Ian Douglas Cave

MECHANICAL PROPERTIES OF FIBRE-REINFORCED MATERIALS

The Wood-water System

A thesis submitted for the degree of Doctor of Philosophy in Physics at the Victoria University of Wellington.

November, 1973.

ACKNOWLEDGEMENTS

It is a pleasure to acknowledge the contributions that Professor N.F. Barber and Dr. M.C. Probine, through an association of many years standing, have made to my understanding of the mechanics of wood. My thanks are due to them also, and to Professor D. Walker, as supervisorsof this thesis, for their help and interest during the period of its preparation.

I thank the members of the staff of the Physics and Engineering Laboratory, D.S.I.R., especially Mr. B.A. Meylan and other members of the wood group for the contributions both direct and indirect that they have made. Thanks are due also to Mr. B.G. Currie who prepared a computer programme in Fortran language for computation of shrinkage and swelling of model wood systems, and to Dr. V.D. Harwood of the Forest Research Institute, Rotorua, for the chemical analysis of a series of wood specimens.

ABSTRACT

The mechanical properties of wood are investigated from a "quasi-elastic" point of view that makes allowance for variation in moisture content. The theoretical work is divided into three parts. The first part shows that wood may be regarded as a fibre-reinforced composite material and then builds up models of wood structure in terms of an assemblage of basic fibre-composite elements. The second part derives the constitutive relations for a fibre-reinforced composite consisting of an inert fibrous phase embedded in a water reactive matrix; and the third part is concerned with the properties of the matrix of wood substance.

The theoretical work is then tested against mechanical data from a set of specimens for which individual models have been devised.

From this work, functions describing the behaviour of the matrix with moisture content are obtained and the structural modelling procedures and the constitutive relation are shown to be not inconsistent with the observations.

It was found that in addition to the mean cellulose microfibril angle, the matrix sorption properties are of great importance in correctly predicting longitudinal shrinkage behaviour.

CONTENTS

Part II

PRACTICAL APPLICATIONS

LIST OF TABLES

LIST OF FIGURES

Chapter 1

INTRODUCTION

Interest in cell-wall mecahnics can be said to have originated with the work of Preston in the 1930's on the influence of plant cell-wall structure on cell growth patterns. In New Zealand this interest has been focused on the problem of relating the properties of wood to the structure of the cell-wall. The first publication from the Wood Group at the Physics and Engineering Laboratory, Department of Scientific and Industrial Research, New Zealand, established the role that the mean cellulose microfibril angle plays in wood shrinkage (Barber and Meylan, 1964). Many papers have since been published reporting experimental and theoretical developments in this and related fields.

The candidate's contributions include work on the theory of the determination of mean microfibril angle in wood from X-ray diffraction diagrams and theoretical work on the influence of structure on the elasticity of the plant cell-wall (with applications to wood). Dynamic properties of wood have also received some attention, together with some discussion of the influence of moisture on mechanical properties.

Two papers covering some of the work of the initial stages of this thesis have already been published. One concerns basic theoretical aspects (Cave, 1972a), and the other is a consequent, but simple, investigation of wood shrinkage, (Cave, 1972b).

The basis of the present work is the derivation of a constitutive relation for a fibre-composite material in which the matrix swells, on the uptake of water. This development has allowed a more complete analytical description of wood behaviour than has formerly been possible. It provides a connection between the thermodynamics of swelling gels developed by Barkas (1949), and the theories of structure-related cell-wall mechanics - by means of a formalism that links the thermodynamic variables of relative humidity, moisture content, temperature stress and strain, with material properties given interms of microscopic structure and the properties of its constituent phases. The new constitutive relation could be important in the study of not only cell-wall mechanics, but also of other multiple phase systems such as soil and water, certain polymers and their solvents and wool and water.

The aim of the present work is to provide, from a "quasi" elastic point of view, a description of wood behaviour that is as comprehensive and as concise as possible. To this end tensors and the reduced tensor matrix notation have been used throughout. A largely self-contained, but brief discussion of tensors as applied to cell-wall mechanics has been appended to this thesis (Appendix I).

With the introduction of moisture content as a variable it has been necessary to find functions describing the moisture-content behaviour of the water-reactive component of wood. In part this has been achieved by deducing the "elastic" properties of the matrix from behaviour under one particular stress-system. As a cross-check the results have been been applied to a second stress system acting on the same material. In the first, longitudinal stress has been applied to give measurements of longitudinal Young's modulus of whole wood at various moisture contents; and in the second, a change in moisture content has been allowed to stress the cell-wall.

The sorption properties deduced in this way (in addition to other information on sorption behaviour) have been applied to the constitutive relations, and then, using models of cell-wall structure, shrinkage properties are predicted. In the light of the comparison between predicted and observed shrinkages, some substantial development has been required of the model representing matrix sorption behaviour and the results have proved most satisfactory.

The work is divided into two parts, theoretical and practical applications.

Part I is divided into three. In the first, the structure of wood is discussed at both the microscopic and submicroscopic levels. In the third chapter, the microscopic structure is used as a basis from which models of wood structure can be built up. The submicroscopic structure suggests a basic mechanical element to which the constitutive

relation applies. The fourth chapter consists of the development of the constitutive relation and then the models of cell-wall structure and the constitutive relation are drawn together in an attempt to form a coherent theory of wood mechanics.

Part II proper consists of four chapters and they are followed by a summary and conclusion. Chapter 5 discusses the preparation of the raw experimental data for a set of specimens that has been gathered together to test the theory. In Chapter 6 the models of the experimental material are set up. In Chapter 7 the "elastic" properties of the matrix are derived from the models and the longitudinal Young's modulus data. Finally, in Chapter 8, the information from the preceding three chapters is pooled to derive and compare the computed shrinkage behaviour with that observed.

In discussing the properties of wood, attention has been confined to the longitudinal components since it is these properties that are most directly determined by cell-wall behaviour. Earlywood from softwood species has been used as the experimental material so as to simplify the considerations of wood structure as far as possible.

Because so many gaps exist in the knowledge of the properties of the phases, and because some of the experimental data is of poor quality, it is suggested that the second part be regarded to some extent as illustrative of a method, rather than as being strictly definitive. However, in spite of some shortcomings in the data, several important results are indicated and these encourage further investigation along the same lines.

References

Barber, N.F., Meylan, B.A. 1964. The Anistropic Shrinkage of Wood. Holzforschung 18 : 146-156.

Barber, N.F. 1968. A Theoretical Model of Shrinking Wood. Holzforschung 22 : 97-103.

_____ 1969. The Shrinkage of Wood, theoretical Models. Proceedings I.P.P.S. Conference on Science of Materials. Auckland. N.Z. 184-195.

Cave, I.D. 1966. X-ray measurement of Microfibril Angle in Wood. Forest Prod. J. 16 : 37-42.

____ 1966. Computation of Diffraction Digrams of Cell Models in X-ray measurement of Microfibril Angle. Appendix to Forest Prod. J. 16 : 37-42.

____ 1968. Elastic Properties of the Plant Cell-wall. A.N.Z.A.A.S. Conf., Christchurch.

____ 1968. Anistropic Elasticity of the Plant Cell-wall. Wood Sci. and Technol. 2 : 268-78.

____ 1969. Longitudinal Young's Modulus of Pinus radiata. Wood Sci. and Technol. 3 : 40-48.

____ 1969. The Mechanical Properties of Wood. Proceedings I.P.P.S. Conference on Science of Materials. Auckland, N.Z. 196-203.

____, Robinson, W.H. 1969. A Model for the Mechanical Damping in Wood. Proceedings I.P.P.S. Conference on Science of Materials. Auckland 109-215.

____ 1970. Note on a Paper by Schniewind and Barrett. Wood and Fiber 2 : 280-281.

____ 1972.(a) Swelling of a Fibre-reinforced Composite in which the Matrix is Water Reactive. Wood Sci. and Technol. 6 : 157-161.

____ 1972.(b) A Theory of the Shrinkage of Wood. Wood Sci. and Technol. 6 : 284-92.

Cousins, W.J. 1972. Measurement of Mean Microfibril Angle of Wood Tracheids. Wood Sci. and Technol. 6 : 58.

_____ 1972. Some Physical Processes involved in Deformation and Fracture. Ph.D. Thesis. Victoria University of Wellington.

_____ 1973. Effects of Strain on the Transverse Strength of Pinus radiata. In press.

Cousins, W.J.1973. A Technique for Microtome Sectioning of Charcoal. In press.

_____ 1973. Effects of Strain Rate on the surface Morphology of Pinus radiata broken in transverse tension. In press.

Exley, R.R. 1964. Technique for lengthwise slicing of single Wood Cells. J. Roy. Mic. Soc. 83 : 479-480.

_____ 1967. Rapid Technique for measuring Cross-sectional Dimensions of consecutive Wood Cells. Forest Prod. J. 17 : 66-67.

_____ 1970. Reference Marks for measurement of small Dimensional Change in Wood. Wood and Fibre 4 : 285.

Gillis, P.P. 1972. On anisotropic Composites. J. Composite Materials 6 : 152-155.

_____ 1972. Orthotropic Elastic Constants of Wood. Wood Sci. and Technol. 6 : 138-156.

_____, Burden, A.K. 1972. Heart Shakes and Growth Stresses. Wood and Fibre. 4 : 95-98.

Harris, J.M., Meylan, B.A. The influence of Microfibril Angle on Longitudinal Shrinkage. Holzforschung 19 : 144-153.

Meylan, B.A. 1967. Measurement of Microfibril Angle by X-ray Diffraction. Forest Prod. J. 17 : 51-58.

_____ 1968. Cause of high Longitudinal Shrinkage in Wood. Forest Prod. J. 18 : 75-78.

_____, Probine, M.C. 1969. Microfibril Angle as a Parameter in Timber Quality Assessment. Forest Prod. J. 19 : 30-34.

_____ 1972. The influence of Microfibril Angle on the Longitudinal Shrinkage - Moisture Content Relationship. Wood Sci. and Technol. 6 : 293-301.

Part I

THEORY

Chapter 2

WOOD STRUCTURE

2.1 Development of Wood Tissue

Practically all of the cells of which wood is composed are derived from a thin zone of living cells, known as the vascular cambium, lying between the bark and the wood. This zone consists of a uniseriate layer of cambial initial cells together with their recent meristematic derivaties, the xylem mother cells on the woody side and the phloem mother cells on the bark side of the initial layer. The phloem mother cells, the initials, and xylem mother cells are arranged in radial files with each file originating from an initial cell. Tree growth proceeds in the main by the formation of new cells by cell division in the tangential plane and by differentiation of the outermost cambial cells into xylem (wood), and phloem tissue, (Kozlowski, T.T. 1971 and Wilson, B.F. 1964).

The process of differentiation generally involves change in shape and often in size; but once the cell has attained full size a much thicker secondary wall is formed in layers on the inside of the primary cell wall. The final stage of development of the wood tissue occurs near the end of the growth phase with the deposition of lignin in the middle lamella and primary wall, and, to a lesser extent, in the secondary layers.

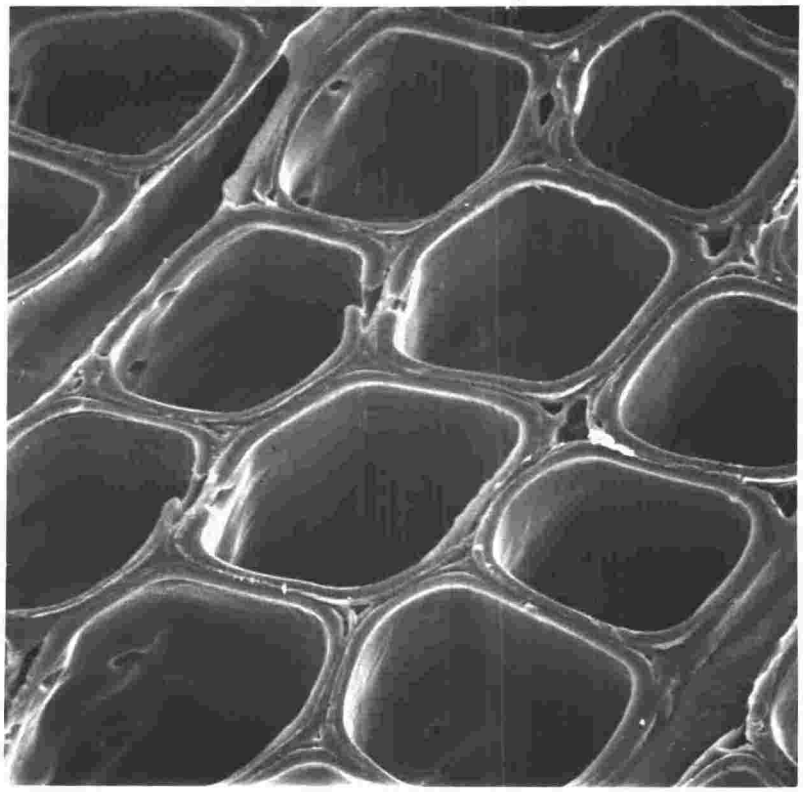

Scanning electron micrograph of a cross-section of

Podocarpus dacrydioides earlywood -- Courtesy B.A. Meylan

Fig. 2.2.1

A cell cut off from the cambium towards the wood may differentiate into one of four types of wood element, each serving one or more special purposes. In hardwoods, cell functions, in general, are more specialised than in softwoods, and result in the appearance of many cell types and structures. On the other hand, softwoods usually consist almost entirely of cells of one type which perform both the functions of tracheary elements (transport of fluids) and fibres (mechanical stiffening). They are known as tracheids.

Because of the relative simplicity of the structures in softwood species, attention in this investigation is confined to wood of this type.

2.2 Softwood Structure

The structure of Pinus species is simple and variation is confined to -

(a) annual banding caused by differences in size, shape and wall thickness between earlywood and latewood tracheids.

(b) vertical resin canals which consist of groups of broken down parenchymatous cells, and

(c) rays which run radially through the tree from pith to bark and consist of clusters of parenchyma cells and ray tracheids.

Between them, the ray structures and resin canals account for no more than 5% of the wood volume in New Zealand grown Pinus radiata. They

are of little account mechanically, for even the ray tracheids, which are elongated in the radial direction, have low stiffness along the cell axis. The parenchymatous tissues are composed of living cells which usually have only thin primary cell walls. From a mechanical point of view Pinus radiata may, therefore, be regarded as consisting of only tracheids and 5% voids, with heterogeneity in structure arising only from the presence of growth rings. In general in the present study, attention has been confined to the wide bands of the earlywood from which homogeneous and thin-walled specimens may be prepared.

2.3 Cell Wall Structures

The wood-cell wall consists, in the main, of a complex of three types of material, namely cellulose, hemicellulose and lignin. Initially, the middle lamella consists merely of the first formed membrane in cell division. The primary wall which is laid down upon the inside of it, is composed of mainly cellulose and pectic substances and the later secondary wall is composed of cellulose and hemicelluloses (Meier 1964). In the closing stages of active cell life the lignin appears as an encrustation in the outer cell-wall layers. The middle lamella and primary wall as a result become composed mainly of lignin and the secondary wall acquires a lignin content of up to 30% (Wardrop 1964).

The cellulose is often termed the "structural" or "framework" component of the cell-wall. It is crystalline and occurs as extremely long "microfibrils" of about 3.5 nm cross-section that generally assume

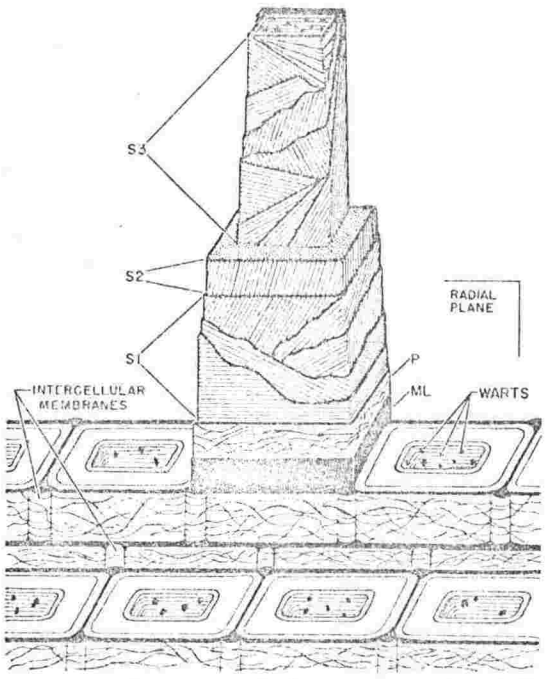

A schematic drawing of "... cell-wall structure" - after Dunning (1969)

Fig. 2.3.1

preferred orientations within the various layers of the cell-wall. In the axial direction it is very stiff (longitudinal Young's modulus 1.37×10^4 kp/mm^2, Sakurada, et al, 1962). On the other hand, the hemicelluloses and lignin which bind the cellulose microfibrils together are each regarded as having low stiffness (Mark 1967). They readily interact with water (though the hemicelluloses do more so than the lignin, (Christensen and Kelsey, 1958)) and have usually been regarded as forming an amorphous complex. However, the hemicelluloses which consist in the main of unbranched polysaccharide chains of various chemical constitutions, with a degree of polymerisation of the order of 100–200, may have a preferred direction associated with the cellulose microfibril alignment. Liang, et al (1960), showed orientation of xylan and glucomannan in the direction of the cellulose by means of polarizing infra-red spectroscopy.

The lignin is a complex three dimensional polymer of polypropane resides which is probably isotropic in nature (Goring, 1971).

The layered structure of the cell-wall is readily observed in the transmission electron microscope, and, to a lesser degree, in the polarizing optical microscope, because the various layers are characterised by differing patterns of cellulose alignment (Wardrop, 1964). However, there are distinct differences in chemical composition also (Meier 1961). The middle lamella and primary wall (usually lumped together and designated M + P) are predominantly composed of lignin with cellulose (10%) and pectic type hemicelluloses (arabinan, galactan and pectic acid) (20%) as other constituents. In the M + P

layer the cellulose microfibrils are uniformly oriented in the plane of the cell-wall and the M + P earlywood thickness is about 10% of the total wall thickness. The first layer of the secondary wall, the S_1 is about as thick as the M + P, Fengel (1969), but the lignin content has dropped to 30%, with equal proportions of cellulose and xylan type hemicelluloses. The S_1 layer is considered by Dunning (1968) to be made up of a series of 4 or 5 lamellae in which the outer lamella has transversely oriented cellulose microfibrils followed by two lamellae with helices at large angles to the cell axes, one left handed and the other right handed. A few lamellae follow with a stepwise transition of microfibril alignment to the steep helix of the S_2 layer.

The S_2 layer is the thickest component of the cell-wall (70-80% in earlywood) and with angles between the microfibrillar axes and the cell axis ranging from 10^{o} - 30^{o} and high cellulose concentration, comprises the most significant component of wood. Dunning (1968), considers that the S_2 layer is laid down in concentric lamellae, and that microfibrillar orientation in each is practically unidirectional throughout the layer.

As in the case of the S_1 layer, the transition from S_2 to S_3 (the final secondary wall layer), is stepwise with regard to microfibril alignment, with the innermost layer of the S_3 having transverse orientation. The S_3 is very thin and comprises less than 2% of the total wall thickness (Fengel, 1969).

Dunning, thus regards the division of the secondary wall into three

layers as somewhat artificial and considers that rather than a sharp division between the layers there is a gradual transition from transverse orientation on the inner and outer faces to the predominant steep helix of the main central portion of the wall.

According to Meier (1961) the chemical composition varies across the secondary wall. The hemicellulose is different from that of the primary wall being composed largely of glucomannan and glucuronoxylan, and the amount of cellulose in the S_2 at 65% is higher than in the inner and outer portions of the secondary wall, (60% and 50% respectively).

2.4 Variation of Structure Across the Tree

Trends in cell-wall composition and structure are noticeable as one moves from the pith of the tree to the bark. The microfibril angle in the S_2 layer usually decreases steadily, from the pith where the largest angles occur, to about the 15th annual growth ring where angles of 15^o - 20^o occur. From there on, small angles (10^o - 20^o) occur that do not correlate closely with annual ring number. In the same way a systematic change can be seen in overall cellulose concentration, the highest values occuring near the outside of the tree where S_2 layer microfibril angles are smallest.

Density also varies across the tree, being lowest near the pith (Nicholls and Dadswell, 1965).

References

Christensen, G.N., Kelsey, K.E. 1958. Sorption of Water Vapour by Wood Constituents. Austr. J. App. Sci. 9 : 263-282.

Dunning, C.E.1968. Cell-wall Morphology of Longleaf Pine Latewood. Wood Sci. 1 : 65-76.

Fengel, D. 1969. The Ultrastructure of Cellulose from Wood. Part I : Wood as the Basic Material for the Isolation of Cellulose. Wood Sci. and Technol. 3 : 203-217.

Goring, D.A.I. 1971. The Lignin polymer in Wood. In : Sarkanen, K.V. and Ludwig C.H. (Eds.) : Lignins, Occurrence, Formation Structure and Reactions. Wiley Interscience, New York.

Kozlowski, T.T. 1971. Growth and Development of Trees. Academic Press, New York and London.

Liang, C.Y., Bassett, K.H., McGinnes, E.A., Marchessa lt, R.H. 1960. Infra-red spectra of Crystalline Polysaccharides. vii. Thin Wood Sections. Tappi. 43 : 1017.

Mark, R.E. 1967. Cell-wall Mechanics of Tracheids. Yale University Press. New Haven and London.

Meier, H. 1961. The Distribution of Polysaccharides in Wood Fibres. J. Polym. Sci. 51 : 11-18.

——— 1964 General Chemistry of Cell-walls and Distribution of Chemical Constituents across the Walls. In : Zimmermann, M.H. (Ed.) The Formation of Wood in Forest Trees. Academic Press. New York and London.

Nicholls, J.W.P., Dadswell, H.E. 1965. Assessment of Wood Qualities for Tree Breeding. III. Division of Forest Products Technological Paper No. 37. C.S.I.R.O., Australia. Melbourne.

Sakurada, I., Nukushina,Y. Ito, T. 1962. Experimental Determination of the Elastic Modulus of Crystalline Regions in Oriented Polymers. J. Polymer Sci. 57 : 651-660.

Wardrop, A.B.1964. The Structure and Formation of the Cell-wall in Xylem. In : Zimmermann, M.H. (Ed.) The Formation of Wood in Forest Trees. Academic Press. New York and London.

Wilson, B.F. 1964. A Model for Cell Production by the Cambium of Conifers. In : Zimmermann, M.H. (Ed.) The Formation of Wood in Forest Trees. Academic Press. New York and London.

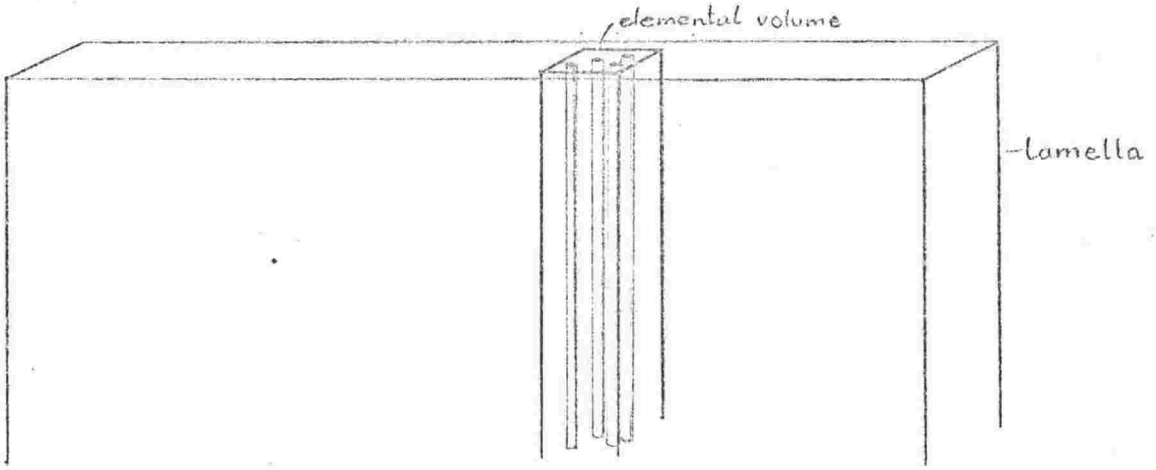

FIG. 3.1.1

Chapter 3

MODELS OF WOOD

3.1 Constitution of the Cell-wall

The concept of the fibre-composite material (that is, the consideration of rigid particles or rodlets of material embedded in a bonding medium) has been used as the basis of the analysis of the mechanics of wood throughout this work. In terms of this concept the elemental component of a cell-wall layer is a "representative volume", as defined by Hill (1963), consisting of a mixture of straight, parallel, cellulose microfibrils embedded in a matrix of hemicelluloses and lignin "that is structurally entirely typical of the whole mixture on average and contains a sufficient number of inclusions for the overall apparent moduli to be independent of surface tractions and displacements ...", Hill (1963). As such, this elemental volume would correspond to a portion of a lamella element of a wall layer, Fig. 3.1.1. Lamellae may be considered to consist of aggregates of identical elemental volumes, cell wall layers to consist of lamellae of various orientations, and cell-walls to consist of layers of various chemical compositions and various orientations.

The cell-wall may thus be described in terms of the behaviour of a series of lamellae bonded together and subject to various bonding conditions. The properties of the lamellae are obtained from the properties of their constituent fibrillar and matrix components by

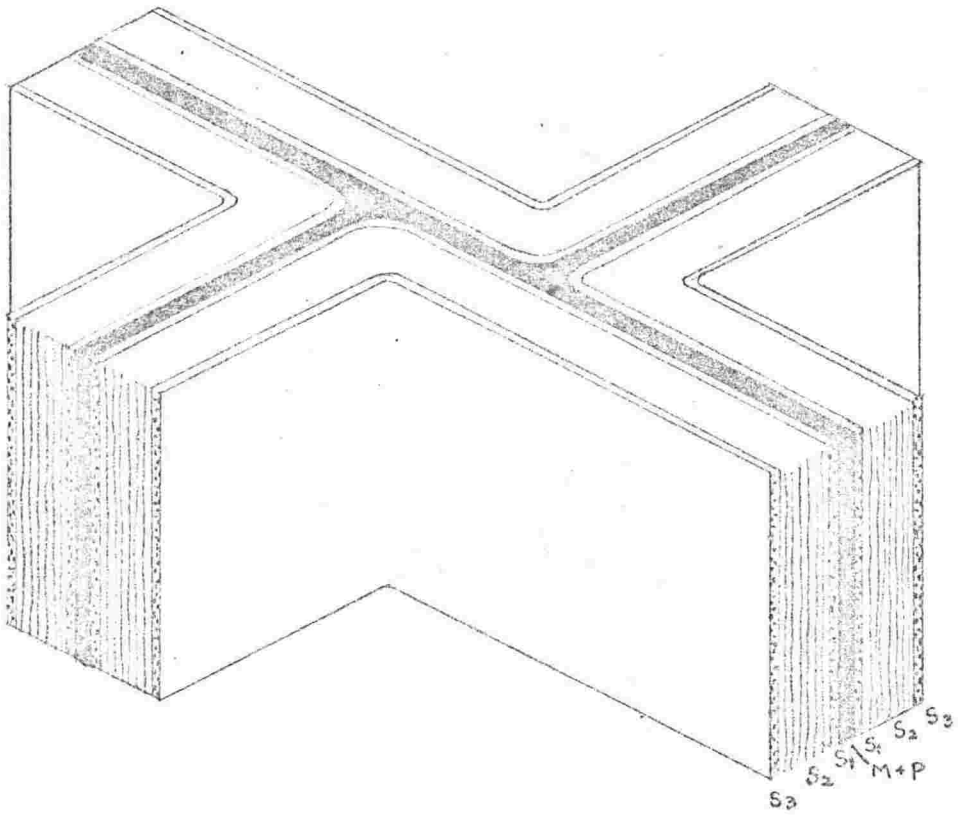

FIG. 3.2.1

Cell-wall pairs

reference to suitable theories of the behaviour of fibre composite materials, e.g. Hill (1965) and Chow and Hermans (1969).

3.2 Model of the Thin Cell-wall

An approximation, appropriate in the consideration of earlywood, results from the assumption that the cell-wall is thin. When a thin walled configuration is assumed it is convenient to consider the wall-pair formed from the cell-walls of adjoining cells. Typically, the cell-walls are flat and the cross-sections appear square or rectangular. A wall-pair thus appears as a symmetric sandwich structure, if the individual cells are identical, with a middle lamella at the centre that is bounded on each face by a primary wall layer followed by the secondary wall. Each lamella in one half of the wall-pair has a complementary lamella in the other half (Fig. 3.2.1). In such wall-pairs the microfibril angle is equal and opposite in complementary lamellae. By assuming a thin wall so that the relative position of the layers is immaterial complementary layers can be lumped together to form balanced laminates. By this means greater symmetry in the elastic constitution of the basic element of the cell-wall is introduced and the boundary conditions applying to the whole cell-wall are simplified. This is at the expense, however, of all information relating to interlayer stresses.

3.3 Model of Wood (Earlywood)

Some properties of whole wood are determined solely by the properties of the multilayered cell-wall. This is the case for longitudinal properties

such as Young's modulus, Cave (1969). For most transverse properties, however, this is not so, and the geometry of the cells themselves and their arrangement with respect to one another, have to be considered before a complete model for wood can be built. The present study is confined to the properties of the cell-wall and so only the longitudinal properties are strictly applicable to whole wood. Transverse shrinkage has been considered; but it is compared only qualitatively with experimental data. (It is too difficult to characterise experimental material for adequate comparison of transverse properties.)

For the properties to be considered in this study, therefore, the wood model (earlywood) is completed by applying the volume factor 0.95 to the cell-wall model, to account for the fact that the tracheids occupy this proportion of the wood volume, and that they are the only elements of importance to the mechanics of wood.

References

Cave, I.D. 1969. Longitudinal Young's modulus of *Pinus radiata*. Wood Sci. and Technol. 3 : 40-48.

Chow, T.S., Hermans, J.J. 1969. The Elastic Constants of Fibre-Reinforced Materials. J. Comp. Materials 3 : 382-396.

Hill, R. 1963. Elastic properties of Reinforced Solids. Some Theoretical Principles. J. Mech. Phys. Solids 11 : 357-372.

——— 1965. Theory of Mechanical Properties of Fibre-strengthened Materials - III Self Consistent Model. J. Mech. Phys. Solids 13 : 189-198.

Chapter 4

A THEORY OF THE MECHANICS OF WOOD

4.1 Constitutive Relations for a Cell-wall Element - General

It has been established that the basic cell-wall element is to be a "representative volume" consisting of parallel cellulose microfibrils embedded in a matrix of hemicelluloses and lignin.

It is now proposed to examine this system from an elastic point of view. Although some experimental phenomena point to a degree of plastic and time dependent behaviour in wood, the view taken here is that the elastic case can usefully take one a long way along the road to understanding much of the behaviour of wood. If necessary, both time dependence and plasticity can easily be accommodated within the formalism used here by the substitution of appropriate material constants. The work of, Cousins (1972), and Nissan and Sternstein (1962), for example, indicates that simple rate theory will account in the main for time dependent phenomena in wood. In considering moisture in wood steady state conditions are assumed, so that diffusion effects are excluded.

The wood material properties considered, however, are not truly elastic, in the conventional sense, since an additional dimension is introduced with which these properties vary. This new dimension is water. Water reacts very readily with the hemicelluloses, and with lignin and thereby affects the stiffness of the matrix. Cellulose, from its X-ray diffrac-

tion properties is known not to interact significantly with water and is taken to be truly elastic. Wood, therefore, has to be considered as a three phase system. Two of the phases, the cellulose microfibrils and the matrix-water complex exist in the solid state, while the third exists in the gaseous state as water vapour. The behaviour of wood is dependent, then, not only on stress and strain, but also on the pressure, temperature and relative humidity of the environs. Consideration will be given to the behaviour of wood at constant atmospheric temperature and pressure.

4.2 Symmetry of the Cell-wall Element

Symmetry in the properties of a composite material is dependent upon the symmetry of its components and the way in which they are arranged with respect to one another. The basic wall element is taken to consist of parallel microfibrils embedded in a matrix that has usually been regarded as amorphous and isotropic. In this case the composite system assumes the symmetry of the microfibril arrangement.

An individual native cellulose microfibril has monoclinic symmetry, but is very nearly orthotropic since its basal angle is nearly 90° ($\beta = 84^{\circ}$). In wood, however, it is assumed that only the "b" crystallographic axis of the cellulose, that is the microfibril axis, is aligned, since there is no evidence that there is alignment of the planes parallel to the "b" axis. The assemblage of cellulose microfibrils is, therefore, assumed to be transversely isotropic and so the composite is also transversely isotropic.

In the present work it is suggested that there is structure in the matrix arising from the alignment of the hemicellulose chains along the microfibril axes. The matrix itself may, therefore, be transversely isotropic, but, because the axis of isotropy is parallel to the cellulose axis of isotropy, the symmetry of the composite system remains the same as before.

4.3 Constitutive Relations of a Swelling Fibre-Composite

4.3.1 Stiffnesses

With transverse symmetry the basic cell-wall element will have five independent "elastic" constants and its stiffness in reduced form (see Appendix I) will be represented by,

$$\begin{matrix} C_{11} & C_{12} & C_{13} & \cdot & \cdot & \cdot \\ & C_{11} & C_{13} & \cdot & \cdot & \cdot \\ & & C_{33} & \cdot & \cdot & \cdot \\ & & & C_{44} & \cdot & \cdot \\ & & & & C_{44} & \cdot \\ & & & & & C_{66} \end{matrix}$$

With $C_{66} = \frac{1}{2}\left(C_{11} - C_{12}\right)$, when the 3 axis is the axis of isotropy. The coefficients C_{ij} are the reduced matrix form of the tensor stiffnesses, which in the present case are not constants but functions of moisture content. They are determined from the geometry and stiffnesses of the constituent microfibrils and binding matrix using Hill's "Self Consistent Theory" of a fibre composite, Hill (1965).

4.3.2 Effect of moisture

When water is taken up by the composite cell-wall element, the matrix swells and becomes more compliant. The swelling process induces internal stress changes, and in the cell-wall situation may also change the external stress through the interaction of the various cell-wall layers upon one another. Strain is, therefore, a function of change in internal and external stress and in matrix compliance.

Internal stress is developed when water is absorbed by the matrix and the matrix attempts to extend the microfibrils. This stress is proportional to the restraint imposed on the swelling of the matrix by the microfibrils. If the unrestrained matrix swelling, relative to the"stress free" state of the composite, (i.e. the state of strain in which the forces of reaction of the cellulose against the matrix are zero), is denoted by ε° and if the strain that the matrix achieves in the presence of the microfibrils and any associated external stress is denoted by ε^{m} then the stress in the matrix is given by,

$$\sigma^{m} = C^{m}(\varepsilon^{m} - \varepsilon^{\circ}), \qquad (1)$$

where C^{m} is the stiffness tensor of the matrix material; and the stress developed in the microfibrils is proportional to the imposed strain, ε^{f} so that,

$$\sigma^{f} = C^{f}\varepsilon^{f}. \qquad (2)$$

In a representative volume of the composite the average stress taken over both the microfibrils and the matrix must equal the average external stress. If we define the average stress by the integral of stress over a specified region divided by the volume of that region then the following connection between the average stress in the two

phases and the overall (external) stress applies, Hill (1963),

$$c^f \bar{\sigma}^f + c^m \bar{\sigma}^m = \bar{\sigma}, \tag{3}$$

where the bar placed above indicates a volume average, and c^f and c^m are the concentrations or volume proportions of the microfibrils and matrix respectively; and we find that,

$$c^f C^f \bar{\varepsilon}^f + c^m C^m (\bar{\varepsilon}^m - \bar{\varepsilon}^\circ) = \bar{\sigma}. \tag{4}$$

Rearranging Eq. 4.3.4,

$$c^f C^f \bar{\varepsilon}^f + c^m C^m \bar{\varepsilon}^m = c^m C^m \bar{\varepsilon}^\circ + \bar{\sigma}, \tag{5}$$

and noting that there is a unique dependence of the average strain in the microfibrils and the matrix on the overall strain, that may be expressed as,

$$\bar{\varepsilon}^f = A^f \bar{\varepsilon}, \quad \bar{\varepsilon}^m = A^m \bar{\varepsilon}, \tag{6}$$

Hill (1963), we find that Eq. 4.3.5 relates a uniform stress, $c^m C^m \bar{\varepsilon}^\circ + \bar{\sigma}$, to the resultant overall strain, $\bar{\varepsilon}$.

$c^f C^f A^f + c^m C^m A^m$ is therefore identical with C, the overall stiffness tensor of the composite, and Eq. 4.3.5 may be written,

$$C\bar{\varepsilon} = c^m C^m \bar{\varepsilon}^\circ + \bar{\sigma}. \tag{7}$$

A^f and A^m are functions dependent on the elastic constants, geometry and concentrations of the two phases and the way in which the phases interact.

If an increment of moisture is added to the composite in the swollen state (relative to the stress free condition) then the resulting increment in strain is given by the differential of Eq. 4.3.5. That is,

$$C\Delta\bar{\varepsilon} = c^m C^m \Delta\bar{\varepsilon}^\circ - c^m \Delta C^m (\bar{\varepsilon}^m - \bar{\varepsilon}^\circ) + \Delta\bar{\sigma}, \tag{8}$$

where, the Δ indicates an increment in the quantity that it precedes

arising from the moisture increment.

Substituting for $\bar{\varepsilon}^m$, Eq. 4.3.8 becomes,

$$C\Delta\bar{\varepsilon} = c^m C^m \Delta\bar{\varepsilon}^\circ - c^m \Delta C^m \left(A^m \bar{\varepsilon} - \bar{\varepsilon}^\circ\right) + \Delta\bar{\sigma}. \qquad (9)$$

Eq. 4.3.9 constitutes a differential equation in overall strain, $\bar{\varepsilon}$, with respect of moisture content.

Eqs. 4.3.7 and 4.3.9 can be evaluated when matrix stiffness as a function of moisture content and the moisture content of the stress free state are known, for,

(i) A^m is given by the relation,

$$C - C^f = c^m \left(C^m - C^f\right) A^m.$$

(ii) C is determined from the elastic constants of the two phases and their concentrations, from theories of fibre composite materials.

(iii) $\bar{\varepsilon}^\circ$ the unrestrained matrix strain may be related to moisture content and relative humidity.

4.4 Moisture Relations

To relate mechanical behaviour to moisture directly Eq. 4.3.9 may be written,

$$C\Delta\bar{\varepsilon} = c^m C^m \left(\frac{\partial\bar{\varepsilon}^\circ}{\partial u}\right)\Delta u - c^m \left(\frac{\partial C^m}{\partial u}\right)\Delta u \left(A^m \bar{\varepsilon} - \bar{\varepsilon}^\circ\right) + \Delta\bar{\sigma}. \qquad (1)$$

An estimate of $\left(\frac{\partial C^m}{\partial u}\right)$ is made in Chapter 7, and the other differential which is dependent on some model of the matrix is discussed in Chapter 8.

The thermodynamic theory of rigid swelling gels developed by Barkas may be used to find the connection between moisture content of wood and

relative humidity. There are four isothermal thermodynamic variables of a rigid gel of which any two taken together are independent. These are stress or pressure, strain, moisture content and humidity; and, defining ambient humidity and pressure for an isotropic gel, for instance, determines the moisture content and the swelling of that gel.

Regarding humidity as one dependent variable, Δh can be written in terms of moisture content change, Δu , and stress change, $\Delta \sigma$. Thus,

$$\Delta h = \left(\frac{\partial h}{\partial u}\right)_{\sigma} \Delta u + \left(\frac{\partial h}{\partial \sigma}\right)_{u} \Delta \sigma \qquad (2)$$

The differential $\left(\frac{\partial h}{\partial u}\right)_{\sigma}$ is the gradient of the familiar sorption isotherm (yet to be produced in a form other than for hydrostatic pressure). It is quite strongly stress dependent and only rough estimates of its general form can be made at present (Chapter 8). Barkas' theory also provides means for estimating $\left(\frac{\partial h}{\partial \sigma}\right)_{u}$ although the term is not required here, as variation in external stress is not considered.

Eqs. 4.4.1 and 4.4.2 (with $\Delta \sigma = 0$) express the formal relationship between mechanical behaviour of a fibre-composite and stress, strain and humidity.

Setting Δu zero in Eq. 4.4.1 gives the simple relation between applied stress and strain for constant moisture content and means for calculating longitudinal Young's modulus for instance*. Taking Eq. 4.4.1 with

---

*Note : This situation strictly requires a change in humidity Δh to maintain Δu zero under an external stress change $\Delta \sigma$, but under test conditions for longitudinal Young's modulus (instaneous elastic deflection) diffusion is too slow to allow a significant change in moisture content.

external stress zero gives shrinkage in terms of moisture content. With both Eqs. 4.4.1 and 4.4.2 operative it is possible to relate mechanical behaviour to humidity change as is done in the discussion of moisture induced deformation in Chapter 8.

4.5 Mechanics of the Cell-wall

4.5.1 Cell-wall reference system

In general, the elements of the cell-wall are aligned with their microfibril axes at differing angles so that strains in terms of a common reference system will have to be determined. This is taken to be the rectangular cartesian cell-wall reference system (x_1', x_2', x_3',) in which the x_3' axis coincides with the longitudinal axis of the tracheid and the x_2' axis lies in the plane of the cell-wall (Fig. 4.5.1).

In this system the constitutive relation Eq. 4.4.1 becomes, with rearrangement,

$$\Delta\bar{\sigma} = C'\Delta\bar{\varepsilon}' - c^m\left[C^{m\prime}\left(\frac{\partial\bar{\varepsilon}^{\circ\prime}}{\partial u}\right)\Delta u - \left(\frac{\partial C^{m\prime}}{\partial u}\right)\Delta u A^{m\prime}\left(\bar{\varepsilon}' - \bar{\varepsilon}^{\circ\prime}\right)\right] \qquad (1)$$

where the tensors C', $C^{m\prime}$, $\bar{\varepsilon}'$, $\bar{\varepsilon}^{\circ\prime}$, $\bar{\sigma}'$ and the matrix $A^{m\prime}$ are transformed from the principal axes of the composite to the cell-wall reference system. The values of the new tensor coefficients are determined uniquely by the principal values and the microfibril angle of the cell-wall elements. The tensor transformation is described in Appendix I.

4.5.2 Position of the stress free state

The cell-wall is made up of a large number of lamellae, each of which is described by a relation of the above type (Eq. 4.5.1) but unless all

lamellae can be said to have the same stress free state there will be differing base lines for measuring strain from. Values must, therefore, be placed on the stress free states before proceeding further. At present, however, there is no basis for doing this. One could postulate that all lamellae could have the same stress free state, perhaps by allowing the assemblage of wall layers to reach equilibrium, after changes in conditions, through the mechanism of creep. However, it is quite uncertain that this could happen in reality.

For convenience it is assumed that this postulate is true. On this basis it is shown in Chapter 8 that the term dependent on the position of the stress free state is likely to be small compared with the swelling stress term and so the stress free state is unimportant in a practical sense.

4.5.3 Interaction of cell-wall lamellae

To discover the average behaviour of the whole cell-wall from a knowledge of its parts it is necessary to specify how the parts interact. The most obvious and also the simplest procedure for a thin cell-wall configuration is to assume that the lamellae are rigidly bonded together, so that each suffers identical strain in the plane of the cell-wall. Under these conditions and with identical stress free states the components of $\bar{\varepsilon}'$ in the plane of the cell-wall will be common to all lamellae. If each lamella is constrained to suffer deformations identical with that of its neighbours, when its elastic constitution by virtue of its different microfibril arrangement, is different, then it will exert stresses on its neighbours given by

Eq. 4.5.1. The sums of the forces acting individually on all the lamellae are the forces acting to produce the deformations in the cell-wall as a whole. Thus a relation between overall stress and overall strain can be obtained.

4.5.4 Overall stress

The summation of these forces can be facilitated by letting it be supposed that the cell-wall is divided into layers (of prescribed chemical composition) and that these layers are divided into unidirectional elemental layers of identical shape and volume. In addition, all the elemental layers from a particular cell-wall layer have microfibril densities consistent with the chemical composition of that layer. The elemental layers just described could be considered to be subunits of the lamellae.

Under this scheme the overall stress is given by,

$$\sigma = \sum_{i=1}^{n} \sigma^i / n \ , \qquad (2)$$

where σ^i is the stress acting on the ith elemental layer and is given by Eq. 4.5.1 and there are n elemental layers in the cell-wall.

Frequently, it is possible to relate the microfibril distribution within a layer to some continuous function. In this case the relative frequencies of elemental layers with the same microfibril angle, will be the same as the microfibril distribution and Eq. 4.5.2 could be rewritten,

$$\sigma = \sum_{r=1}^{N} \int_{-\frac{\pi}{2}}^{\frac{\pi}{2}} \sigma^r(\theta) f^r(\theta) \, d\theta \Big/ \sum_{r=1}^{N} \int_{-\frac{\pi}{2}}^{\frac{\pi}{2}} f^r(\theta) \, d\theta \qquad (3)$$

where $\sigma^r(\theta)$ is the elemental layer stress distribution in the rth cell-wall layer, N is the number of layers in the cell-wall and

$f^r(\theta)d\theta$ is the number of elemental layers in the rth cell-wall layer with microfibril angles in the range $\theta - d\theta$ to $\theta + d\theta$;

$$n = \sum_{r=1}^{N} \int_{-\frac{\pi}{2}}^{\frac{\pi}{2}} f^r(\theta)d\theta. \qquad (4)$$

Continuous microfibril angular distributions are assigned to the cell-wall layer, in Part II using the techniques of Cave (1968) who demonstrated that the integration of lamella stresses for a quasi normal distribution is easy, and that the assumption of a normal distribution for plant cell-wall material is reasonable.

4.5.5 Cell-wall layer-pairs

It is convenient at this stage to introduce the concept of the layer-pair balanced laminate discussed in Chapter 3. Reference to Table A1.7.1 in the appendix will show that there are no terms in the composite stiffness tensor C that relate shear stress to tensile strain or conversely tensile stress to shear strains, in a balanced laminate. Thus for the present we may conveniently consider only the relation between the stresses σ_1', σ_2', σ_3' and their dependence on the strains ε_1', ε_2', ε_3'.

4.5.6 Overall stress in terms of strain

From the preceding discussion it will be clear that the stress normal to the plane of the cell-wall σ_1', is zero since there are no constraints placed on the lamellae in that direction. Thus in each elemental layer an expression for the ε_1' strain of the elemental layer can be obtained in terms of the overall ε_2' and ε_3' strains. These can then be used to eliminate ε_1' from the expressions for the elemental layer stresses

σ_2' and σ_3', and so the relation between the overall stress and the overall strains ε_2' and ε_3' can be obtained by the summation of forces over the elemental layers.

The overall strain in the '1' direction is obtained from,

$$\varepsilon_1' = \sum_{i=1}^{n} \varepsilon_1'^{i} / n \,, \qquad (5)$$

once the elemental layer strains $\varepsilon_1'^{i}$ have been calculated from the solutions for ε_2' and ε_3'.

4.6 Evaluation of Composite Stiffnesses of Wood Substance

Hill's "Self Consistent Model" of the fibre-composite has been used to evaluate the stiffness coefficients of the cellulose-matrix composite in terms of the stiffness of its components and their relative proportions.

For a transversely isotropic system of parallel fibres embedded in a matrix Hill (1963) discovered that only three out of the five elastic constants are independent. He found quite generally that,

$$\frac{k-k_1}{\ell-\ell_1} = \frac{k-k_2}{\ell-\ell_2} = \frac{\ell - c_1\ell_1 - c_2\ell_2}{n - c_1 n_1 - c_2 n_2} \,, \qquad (1)$$

where k is the transverse bulk modulus, $k = \frac{1}{2}(c_{11} + c_{12})$, $\ell = c_{13}$, $n = c_{33}$ and c_1 and c_2 are the volume proportions of the two phases. Absence of a subscript implies a property of the composite, while a subscript 1 or 2 refers to a property of one of the two phases.

Thus if k is known ℓ and n can be determined. Hill (1965) determined k, $\mu = c_{44}$ and $m = c_{66} = \frac{1}{2}(c_{11} - c_{12})$ by means of a

"self consistent" method in which he imagined a single fibre to be embedded in a homogeneous medium with the same properties as the composite. The strain developed in this fibre by a uniform load applied to the unbounded medium was adopted as the average strain over all the fibres in the actual composite. This lead to a relation amongst the longitudinal shear moduli, of,

$$\frac{c_1}{\mu - \mu_2} + \frac{c_2}{\mu - \mu_1} = \frac{1}{2\mu} , \qquad (2)$$

and m was found to be given by,

$$\frac{c_1 k_1}{k_1 + m} + \frac{c_2 k_2}{k_2 + m} = 2\left(\frac{c_1 m_2}{m_2 - m} + \frac{c_2 m_1}{m_1 - m}\right). \qquad (3)$$

k was obtained from,

$$k + m = \left(\frac{c_1}{k_1 + m} + \frac{c_2}{k_2 + m}\right)^{-1} . \qquad (4)$$

More recently, Chow and Hermans (1969) have published a more accurate evaluation of k , μ and m using a method that takes into account the interaction of a fibre with its closest neighbour.

4.7 Computation

The complex computations represented by Eqs. 4.6.1 - 4.6.4 (composite stiffness coefficients) and table A1.7.1 (tensor transformation of stiffnesses) substituted in Eq. 4.5.1 (elementary layer stresses) together with the stress summation procedures in sections 4.5.4 - 4.5.6 have been performed on both a basic Hewlett-Packard HP9800-10 programmable desk calculator and a Hewlett-Packard 2100 mini-computer. The integrations over moisture content required to solve for total strain have been run only on the mini-computer, but the desk calculator has been used to check these runs by comparing strain increments from both programmes.

References

Barkas, W.W.1949. The Swelling of Wood under Stress. His Majesty's Stationery Office, London.

Cave, I.D. 1968. The Anisotropic Elasticity of the Plant Cell-wall. Wood Sci. Technol. 3 : 268-278

Chow, T.S., Hermans, J.J. 1969. The Elastic Constants of Fibre Reinforced Materials. J. Comp. Materials. 3 : 382-396.

Cousins, W.J. 1972. Some Physical Processes involved in Deformation and Fracture. Ph.D. Thesis, Victoria University of Wellington, Wellington, New Zealand.

Hill, R. 1963. Elastic Properties of Reinforced Solids : Some theoretical Principles. J. Mech. Phys. Solids 11 : 357-372.

____ 1964. Theory of the Mechanical Properties of Fibre-Strengthened Materials : I. Elastic Behaviour. J. Mech. Phys. Solids. 12 : 199-212.

____ 1965. Theory of Mechanical Properties of Fibre-Strengthened Materials:III Self Consistent Model. J. Mech. Phys. Solids. 13 : 189-198.

Nissan, A.H., Sternstein, S.S. 1962. Cellulose as a Viscoelastic Material. Pure App. Chem. 5 : 131-146.

Flow-chart for use of Models and Data.

FIG. 5.1.1

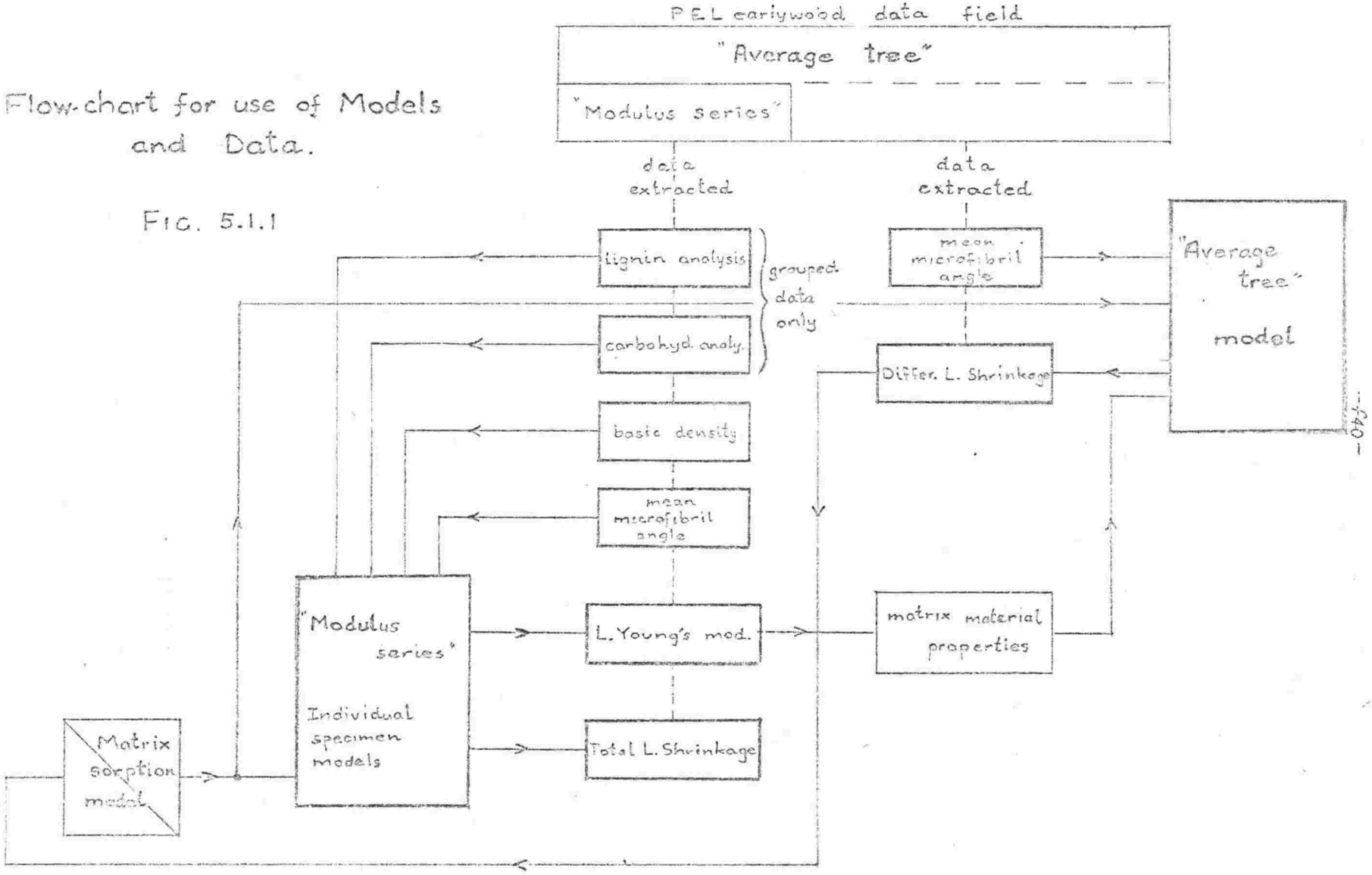

Part II

PRACTICAL APPLICATIONS

Chapter 5

EXPERIMENTAL DATA

5.1 Introduction

The aim of this work has been to explain the behaviour of wood in terms of its structure and the properties of its components. However, the properties of some components are not completely known and in particular the stiffness constants of the matrix are unknown. By making some assumptions about the nature of the matrix a value of the shear modulus consistent with these assumptions has been deduced from longitudinal Young's modulus data; and the system has been cross-checked by comparing the shrinkage of the same specimens used in the longitudinal Young's modulus experiment with computations of shrinkage using these values. To do this, the individual experimental specimens have been modelled on the basis of chemical composition, density, and mean microfibril angle.

The data on longitudinal Young's modulus, shrinkage and density have been obtained from experiments conducted by the Wood Group of the Biophysics Section at the Physics and Engineering Laboratory, Department of Scientific and Industrial Research, Gracefield, on a small set of earlywood Pinus radiata specimens. For convenience later these specimens are termed the "Modulus series".

Shrinkages were determined according to the methods of Meylan (1972), and the longitudinal Young's modulus according to the procedures of Cave (1969), except that photographic recording of strain was replaced by a direct measurement of strain using a strain gauge extensometer. Chemical analyses of the specimens have been determined by Dr. V.D. Harwood of the Forest Research Institute, New Zealand Forest Service, Rotorua. The chemical work involved carbohydrate analysis and gravimetric lignin determination. Unfortunately lignin determination on 30 mgm specimens is very difficult and so specimens were grouped to make more conventional sample sizes for lignin analysis. This meant that the ideal situation of individual determinations of lignin, cellulose and hemicelluloses relative to whole wood was not attained and means have had to be devised to obtain models of best fit for the grouped data.

A larger body of earlywood Pinus radiata data is available from the work of the Wood Group that includes longitudinal shrinkage and mean microfibril angle information only. This set is presented in Fig. 8.2.1 and is used against the "Average tree" model of section 6.4.

5.2 Experimental Data and its Preparation

5.2.1 Need for correction and conversion

Before the raw experimental data on longitudinal Young's modulus, basic density, and chemical composition, can be used it needs to be converted to make it consistent with the theoretical parameters. For instance experimental Young's modulus has been obtained with longitudinal stress equated to load per unit dry cross-sectional area. This needs to be

corrected for a true cross-sectional area - a variable dependent on moisture content. Similarly basic density has to be converted to give cell-wall thickness which is another variable that depends on moisture content.

5.2.2 Longitudinal Young's modulus

Longitudinal Young's modulus has been recorded from experiments as load/dry cross-sectional area/strain, for a range of moisture contents. For use in the present context plots of this parameter versus moisture content have first been smoothed and then multiplied by an area-correction factor to account for the changing area of the cross-section with moisture content. This procedure results in a longitudinal Young's modulus for wood substance.

The area correction factor is,

(dry cross-sectional area)/(cross-sectional area at moisture content u),

with the denominator calculated from,

cross-sectional area = (volume of wood substance)/(length),

all at moisture content u .

That is, the area correction factor is,

$$\left(w_d / 1{\cdot}46\ell\right) \Big/ \left[\left(w_d / 1{\cdot}46 + w_d\, u/\rho_s\right)/\ell\,(1+\varepsilon_3)\right], \qquad \text{or}$$

$$(1+\varepsilon_3)\Big/(1 + 1{\cdot}46\, u/\rho_s),$$

where w_d is the dry weight of the specimen, ℓ is its length dry ρ_s is the density of sorbed water (Table 5.2.1), ε_3 is the longitudinal swelling and u , the moisture content, is the ratio of the weight of water sorbed to the dry weight of the wood. In this

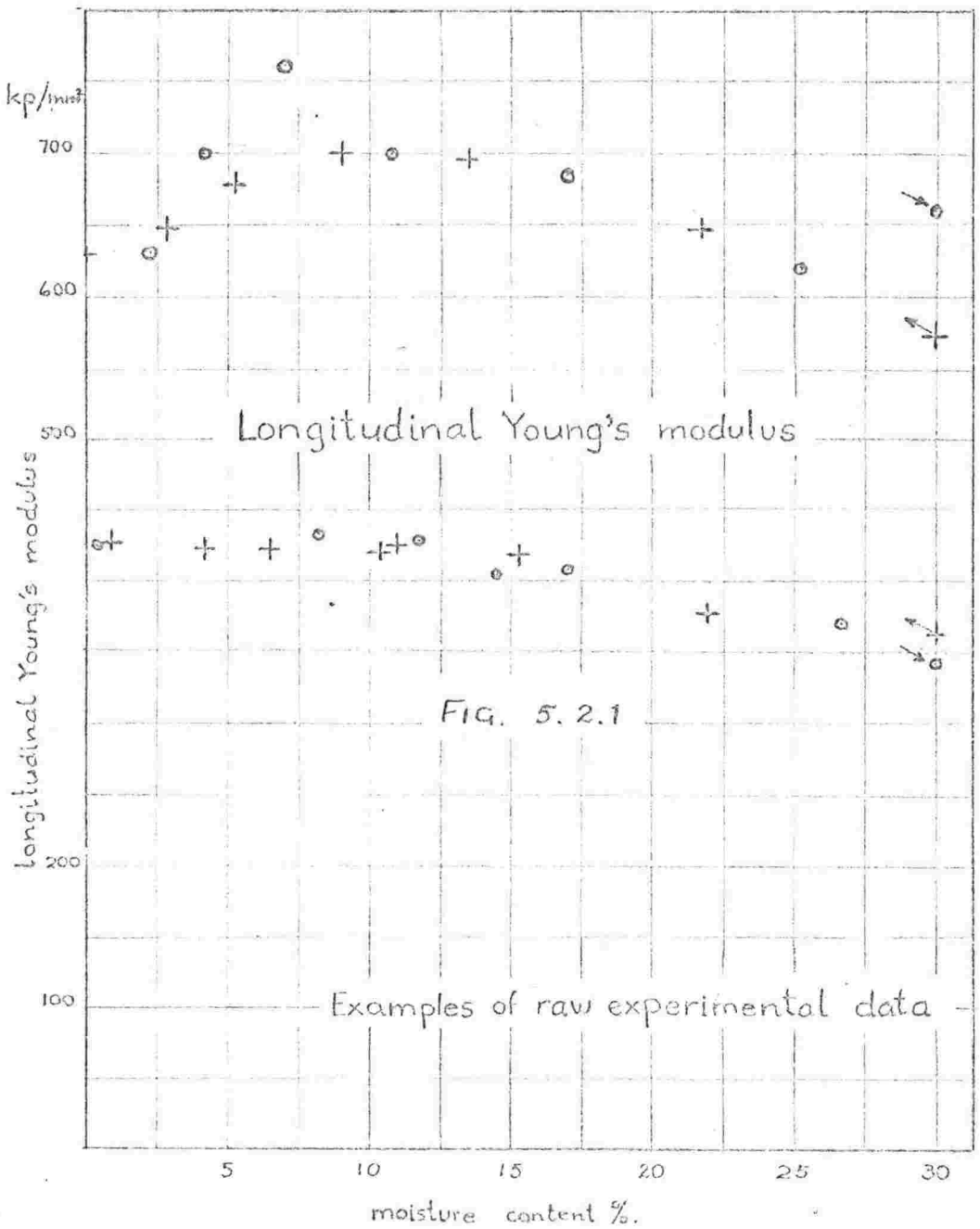

FIG. 5.2.1

Examples of raw experimental data

context dry means a state of dryness in equilibrium with P_2O_5 . The density of dry wood substance is taken to be 1.46 (Stamm, 1938).

Two raw longitudinal Young's modulus curves are shown to demonstrate the nature and the extremes of quality of the data (Fig. 5.2.1).

5.2.3 Shrinkage

Curves of longitudinal (and transverse) shrinkage versus moisture content (e.g. Fig. 8.2.6) as obtained from experiment are in a form that can be directly compared with the output from model computations of shrinkage. Consequently, in distinction to the longitudinal Young's modulus case there is no need for correction or conversion of shrinkage data.

5.2.4 Microfibril angle

The mean microfibril angle in the S_2 layer has been measured by an X-ray diffraction technique described by Meylan (1967).

In the models it has been assumed that the microfibrils in the S_2 layer have an angular distribution about the mean angle that can be represented by a gausian or normal function whose standard deviation is one third of the mean angle. This assumption has been discussed in Cave (1966) and has subsequently been supported by Okano (1968).

5.2.5 Basic density

Basic density has been measured simply as ,

(dryweight)/(wet volume),

and this figure has been converted to,

(dryweight)/(dry volume),

to provide a basis for calculating wall thickness of model cells with a standard diameter of 34 μm.

(Dry weight)/(dry volume) is obtained from basic density through the relation,

basic density = (dry weight)/(dry volume + dry weight $\times u_s/\rho_s$),

where u_s is the moisture content of the saturated cell-wall (28.5%) and ρ_s is the mean density of water in the saturated cell-wall (1.115, Stamm 1938).

5.2.6 Chemical analyses

The chemical data has been provided in terms of gravimetric percentages and these have been converted to volumetric ratios using the densities quoted by Fengel (1969, 1970) for lignin, hemicellulose and cellulose. These are lignin 1.34, hemicellulose 1.50 and cellulose 1.55.

5.2.7 Sorption in the matrix

The density of sorbed water at various moisture contents, ρ_s, has been taken from Stamm (1938).

The values used are given in Table 5.2.1. From this table the volumetric strain of wood substance arising from an increment in moisture content of amount Δu is,

$$\frac{\Delta V}{V} = \frac{1.46}{\rho_s} \Delta u \qquad (3)$$

If it is assumed that Stamm's wood contained 50% cellulose then the linear strain in an isotropic matrix is given by,

$$\Delta\varepsilon^{\circ} = \frac{1{\cdot}46}{3\varepsilon_s} \times \Delta mmc$$

where mmc is the matrix moisture content ($\simeq 2\times$ moisture content of wood).

This relation has been adopted initially as the matrix sorption property and values of the sorbed moisture volume as a function of matrix moisture content are also given in Table 5.2.1.

Table 5.2.1

Density and volume of sorbed water

moisture content %	0	5	10	15	20	25	30
sorbed water density(1)	1.300	1.244	1.201	1.169	1.144	1.126	1.113
sorbed moisture vol.(2)	0.000	0.114	0.232	0.355	0.480	0.608	0.739

(1) From Stamm (1938)

(2) Sorbed water volume expressed as a fraction of dry matrix volume. Derived from (1) and Eq. 5.2.4.

Table 5.2.2

Elastic constants of cellulose

Elastic constant stated by MARK (1965)		Derived stiffnesses	Source
longitudinal YOUNG'S modulus	$E_L = 1.37 \times 10^4$ kp/mm^2	$c_{33} = 13{,}730$ kp/mm^2	SAKURADA et al. (1962). Experimentally determined by X-ray technique
transverse YOUNG'S modulus	$E_T = 0.157 \times 10^4$ kp/mm^2	$c_{11} = 1{,}572$ kp/mm^2	MARK (1965). Theoretical computation
		$c_{12} = 12$ kp/mm^2	Obtained by setting $s_{12} = 0$
POISSON'S ratio of contraction transverse to longitudinal extension under longitudinal stress	$\nu_{LT} = 0.1$	$c_{13} = 157$ kp/mm^2	MARK (1965). Theoretical computation
Shear modulus of rigidity average for 101 and 101 planes	$G_{LT} = 380$ kp/mm^2	$c_{44} = 380$ kp/mm^2	MARK (1965). Theoretical computation

5.3 Established Data

The elastic constants of cellulose are regarded as established even though only the axial Young's modulus has been subjected to experimental determination. Figures first given by Mark (1965) and subsequently used by Cave (1968, 1969, 1972) are used here and are quoted in Table 5.2.2.

References

Cave, I.D. 1969. The Longitudinal Young's Modulus of *Pinus radiata*. Wood Sci. Technol. 3 : 40-48.

——— 1966. X-ray Measurement of Microfibril Angle. For. Prod. J. 16 : 37-42.

——— 1972. A Theory of the Shrinkage of Wood. Wood Sci. Technol. 6 : 284-92.

Fengel, D. 1969. The Ultrastructure of Cellulose from Wood. Part 1 : Wood as the Basic Material for the Isolation of Cellulose. Wood Sci. Technol. 3 : 203-217.

——— 1970. The Ultrastructure of Cellulose from Wood. Part 2 : Problems of the Isolation of Cellulose. Wood Sci. Technol. 4 : 15-35.

Mark, R.E. 1965. in W.A. Cote, Jr.(Ed) : Cellular Ultrastructure of Woody Plants. Syracuse, Syracuse Univ. Press.

Meylan, B.A. 1972. The Influence of Microfibril Angle on the Longitudinal Shrinkage - Moisture Content Relationship. Wood Sci. Technol. 6 : 293-301.

——— 1967. Measurement of Microfibril Angle by X-ray Diffraction. For. Prod. J. 17 : 51-58.

Okano, T. 1968. The Relationship between Micelle Angle and X-ray Diffraction Diagrams. Jap. Wood Res. Soc. J. 14 : 358-362.

Sakurada, I., Nukushina, Y., Ito, T., 1962. Experimental Determination of the Elastic Modulus of Crystalline Regions in Oriented Polymers. J. Polymer Sci. 57 : 651-660.

Stamm, A.J. 1938. Calculations of the Void Volume in Wood. Ind. Eng. Chem. 30 : 1280-1281.

Chapter 6

MODELLING

6.1 Structural Data

It was intended at the outset to model the individual specimens from which data was to be drawn. However, while data on an individual basis is available for mean microfibril angle and basic density, the chemical analyses are related to grouped values only. The groupings were made according to the sugar composition of the carbohydrate, the twelve normal wood specimens of the sample being divided into two groups, corresponding to specimens that were supposed to have come from inside or outside the tenth growth ring of the tree. (Ring number information was not recorded in the P.E.L. experiments.) The models adopted have accordingly been fitted to give the best grouped fit of the chemical data and, therefore, regretably, fall short of being models of individual specimens.

6.2 Specimen Models

6.2.1 Two layer model

To provide a model of sufficient complexity to describe wood in the desired detail it has been necessary to assume at least a two layer model. However, the density and chemical data alone is not sufficient to determine such a model, and so some assumptions about cell-wall structure and composition have to be made.

These assumptions have been based on information available on softwood species elsewhere, and they are generally in line with experience at the Physics and Engineering Laboratory over the years on locally grown Pinus radiata.

The observed variation in chemical composition with cell-wall thickness attributed by Fengel (1969) to the change in the thickness of the S_2 layer, suggested a basis for cell-wall models that has proved to be useful. The model applied consists of two layers one representing the combined middle lamella, primary and secondary S_1 and S_3 layers, and the other representing the S_2 layer.

6.2.2 The layers

For a given moisture content the "combined layer" is fixed in size and composition and is regarded as being a binding layer, while the S_2 fixed in chemical composition, but varying in thickness, is regarded as being entirely responsible for any change in overall thickness or chemical composition. The combined layer consists of an M + P layer and an S_1 plus S_3 layer, lumped together, each of the same thickness but differing in chemical constitution. M + P and S_1 + S_3 thicknesses are generally quoted as being about 10% of the total wall thickness, and in these models, thickness has been set at 10% of the thickness of the median total cell-wall thickness in the sample, i.e. 0.24 μm . To account for the material in the cell corners, which is largely lignin, an extra 50% is added to the M + P thickness to make an equivalent thickness for the M + P of 0.36 μm .

However, the observations of Fengel (1969) on which this model has been based, were made on the variation in cell-wall thickness within an annual ring and not on the variation in earlywood cell-wall thickness from pith to bark, and so some degree of circumspection needs to be exercised here.

In a later publication, Fengel & Stoll (1973), give evidence that supports a model in which the binding layer in earlywood is a constant proportion of the total cell-wall thickness. Again, however, the variation is across an annual ring. This possibility is examined in the later stages of the discussion of shrinkage (Section 8.4).

6.2.3 Lignin in the secondary wall

Fergus, Procter, Scott and Goring (1969) found that for black spruce, lignin concentration is high in the middle lamella, being nearly 100% at the cell corners, and is nearly uniform throughout the secondary wall with a value of 0.22. It can be shown from overall composition values that New Zealand grown Pinus radiata also has a similar lignin concentration, if the model presented here applies, and so this value is accepted as another fixed parameter in the model.

6.2.4 Polysaccharide ratios in the binding layer

The ratios of cellulose to all other polysaccharides given by Meier (1961) for M + P and S_1 in Pinus sylvestris have been adopted as polysaccharide ratios in the M + P and S_1 + S_3 layers. They are 0.355 and 0.615 respectively.

6.2.5 Standard cell diameter

The polysaccharide ratios for the M + P and S_1 + S_3 layers together with the adoption of a figure for the standardised cell diameter, completes the set of fixed parameter required to make the model determinate from chemical and basic density data. The standardised cell diameter has been taken to be 34 μm and represents the mean diameter of a set of New Zealand grown Pinus radiata earlywood specimens measured at the Physics and Engineering Laboratory some years ago (unpublished). The figure is consistent also with the average radial diameter of black spruce earlywood measured by Fergus et al (1969).

6.2.6 The fitted model

Using, for each specimen, the total wall thicknesses as obtained from the ratio (dry weight)/ (dry volume) (derived from basic density) figures for lignin concentration in the M + P layer and cellulose concentration in the S_2 layer have been obtained that give a best fit to the overall chemical composition of the whole sample.

The value deduced for cellulose concentration in S_2 is 0.685 which is to be compared with the figure of 0.665 given by Meier (1961) for Pinus sylvestris. The figure deduced for the lignin concentration in the M + P layer proper (0.69) is greater than that suggested by Fergus et al (1969) (0.50 ..... .60) for black spruce. This may suggest (recalling, Sect. 6.2.2, that the model M + P layer thickness includes an allowance (50%) for the material of the cell corners) that a greater volume should be attributed to the lignin rich cell corners.

The model is summarised in Table 6.2.1.

Table 6.2.1

Layer thicknesses and chemical compositions

	Thickness	Lignin Concentration	Cellulose/hemicellulose
M + P	0.36 μm	0.796*	0.355
$S_1 + S_3$	0.24 μm	0.22	0.615
S_2		0.22	0.685*

* fitted to whole sample chemical data.

The deviation in the lignin and cellulose concentrations of the model, as deduced from the analytical figures supplied, range up to 60% and 45% respectively of the values in the table. These figures reflect the unsatisfactory nature of both the chemical determinations of the specimens and the large likely error in cell-wall thickness (25%) derived from basic density as much as any shortcomings in the model.

Nevertheless, the models derived from the data are sufficiently good to show the individual differences between the "Modulus series" specimens (Fig. 8.8.1).

6.2.7 Microfibril angular distribution

The microfibril-angle distribution in the binding layer has been taken to be that reported by Dunning (1968) for the P, S_1 and S_3 layers. In the model it is represented by a normal distribution of mean angle 70° and standard deviation 12.5°.

The mean angle of the microfibrils in the S_2 layer was measured for each specimen and a normal distribution about this mean angle with a standard deviation equal to one third the mean angle has been assumed, (Cave, 1966 and Okano, 1968).

6.3 Variation of Model Parameters with Moisture Content

Table 6.2.1 refers to the dry state. On the addition of water to wood the volume of the matrix rises by up to 80% and the proportion of matrix in the cell-wall rises accordingly. To account for this volume change, the matrix volume ratio, c^m as a function of moisture content has been calculated according to the following formula,

$$c^m = \left[M/\varrho_m + (M \times mmc)/\varrho_s\right] \Big/ \left[M/\varrho_m + M \times mmc/\varrho_s + C/\varrho_c\right]$$

Where M and C are the dry masses of matrix and cellulose respectively, ϱ_m , ϱ_c and ϱ_s are the densities of matrix, cellulose and water at the matrix moisture content mmc .

The wood moisture content, u , for the model, is obtained from the matrix moisture content, mmc , through the relation

$$u = M \times mmc/(M+C)$$

6.4 General Model for Pith to Bark Tree Sampling - "Average tree"

In actual trees, the basic density and with it cellulose volume ratio increases continuously from the inside to the outside of the tree, while mean microfibril angle shows a converse tendency, the angle being large, 35° - 40°, near the pith dropping steadily to 15°near the 15th annual

growth ring and thereafter being somewhat random in the range 10^{o} - 20^{o} (this for specimens of about 1mm cross section).

The "Average tree" model in Table 6.4.1 is an attempt to represent these structural variations from the pith to the bark. In this model cell-wall thickness varies linearly with the mean microfibril angle. The lower end of the range of wall thickness corresponds to the lowest values found in earlywood specimens extracted from the wide growth rings near the pith, of locally grown Pinus radiata. The upper end intentionally represents a value somewhat higher than would be found in pure earlywood material from near the bark. The value in the table corresponds to a basic density of 0.42 and represents a 20% admixture of latewood (characteristics taken from one set of data given by Cousins (1972)). A specimen nominally designated earlywood from near the bark, would contain some latewood as the growth rings there are too narrow to extract pure earlywood specimens of 2 x 2 mm cross-section. Such an admixture of latewood was probably present in the experimental specimens whose behaviour is summarised later in Fig. 8.2.1.

Table 6.4.1.

"Average tree" model

Relative S_2 layer thickness

Microfibril Angle S_2 layer	Moisture Content %						
	0	5	10	15	20	25	30
10°	.800	.795	.790	.785	.781	.777	.773
15°	.758	.752	.746	.741	.736	.731	.727
20°	.716	.709	.703	.697	.691	.687	.682
25°	.674	.667	.660	.653	.648	.642	.638
30°	.632	.624	.617	.610	.602	.599	.594
35°	.590	.582	.575	.568	.561	.556	.551

Volume Ratio								
	S_2 layer	.466	.492	.518	.542	.565	.585	.604
	Binding layer	.766	.785	.802	.817	.831	.843	.853

"Average tree" relative wall layer thickness, and cellulose volume ratio in the wall layers as functions of mean microfibril angle and moisture content.

References

Cave, I.D. 1966. X-ray Measurement of Microfibril Angle. For. Prod. J. 16 : 37-42.

Cousins, W.J. 1972. Some Physical Processes involved in Deformation and Fracture. Ph. D. thesis, Victoria University of Wellington, Wellington, New Zealand.

Dunning, C.E. 1968. Cell-wall Morphology of Longleaf Pine Latewood. Wood Sci. 1 : 65-76.

Fengel, D. 1969. Ultrastructure of Cellulose from Wood. Part 1 : Wood as the Basic Material for the Isolation of Cellulose. Wood Sci. Technol. 3 : 203-217.

_____, Stoll, M. 1973. Uber die Veranderungen des Zellquerschnitts, der Dicke der Zellwand, und der Wandschichten von Fichtenholz-Tracheiden innerhalb eines Jahrringes. Holzforschung. 27 : 1 - 7.

Fergus, B.J., Proctor, A.R., Scott, J.A.N., Goring, D.A.I. 1969. The Distribution of Lignin in Sprucewood as determined by Ultraviolet Microscopy. Wood Sci. Technol. 3 : 117-138.

Meier, H. 1961. The Distribution of Polysaccharides in Wood Fibres. J. Polym. Sci. 51 : 11-18.

Okano, T. 1968. The Relationship between Micelle Angle and X-ray Diffraction Diagrams. J. Wood Res. Soc. J. 14 : 358-362.

Chapter 7

SHEAR MODULUS OF THE MATRIX

7.1 Model for the Matrix

Values for the shear modulus of the matrix have been deduced by adjusting the shear modulus used in predicting the longitudinal Young's modulus until the predicted and experimental longitudinal Young's moduli of the specimens have agreed. The "Modulus series" of specimens were used for this purpose. The computation of longitudinal Young's modulus has been carried out using the methods and equations developed in Chapter 4. Moisture content remains approximately constant during a Young's modulus test so that Δu in the equation for layer stress (Eq. 4.5.1) is zero. An external longitudinal tensile force (represented by setting $\sigma_1' = \sigma_2' = 0$ in the layer force summation, section 4.5.6) is applied to deform the specimen. The longitudinal Young's modulus is then predicted by the ratio of the applied stress, σ_3', to the consequent longitudinal strain, ε_3'.

The shear modulus of the matrix, S, appears in the equations for composite stiffnesses (Eq. 4.6.1 - 4.6.4) as m_2 and indirectly through the other non-independent matrix constants k_2, ℓ_2, n_2, μ_2. (Matrix elasticity is discussed below.)

The structural data for each specimen enters the equations in the form of,

(i) cellulose concentration, which is applied to the computation of composite stiffnesses (Eq. 4.6.1 - 4.6.4) and the computation of layer stresses (Eq. 4.5.1);

(ii) layer thicknesses, which are required to convert the layer stresses for forces for the force equilibrium summation over the layers (Section 4.5.6).

The shear modulus of the matrix has been deduced from the longitudinal Young's moduli determined for a range of moisture content values to derive a relation between the shear modulus of the matrix and its moisture content for each separate specimen.

To obtain a one to one relationship between the shear modulus of the matrix and the longitudinal Young's modulus of the specimen, it is necessary, even given all the relevant parameters other than the elastic constants of the matrix, to make some assumptions about the nature of the matrix.

Even if one assumes that the matrix is elastically isotropic one needs to assume some value for the bulk modulus in order to determine the shear modulus. However, the bulk modulus does not vary greatly between materials of similar type, for instance the bulk modulus of water is 220 kp/mm^2*, ice IV 800 kp/mm^2 and polystyrene 300 kp/mm^2.

In fact it may be reasonable to assume that the bulk modulus of the matrix

---

* Note on units : Kiloponds (or kilograms-weight) per square millimeter (kp/mm^2) have been used throughout as the units of stress and stiffness. It is a unit widely used in the field of wood mechanics and is of convenient magnitude. It is equivalent to 9.81×10^6 pascals in the S I system.

does not vary with moisture content.

Barkas (1949) provides the only estimates known to the author of the bulk modulus of wood substance. He estimated it to be approximately 1000 kp/mm^2 across the whole moisture content range. The slight variation that he did observe ran contrary to expectation, the wood being more compressible in the dry state than in the wet and he concluded that this result was false.

If one assumes that the cellulose is relatively incompressible compared with the matrix then Barkas' value for entire wood-substance would suggest a bulk modulus for the matrix of approximately 500 kp/mm^2. This is compatible with the values quoted for water and ice and it is probably reasonable to compare the matrix with them since the interchain bonding of the matrix is similar to that of the inter-molecular bonding in water and ice.

Accordingly, the bulk modulus of the matrix is taken to be 500 kp/mm^2 across the whole moisture content range.

A lower limit, set by the experimental data is discussed in Section 7.3.

7.2 Derivation of the Shear Modulus Function of the Matrix

Using the model of the matrix just discussed six out of the twelve "Modulus series" model specimens gave plausible values for matrix shear modulus over the whole moisture content range (Fig. 7.2.1). The models showed an

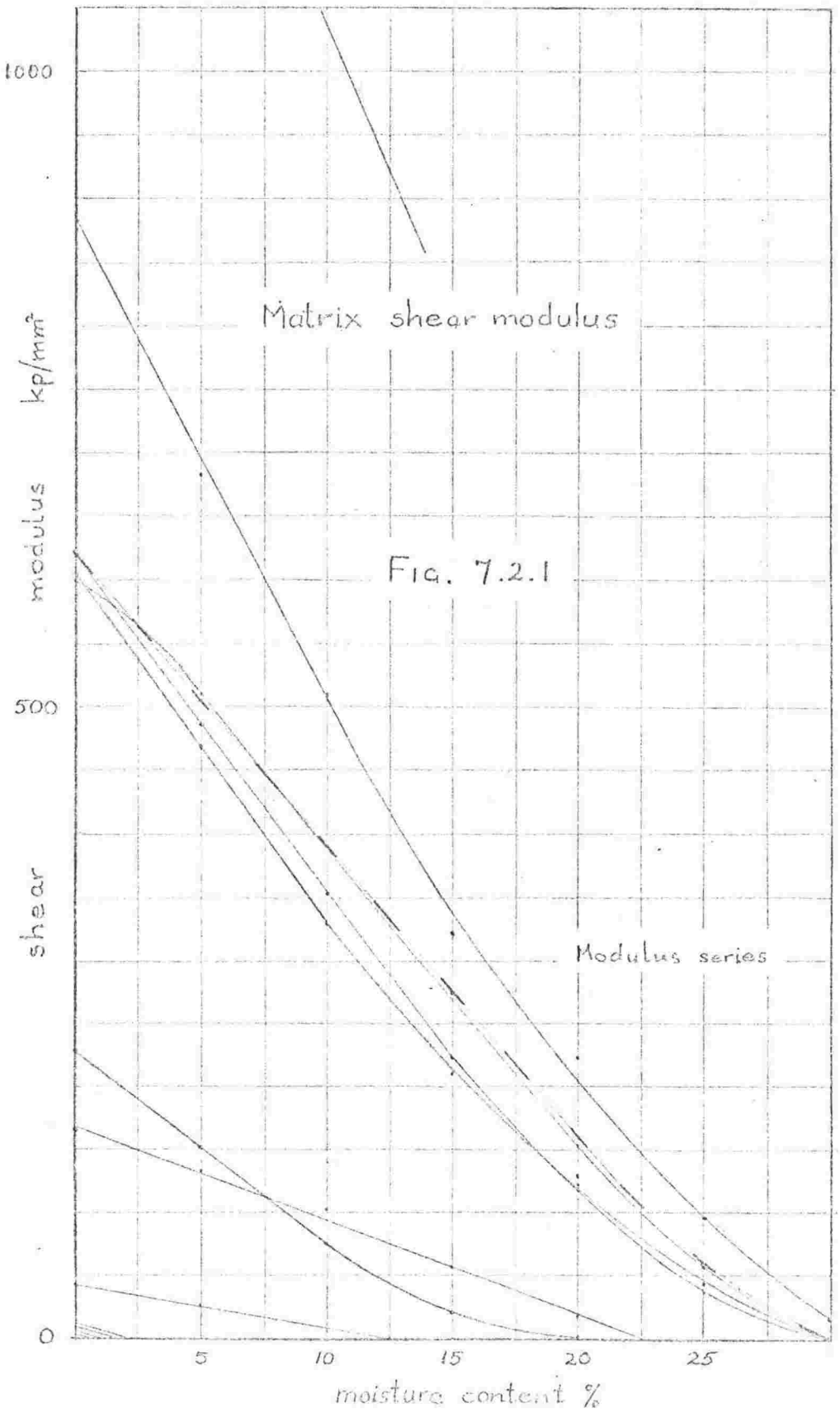
1000
500
0
shear modulus kp/mm²
Matrix shear modulus
Modulus series
5
10
15
20
25
moisture content %

Fig. 7.2.1

approximately linear relationship between shear modulus and moisture content and thereafter a rate of fall of shear modulus decreasing with increasing moisture content. The unsatisfactory specimens gave either very low values (less than 40 kp/mm^2) or very high values (greater than 1500 kp/mm^2) in the dry state and have been rejected as unrealistic. The large variance in shear modulus arises from the sensitivity of this property to the longitudinal Young's modulus of the wood substance, basic density and chemical composition, all of which have substantial uncertainties. Typical or expected errors in these values are shown in table 7.2.1 together with the associated errors in matrix shear modulus.

Table 7.2.1

Error estimates for shear modulus of the matrix, S.

	Typical expected error	Consequent error in S kp/mm^2
Young's modulus	+10%	+900
Basic density	-10%	+1900
Cellulose concentration	+10%	-520

Calculated error in the shear modulus of the matrix, S for a typical specimen in the dry state, arising from typical or expected errors in longitudinal Young's modulus, basic density and cellulose composition ratio.

Three of the specimens in the sample gave nearly identical results and a function for matrix shear modulus versus moisture content close to these

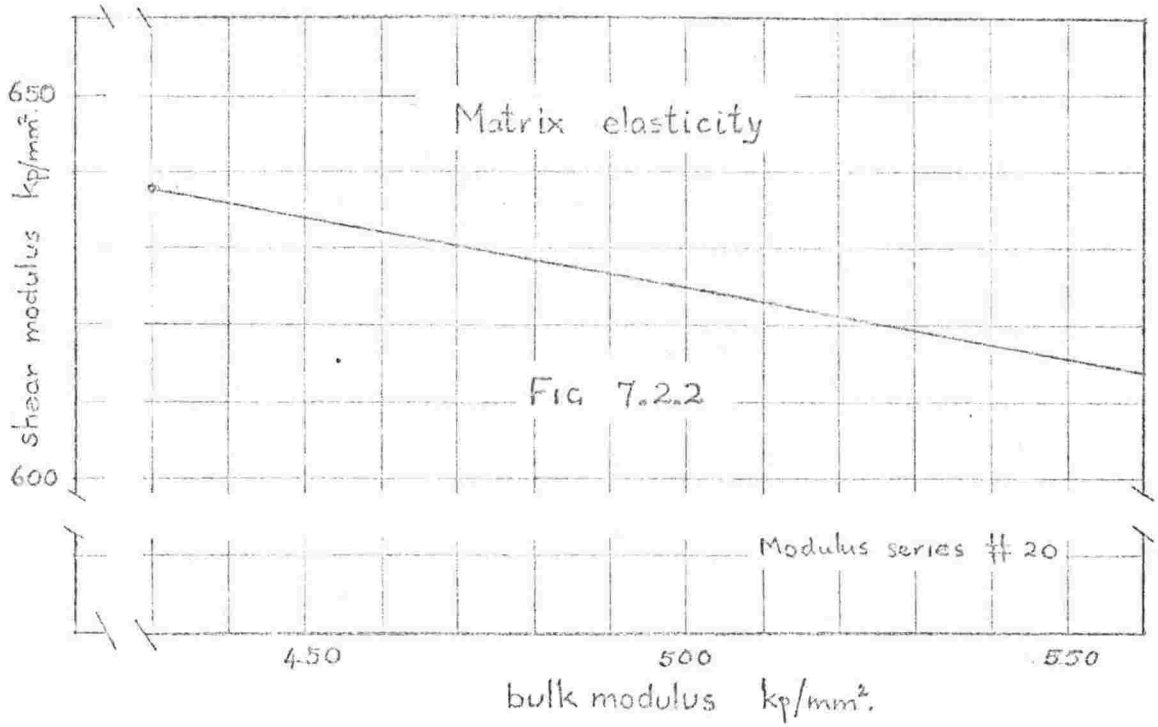
Matrix elasticity
650
600
shear modulus kp/mm²
Modulus series # 20
4.50
500
550
bulk modulus kp/mm².

Fig 7.2.2

has been chosen (Fig. 7.2.1 - dashed line).

Barkas' (1949) figures for wood-substance shear modulus suggest values of matrix shear modulus of approximately 560 and 80 kp/mm^2 at 10% and 90% relative humidity respectively, on the assumption that the cellulose is rigid and comprises 50% of the wood volume. The corresponding values for the model matrix (the dashed line in Fig. 7.2.1) are 550 and 110 kp/mm^2, which makes a satisfactory comparison.

The sensitivity of shear modulus to variation in bulk modulus is small. The relationship for one typical specimen of the experimental set is shown in Fig. 7.2.2.

7.3 Bounds to the Bulk and Shear Moduli of the Matrix

Love (1944) has stated that there is no isotropic substance possessing a negative Poisson's ratio, ν, even though theoretical limits allow negative values ($-1 < \nu < 0{\cdot}5$). Perusal of the Landolt-Börnstein tables also, indicates no negative value in any other symmetry system. If one accepts that the Poisson's ratio of the matrix is always positive, then the experimental data places limits on both the bulk modulus, k, and the shear modulus, S, of the matrix. If Poisson's ratio,

$$\nu = -s_{12}/s_{11} = c_{12}/(c_{11} + c_{12}),$$

is to be positive then c_{12} must be positive. It can be seen for the specimen depicted in Fig. 7.2.2 that,

$$c_{12} = k - 2S/3,$$

can be positive only if k is greater than about 430 kp/mm^2 and S is less than about 640 kp/mm^2.

The upper limit to the bulk modulus set by the condition that,

$$\nu < 0{\cdot}5, \qquad (S>0),$$

is so large, about 4,000 kp/mm^2, that it would appear to be of little significance.

References

Barkas, W.W. 1949. The Swelling of Wood under Stress. London. His Majesty's Stationery Office.

Landolt-Börnstein. 1969. Numerical Data and Functional Relationships in Science and Technology, Group III, Vol 2. Berlin-Heidelberg : Springor-Verlag.

Love, A.E.H. 1944. A Treatise on the Mathematical Theory of Elasticity. New York: Dover Publications.

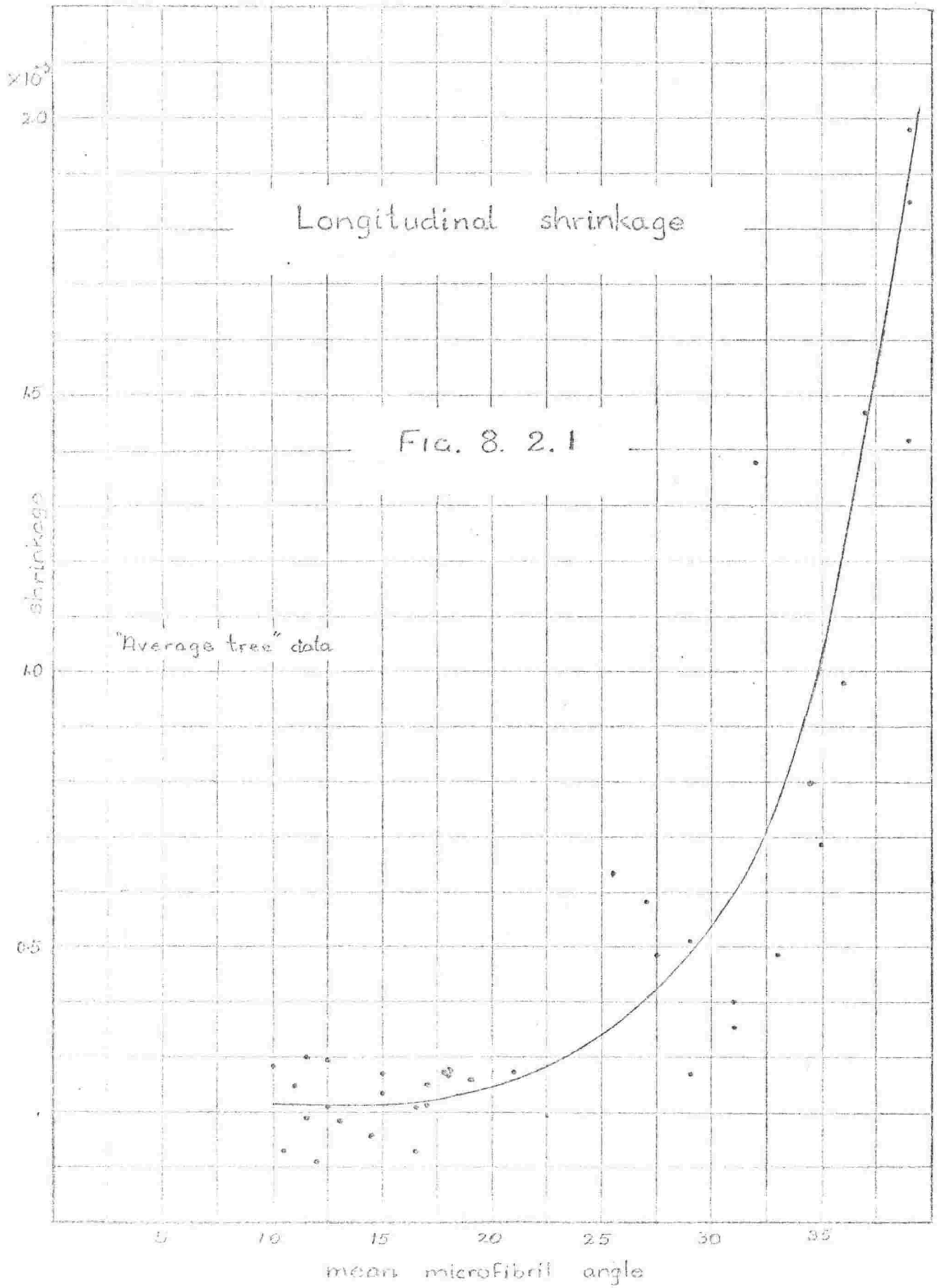
Longitudinal shrinkage
×10⁻³
2.0
1.5
1.0
0.5
shrinkage
"Average tree" data
5
10
15
20
25
30
35
mean microfibril angle

Fig. 8. 2.1

Chapter 8

MODEL SHRINKAGE

8.1 Introduction

So far, we have set up models for wood structure and for matrix behaviour and have chosen values for material constants. We are now in a position to test the models against independent data, (the shrinkage data). It will quickly become apparent that the models proposed so far are inadequate and that further development of the matrix model in particular will be necessary.

8.2 Model of Sorption in the Matrix

8.2.1 Isotropic sorption

Data collected over the years at Physics and Engineering Laboratory is illustrated in Fig. 8.2.1 where the total longitudinal shrinkage is plotted against its mean microfibril angle. The model structure proposed in table 6.4.1 and designated "Average tree" is intended for comparison with this data. The theoretical longitudinal shrinkages have been computed in much the same way as that described in Section 7.1 for the longitudinal Young's modulus. In this case Δu is not zero, and there are no externally applied forces. The differential longitudinal shrinkage is given by ε_3' when the procedures of Sections 4.5.1-4.5.6 and Section 4.6 have been followed and the relevant equations have been solved under these

conditions. Total shrinkage is obtained by integrating the strains $\varepsilon_z', \varepsilon_3'$ over moisture content starting from the moisture content of the stress free state, and integrating towards both ends of the moisture content scale (e.g. see Fig. 8.6.1).

Using the "Average tree" structure and the provisional isotropic matrix sorption model (given in table 5.2.1) and assuming the stress free state to be at zero moisture content we obtain the relationship between longitudinal shrinkage and mean microfibril angle that is shown in Fig. 8.2.2. Comparison of Figs 8.2.1 and 8.2.2 shows clearly that the shrinkages predicted are overestimated by about a factor of seven. Setting the 'stress free state' to some value higher than zero moisture content makes the situation worse. (Compare Figs. 8.6.1 and 8.6.3)

Cave (1972) has shown that only small adjustments of magnitude can be achieved by manipulating values of matrix stiffness, binding layer thickness and cellulose composition ratio within reasonable limits and so it is necessary to look to other factors to explain the discrepancy.

8.2.2 Anisotropic sorption

The most obvious idea that comes to mind that might reduce longitudinal shrinkage is that moisture up-take in the cell-wall is anisotropic. If the matrix is structured with its polysaccharide chain direction associated with the cellulose microfibril direction, then it could be expected that more swelling would take place in the transverse direction than in the chain direction. This would result in lower longitudinal swelling stress

and consequent lower longitudinal strain.

To accommodate this idea the swelling matrix, $\bar{\varepsilon}^{\circ}$, could be written,

$$\left[\bar{\varepsilon}^{\circ}\right] = \begin{bmatrix} n \\ n \\ 1 \end{bmatrix} \frac{1}{2n+1} \cdot \frac{\Delta V}{V} \quad , \qquad (1)$$

where the scalar $\Delta V/V$ is taken from Table 5.2.1 and n is the anisotropic swelling factor. It turns out, however, that the swelling stress is not greatly influenced by swelling represented in this form because the non-diagonal matrix stiffnesses, C_{12}^{m} , are of considerable magnitude and so little difference between the axial and transverse components of the swelling stress, $c^{m} C^{m} \Delta \bar{\varepsilon}^{\circ}$, can be generated.

For example, the matrix stiffnesses in the dry state have been taken to be,

$$C_{11}^{m} = 1326.7 \text{ kp/mm}^2 \quad \text{and} \quad C_{12}^{m} = 86.7 \text{ kp/mm}^2$$

which for an anisotropy factor of 5 leads to a ratio between the longitudinal and transverse components of the swelling stress, $c^{m} C^{m} \Delta \bar{\varepsilon}^{\circ}$, of 1:3 and, towards the wet state the values of C_{12}^{m} and C_{11}^{m} approach each other so that the stress ratio tends to unity at saturation. Even an anisotropy factor of 50 is not sufficient to explain the difference between computed and observed longitudinal strains.

It is apparent that transverse swelling leads to considerable longitudinal stress under this scheme, and it is necessary to find some way of decoupling these quantities.

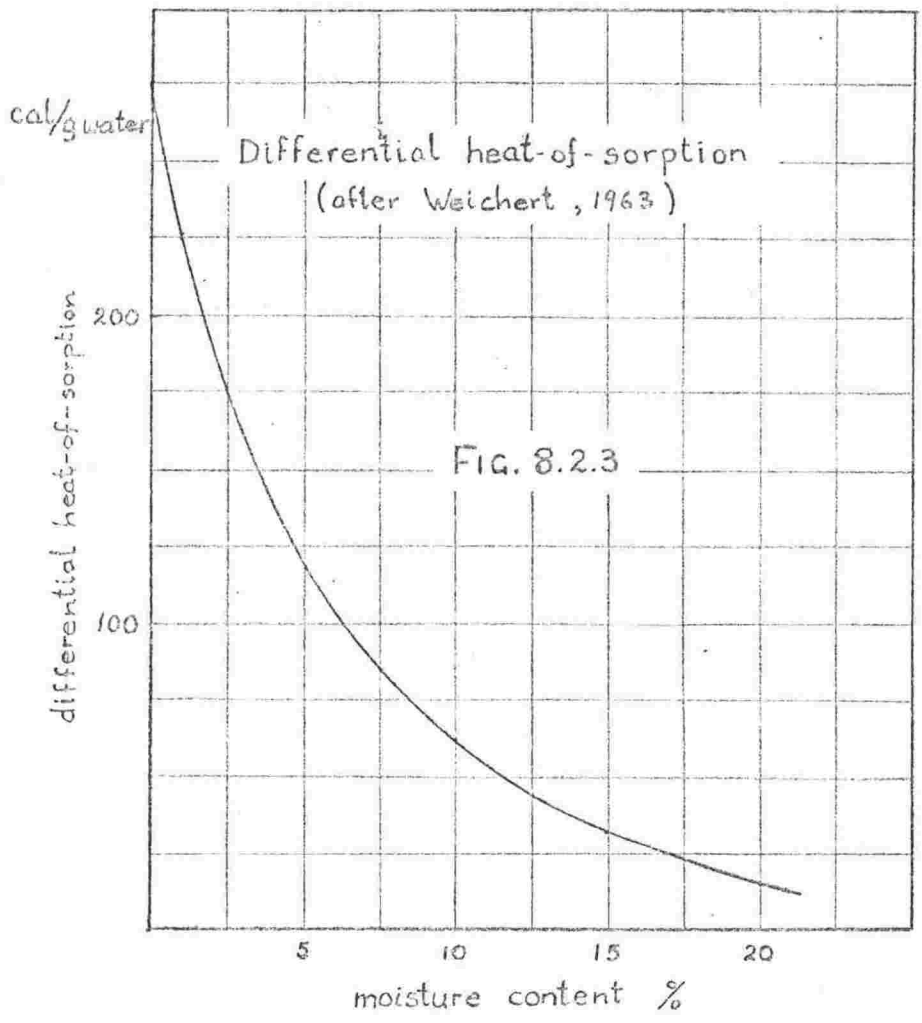
cal/g water
Differential heat-of-sorption
(after Weichert, 1963)
differential heat-of-sorption
200
100
5
10
15
20
moisture content %

FIG. 8.2.3

8.2.3 Interlamella water

The lamella structure of the cell-wall suggests a means whereby this decoupling could be achieved.

Suppose that the water is sorbed on two different types of sites, as is commonly taken to be the case (Smith, 1947; Hailwood and Horobin, 1946), and suppose further that each type occurs in definite regions of the cell-wall. Sorption within the matrix has already been considered, and, it might reasonably be argued that the interlamella regions could provide an alternative site for water sorption. Very little reaction against the lamellae would result from interlamella sorption since water could be accommodated merely by the radial displacement of the inert lamellae relative to one another as the cell-wall swelled. With the interlamella bonding being relatively week (Stamm, 1964) it could be expected that the interlamella waterbonding energy is lower than that in the matrix so that sorption on to matrix sites would take preference over sorption onto interlamella sites, at the lower moisture contents. This would be in accord with differential heat-of-sorption patterns, (e.g. Fig. 8.2.3), and would lead one to expect that mechanical effects dependent on swelling within the plane of the cell-wall would take place at lower moisture contents (e.g. moisture induced deformation, Armstrong and Kingston, 1962, longitudinal shrinkage, Meylan, 1972, see Fig. 8.10.1), while the bulk of the swelling in wall thickness would take place towards the higher moisture contents.

Because the water absorbed in the interlamella regions is virtually mechanically inert its presence can be ignored in computations of

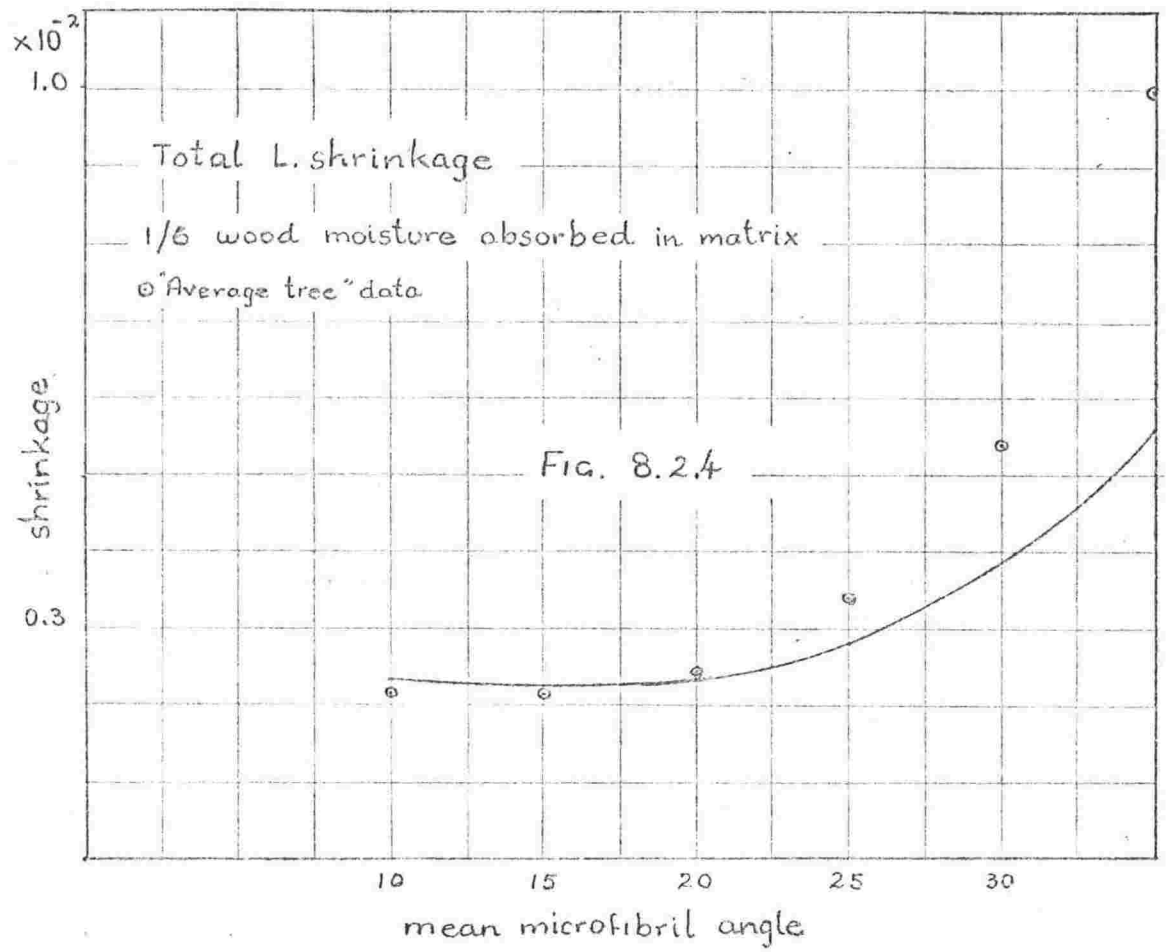
×10⁻²
1.0
Total L. shrinkage
1/6 wood moisture absorbed in matrix
⊙ "Average tree" data
shrinkage
0.3
10
15
20
25
30
mean microfibril angle

FIG. 8.2.4

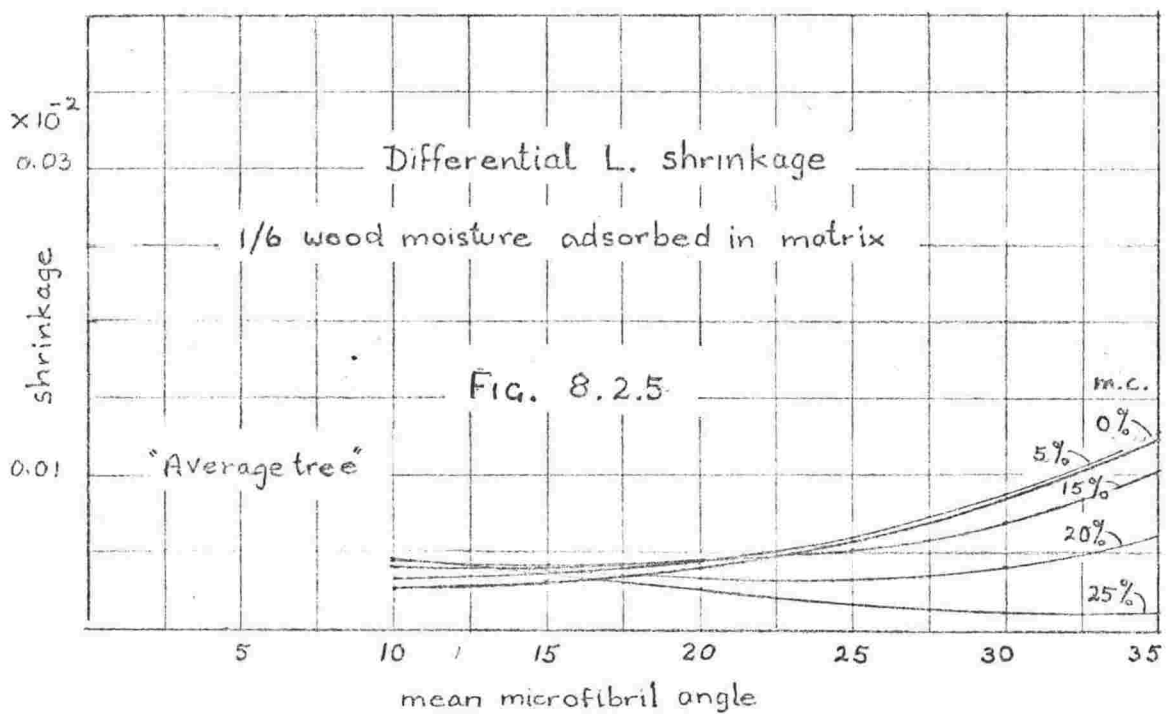
Differential L. shrinkage
1/6 wood moisture adsorbed in matrix
"Average tree"
shrinkage
x10⁻²
0.03
0.01
m.c.
0%
5%
15%
20%
25%
5
10
15
20
25
30
35
mean microfibril angle

Fig. 8.2.5

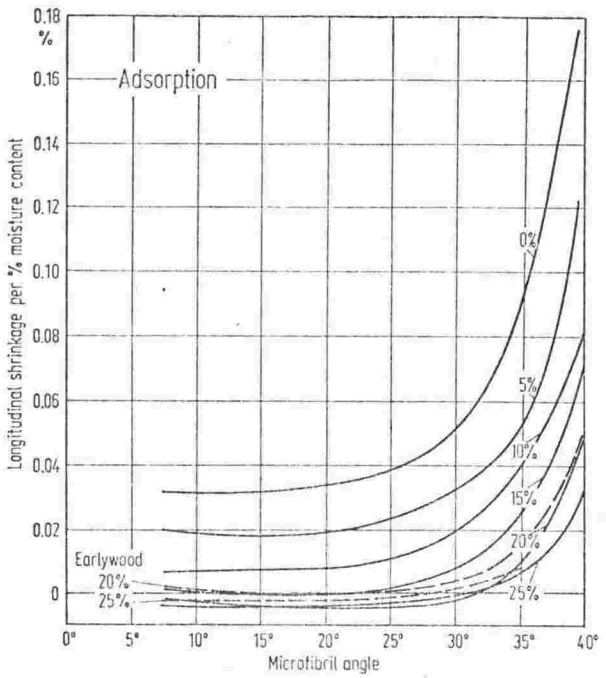

The relationship between incremental longitudinal shrinkage during absorption and microfibril angle for moisture contents between 0 and 25%. The broken lines indicate earlywood shrinkage at moisture contents of 20% and 25%

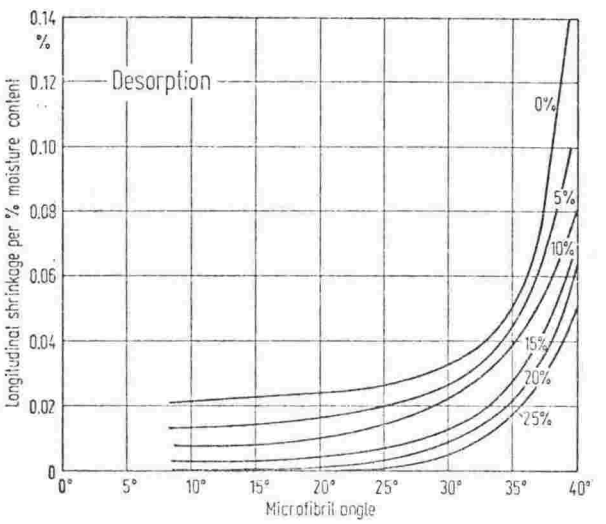

The relationship between incremental longitudinal shrinkage and microfibril angle during desorption for moisture contents between 0 and 25%

FIG. 8.2.6

[After Meylan (1972)]

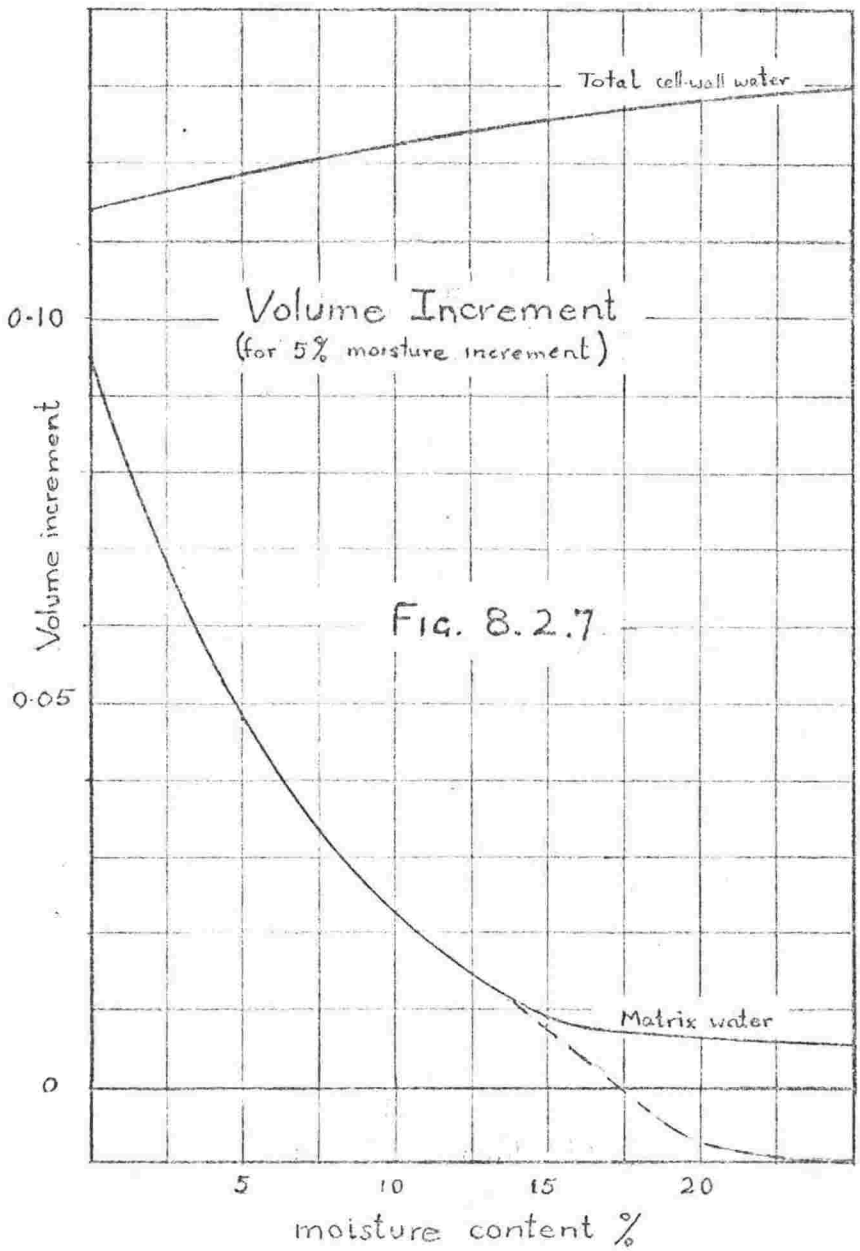
Total cell-wall water
Volume Increment
(for 5% moisture increment)
0·10
0·05
0
Volume increment
Matrix water
5
10
15
20
moisture content %

FIG. 8.2.7

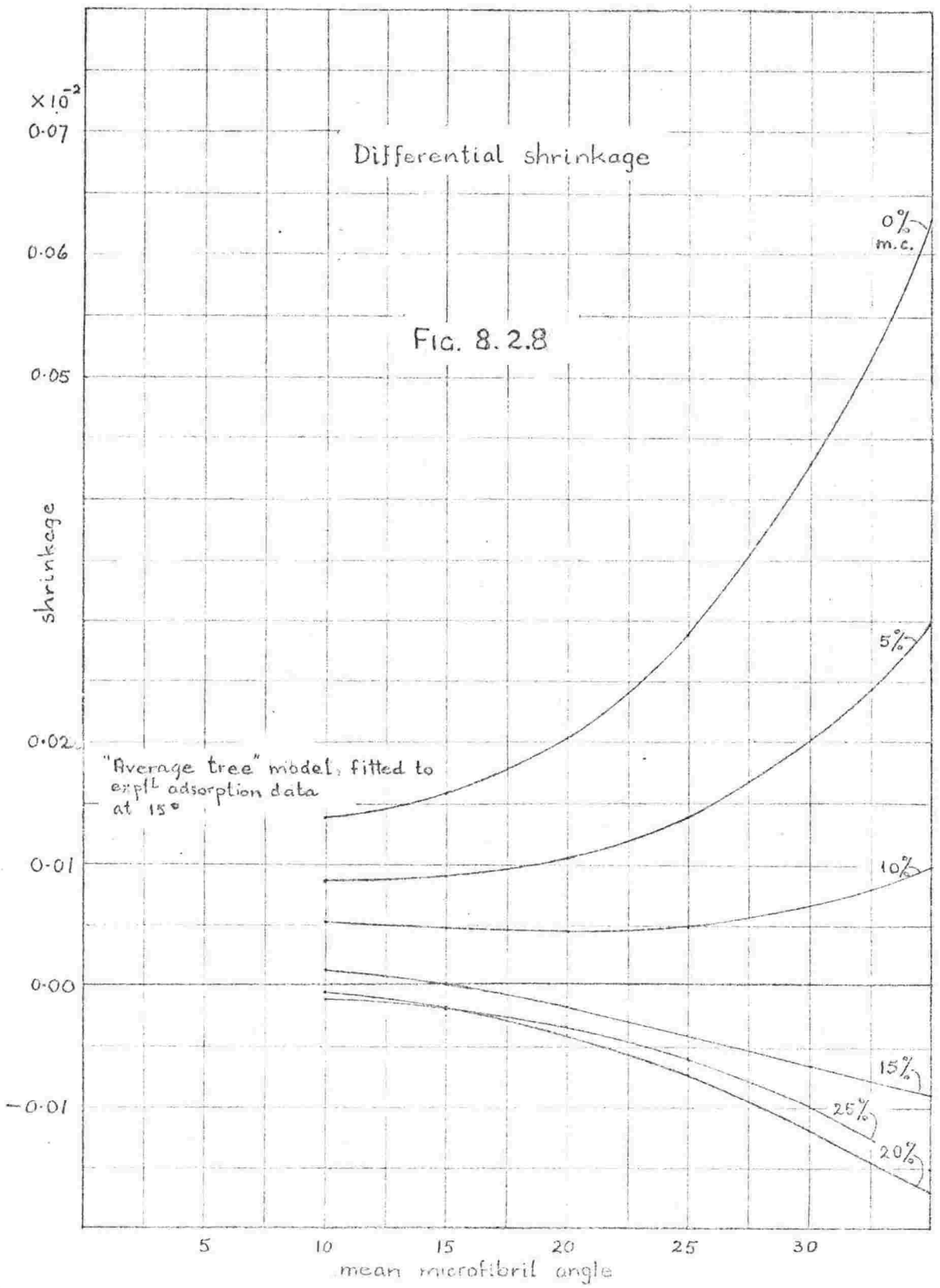
Differential shrinkage
FIG. 8.2.8
$\times 10^{-2}$
0·07
0·06
0·05
0·02
0·01
0·00
−0·01
shrinkage
0% m.c.
5%
10%
15%
25%
20%
"Average tree" model, fitted to expt^L adsorption data at 15°
5
10
15
20
25
30
mean microfibril angle

longitudinal shrinkage. It was found that one sixth of the water taken up by the wood as a whole was required to be present in the matrix to produce the observed total longitudinal shrinkage. The result for the "Average tree" is shown in Fig. 8.2.4.

8.2.4 Matrix water

Looking at the differential longitudinal shrinkages (shrinkage increments corresponding to 5% increment in moisture content, calculated in the manner related in Section 8.2.1) for the "Average tree" with one sixth of the total water residing in the matrix (Fig. 8.2.5) and comparing them with figures published by Meylan (1972), (reproduced in Fig. 8.2.6), it is apparent that the theoretical, low angle differential shrinkages at low moisture-contents are too small while at high moisture-contents they tend to be too large. If the moisture-content increments (Table 5.2.1) are adjusted so that the differential shrinkages at a microfibril angle of 15^{o} correspond to Meylan's adsorption figures then the "Average tree" model gives the results shown in Fig. 8.2.8. The required moisture content increments are shown in Fig. 8.2.7 (dotted line) with the total moisture increment for whole wood for comparison. It can be seen that negative increments in the matrix are required at high moisture contents which does not seem very credible,

Table 8.2.1

Sorption by the matrix

Moisture Content %	0	5	10	15	20	25	30
Sorbed Moisture Vol. (1)	0	0.095	0.143	0.166	0.175	0.182	0.187

(1) Sorbed water volume in matrix expressed as a fraction of dry matrix volume.

and so the full line shown in the figure has been arbitrarily adopted as the matrix sorption property (Table 8.2.1). This line conforms with the differential heat-of-sorption data of Weichert (1963), Fig. 8.2.3. The new line strictly requires adjustment in overall magnitude to make the total amount of water (given by the area contained beneath the line) equal to that of the original curve. The error has the effect of raising the total shrinkage at a microfibril angle of 15^{o} above the "Average tree" value to which the original sorption curve was fitted (see Fig. 8.2.10) and is the reason for the correction factor shown in Fig. 8.8.1. Considering more important refinements required in other matters such as in the deduction of the shear modulus of the matrix from the longitudinal Young's modulus data it was not felt worthwhile to make corrections for this error at this stage. Work to refine the models of the shear modulus and the sorption properties of the matrix is continuing and these points will be dealt with in due course.

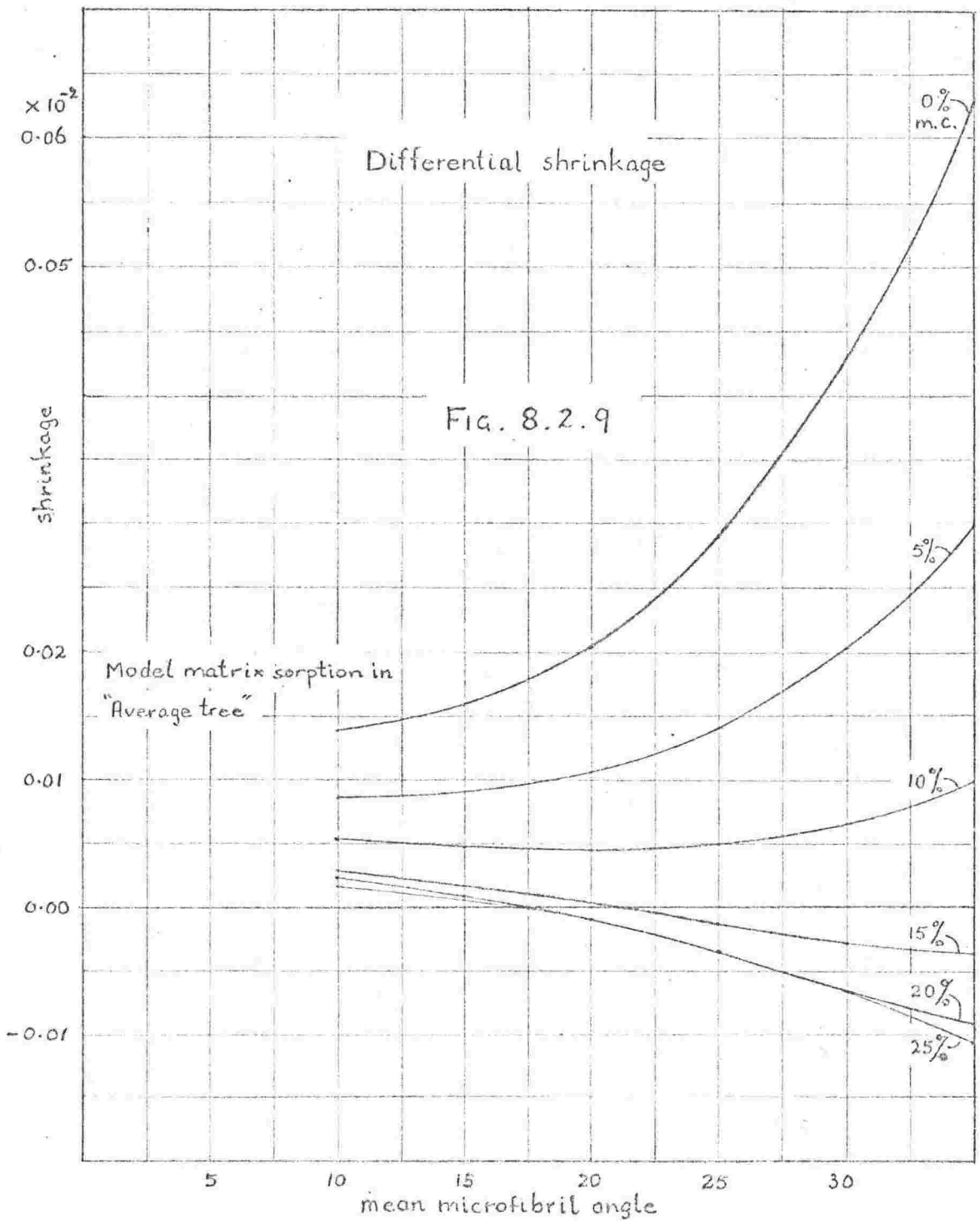
Differential shrinkage
Fig. 8.2.9
Model matrix sorption in "Average tree"
shrinkage
× 10⁻²
0·06
0·05
0·02
0·01
0·00
-0·01
0% m.c.
5%
10%
15%
20%
25%
5
10
15
20
25
30
mean microfibril angle

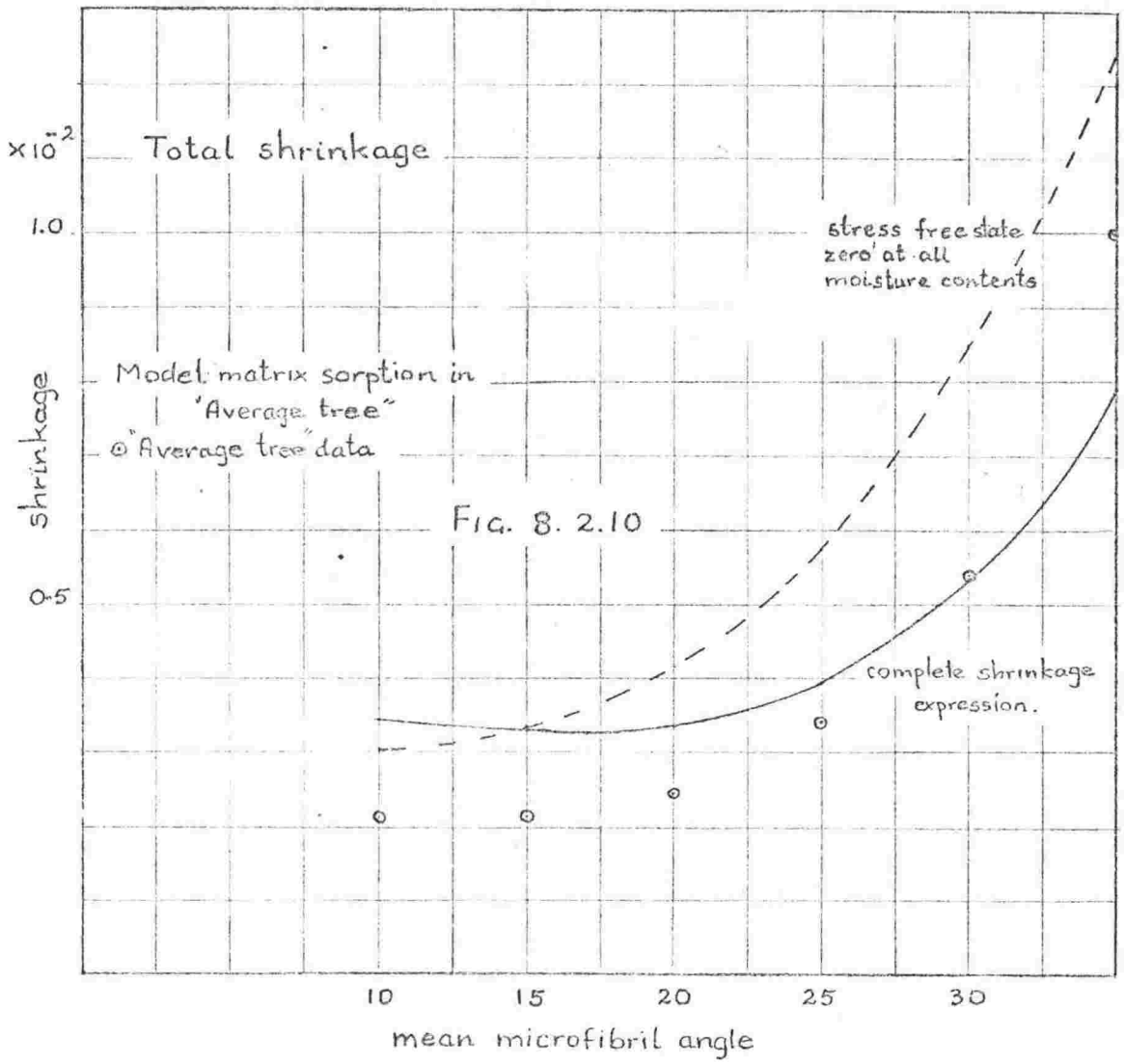
Total shrinkage
×10⁻²
1.0
0·5
shrinkage
stress free state zero at all moisture contents
Model matrix sorption in "Average tree"
⊙ "Average tree" data
complete shrinkage expression.
10
15
20
25
30
mean microfibril angle

FIG. 8.2.10

According to the model, at the dry state most of the moisture is taken up into the matrix (84%) while in the saturated condition very little of the moisture increment (< 5%) goes into the matrix, as was anticipated earlier. At saturation, 25% of the total wood moisture is to be found in the matrix. The shape of the moisture-increment plot for the matrix component of cell-wall water and the total amount sorbed in the matrix at saturation (7.0 - 7.5% mc.) corresponds closely with that quoted widely for "Langmuir adsorption" in wood (Smith, 1947; Skaar, 1972).

Returning now to the consideration of the differential shrinkage plots, the adoption of this new matrix sorption relation in the "Average tree" model, (using the prescriptions in Sections 7.1 and 8.2.1), Fig. 8.2.9, leads to only a slight improvement in the gross negative deviation of the high angle, high moisture content differential shrinkages, from the observed values. This negative-going is caused by the increasingly large contributions made by the compliance change component, $c^m \Delta C^m (A^m \bar{\varepsilon} - \bar{\varepsilon}^o)$, of the internal stress as moisture content and strain increase, while the swelling stress component steadily decreases. Since total shrinkage at high angle is falling behind observation it seems likely that the compliance change component is contributing too much to the internal stress. Without the compliance change term, total shrinkage follows the dashed curve in Fig. 8.2.10 and the high angle shrinkage is in good agreement with practice. (The mismatch at 15^o microfibril angle between the "Average tree" data and the theoretical shrinkages is due to the introduction of the positive matrix moisture-content increments at high moisture contents as noted above.)

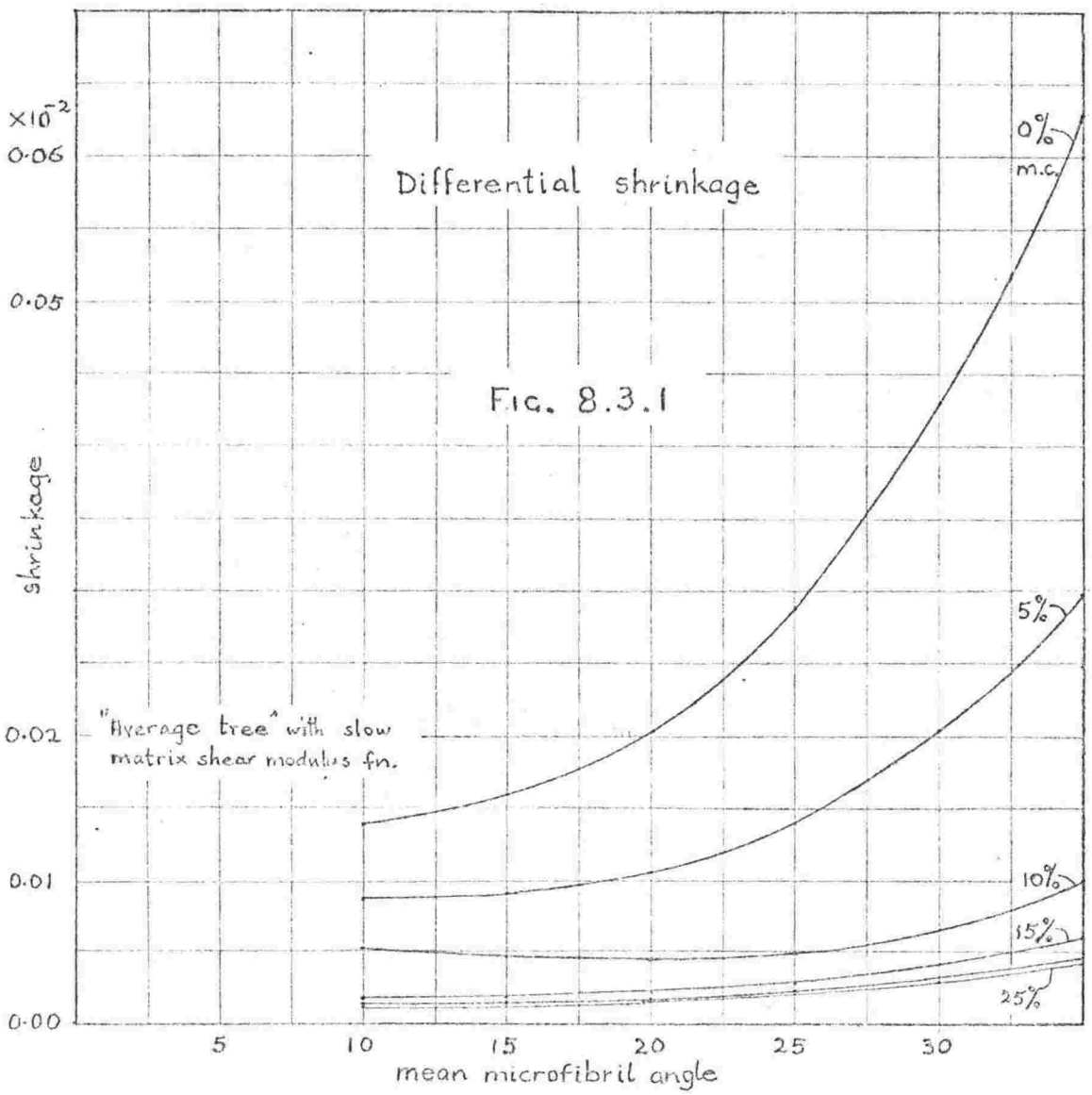
Differential shrinkage
Fig. 8.3.1
shrinkage
×10⁻²
0·06
0·05
0·02
0·01
0·00
"Average tree" with slow matrix shear modulus fn.
0% m.c.
5%
10%
15%
25%
5
10
15
20
25
30
mean microfibril angle

8.3 Stiffness of the Matrix

The magnitude of the compliance change term is dependent on the size of the decrement (for adsorption) in matrix stiffness as well as total strain, and, if the matrix shear modulus were to tail off rather more slowly than it does in Fig. 7.2.1, then the compliance change term would be reduced at high moisture contents. The effect is illustrated in Fig. 8.3.1, for a model in which the shear modulus of the matrix follows the regular course (dashed line in Fig. 7.2.1) until reaching a steady value of 275 kp/mm^2 at 15% moisture content and above. The general pattern of differential shrinkage now agrees with that observed except that it would not be possible to produce the small negative shrinkages observed by Meylan for adsorption between 10^o and 30^o by manipulating moisture increments or matrix shear modulus. The figure as it stands corresponds quite well with Meylan's desorption curves.

The larger proportion of the wood moisture content that has been assigned to the interlamella regions (Section 8.2.4) of the cell-wall is virtually discounted from a mechanical point of view and this has important implications for the matrix shear modulus function. To be compatible it should now be recalculated making appropriate allowance for the new matrix model in the area correction factors. If this is done, the cross-section changes produced by moisture content increase will be reduced and the shear modulus function will fall less steeply, in line with the requirements just discussed.

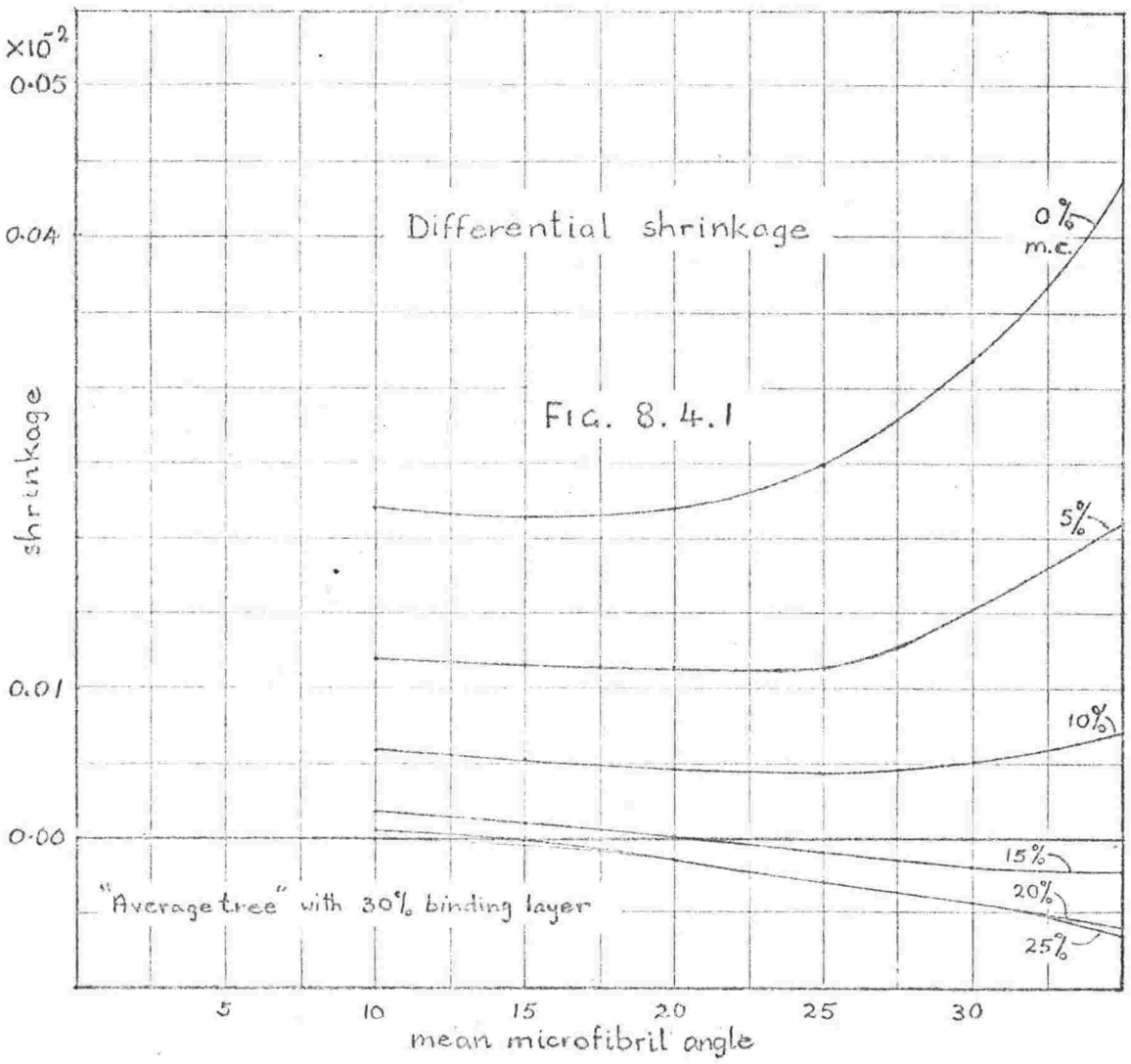
×10⁻²
0·05
0·04
0·01
0·00
shrinkage
Differential shrinkage
0% m.c.
5%
10%
15%
20%
25%
"Average tree" with 30% binding layer
5
10
15
20
25
30
mean microfibril angle

FIG. 8.4.1

8.4 Cell-wall Structure

The differential shrinkage curve shapes can be influenced quite strongly by the size of the binding layer. By increasing the binding layer of the "Average tree" model from 20% to 30% of the total wall thickness at a microfibril angle of 10^{o} and leaving the binding layer substantially unchanged (30%) at a microfibril angle of 25^{o} calculations made from the prescription of Section 8.2.1 agree better with the experimental adsorption curve, (Fig. 8.4.1). It is likely, therefore, that the variation of model wood structure with basic density that was postulated in Section 6.2 is not suitable and that the actual size of the binding layer varies with total wall thickness rather than remaining constant. This is in accord with more recent observations on the cross-sections of fresh material (Fengel and Stoll, 1973) in which the components of the binding layer are shown to be nearly a constant proportion (~15%) of the total cell-wall thickness as total cell-wall thickness varies across an annual ring.

8.5 Multiple Factor Influences

From the preceding sections in this chapter it seems likely that no single factor in the model set up at the start of this investigation is entirely responsible for the deviation between model shrinkage and observation. It is certain that the matrix sorption must fall in a somewhat exponential manner as shown in Fig. 8.2.6 and it then seems likely that the matrix shear modulus must fall more slowly at high moisture contents than the function deduced from Young's modulus data, in order to avoid large

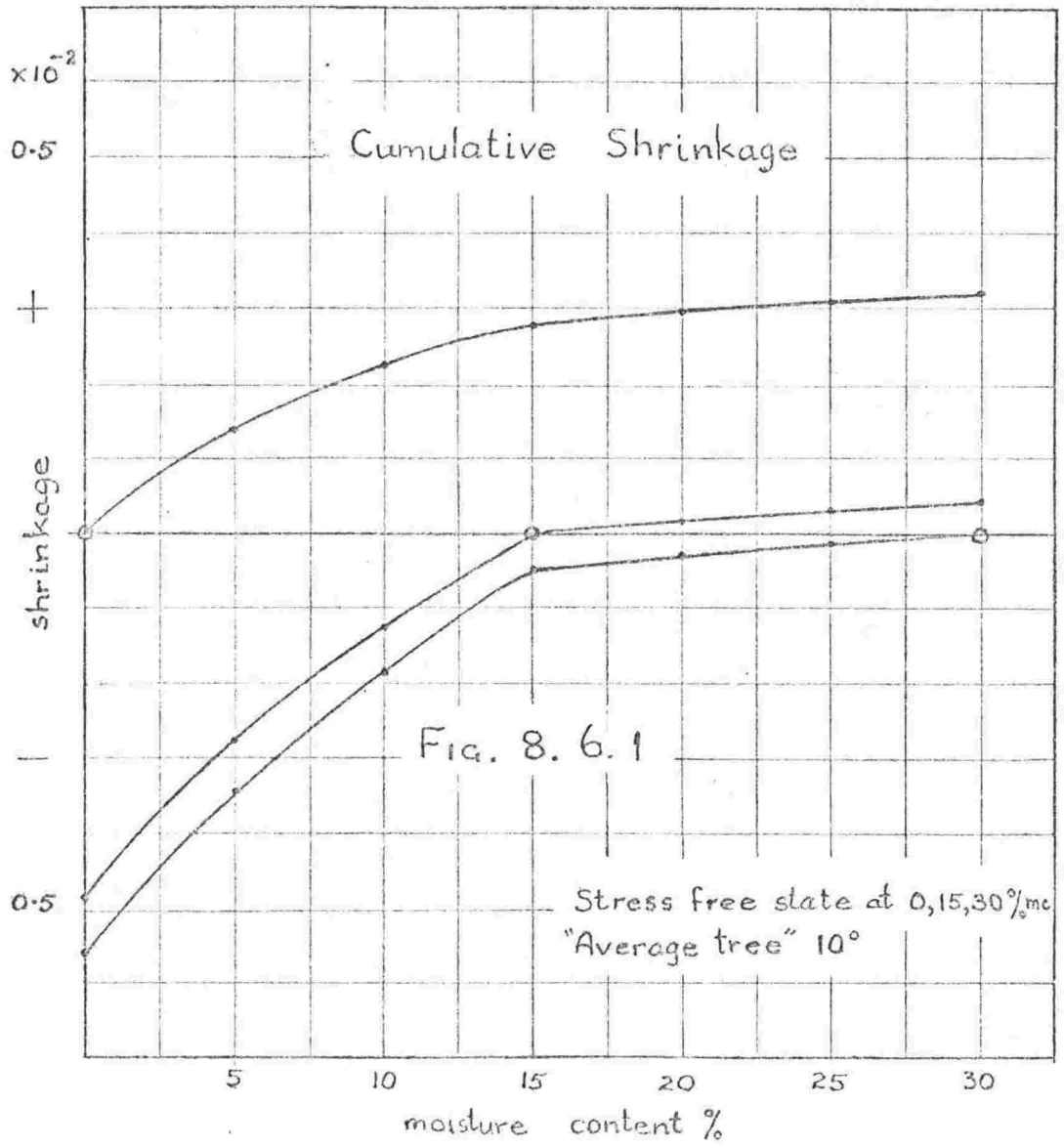
Cumulative Shrinkage
x10⁻²
0·5
+
shrinkage
−
0·5
Stress free state at 0,15,30% mc
"Average tree" 10°
5
10
15
20
25
30
moisture content %

Fig. 8.6.1

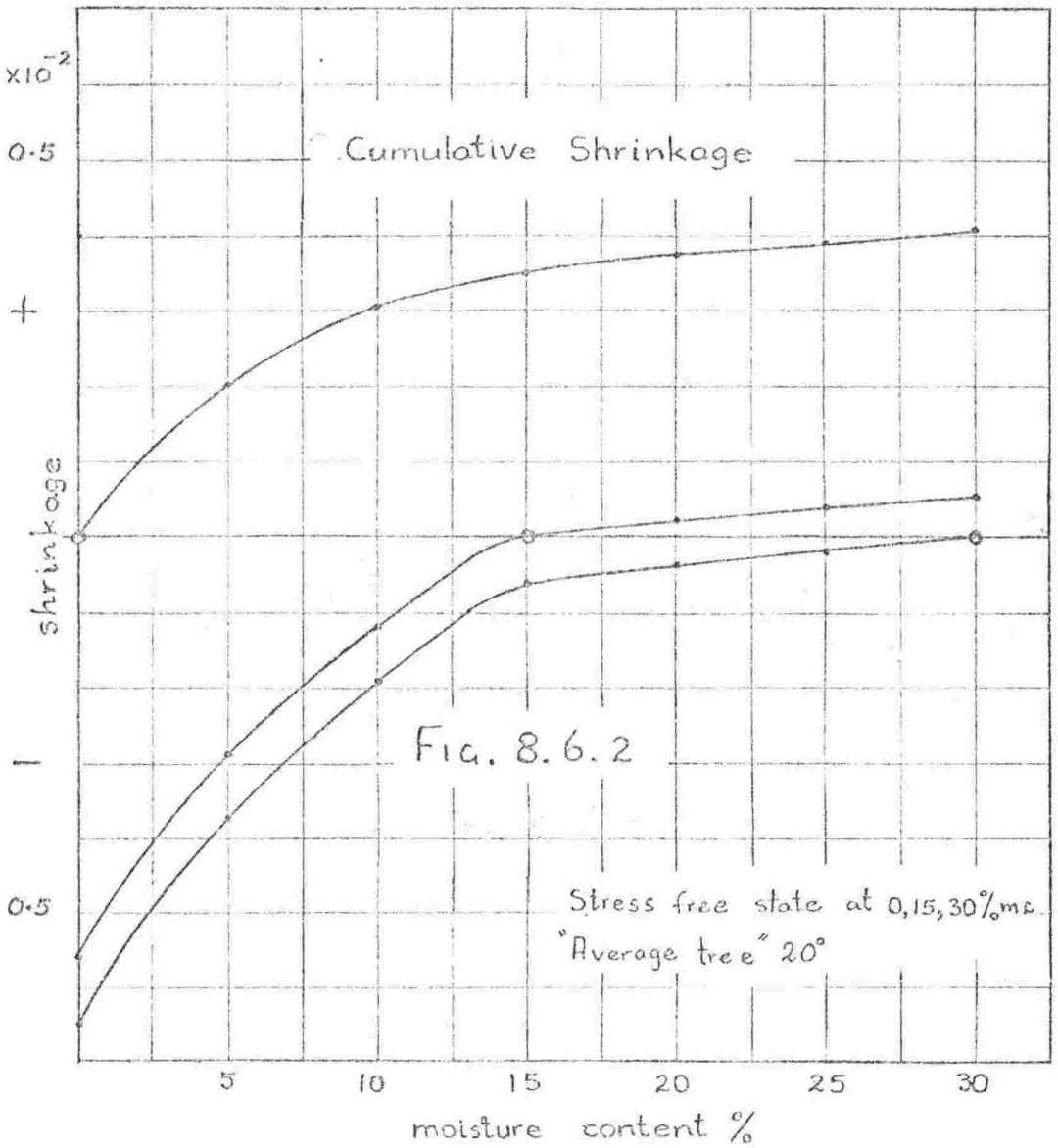
x10⁻²
0·5
Cumulative Shrinkage
+
shrinkage
–
0·5
Stress free state at 0, 15, 30% mc.
"Average tree" 20°
5
10
15
20
25
30
moisture content %

Fig. 8.6.2

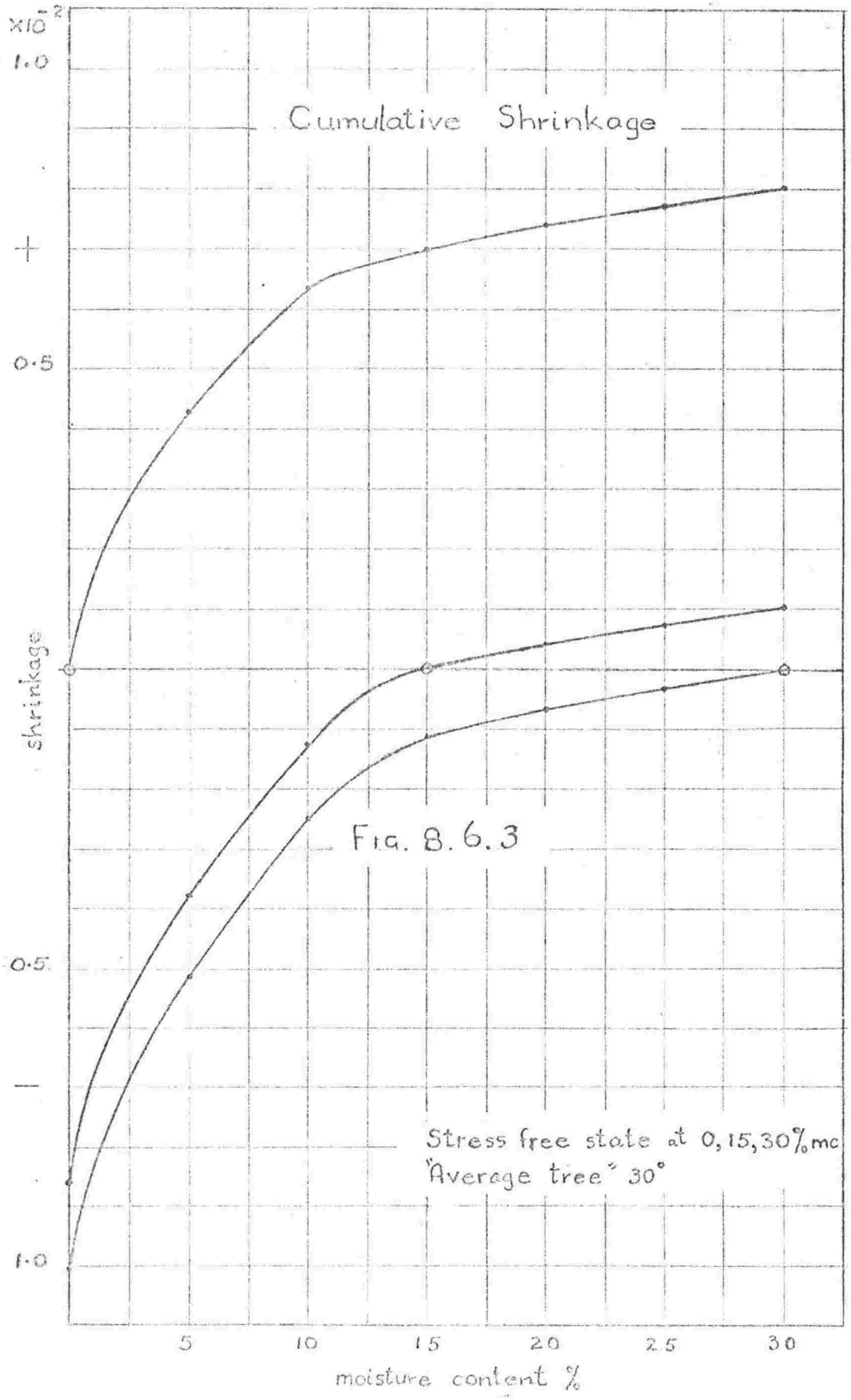
x10⁻²
1.0
Cumulative Shrinkage
+
0.5
shrinkage
0.5
—
1.0
Stress free state at 0, 15, 30% mc
"Average tree" 30°
5
10
15
20
25
30
moisture content %

Fig. 8.6.3

negative high-angle, high moisture-content differential shrinkages. There appears to be no factor other than binding layer thickness that could produce the slight negative going low angle, high moisture content adsorption differential shrinkages and yet be consistent with other considerations, such as positive stiffness and moisture increments. While setting the binding layer at a uniform 30% of the cell-wall thickness reduces the high angle negative differential shrinkages, a modified high moisture content shear mosulus is still required to produce positive shrinkages in this region; and so it must be concluded that all the variations suggested must apply simultaneously in some degree or other.

8.6 Stress Free State

It was mentioned in passing in Section 8.2.1 that the agreement between theoretical and experimental shrinkages is made worse by assuming that the stress free state occurs at moisture contents greater than zero. The cumulative-shrinkage (i.e. shrinkage between the initial moisture content state and the state in question) versus moisture-content curves illustrated in Figs. 8.6.1,2,3, show that at low angles the total shrinkage increases by 70% between the stress-free states at zero and 30% moisture content (Fig. 8.6.1) and at high angles the total shrinkage magnitude is affected to a much smaller extent (Fig. 8.6.3). (The abrupt change in slope in each curve is caused by terminating the fall of the matrix shear modulus function at 15% moisture content with a value of 275 kp/mm^2, as was done for the computations of Section 8.3 and Fig. 8.3.1.)

Theoretically there is no reason why the stress free state could not lie

outside the range of real moisture content values. It would be expected that if it lay in the negative region (i.e. the matrix is always under longitudinal compressive stress), that the initial discrepancy between theoretical and experimental magnitudes remarked on in Section 8.2.1 would be reduced. However, difficulties would then arise in assigning the state of internal stress existing at some real moisture content value and it is not proposed to tackle this problem here.

8.7 Compliance Change Component of Swelling Stress

The compliance change term, $c^m \Delta C^m \left(A^m \bar{\varepsilon} - \bar{\varepsilon}^\circ\right)$, by which the stress free state is introduced into the internal stress of the constitutive relation is new to theories of wood shrinkage. In Table 8.7.1 the magnitude of the axial component of this term is compared with that of the swelling stress, $c^m C^m \Delta \bar{\varepsilon}^\circ$, for the S_2 layer of the "Average tree" 15° specimen, with a stress free state at zero moisture content.

Table 8.7.1

Comparison of the components of internal stress

Moisture Content %	0	5	10	15	20	25
$c^m C^m \Delta \bar{\varepsilon}^\circ$, kp/mm^2	7.82	5.02	2.96	0.13	0.03	-0.08
$c^m \Delta C^m \left(A^m \bar{\varepsilon} - \bar{\varepsilon}^\circ\right)$, kp/mm^2	0.00	0.81	1.23	1.42	1.23	0.53

Overall the term is not of great importance, the maximum value, at 15% moisture content, being less than one fifth the maximum value of the

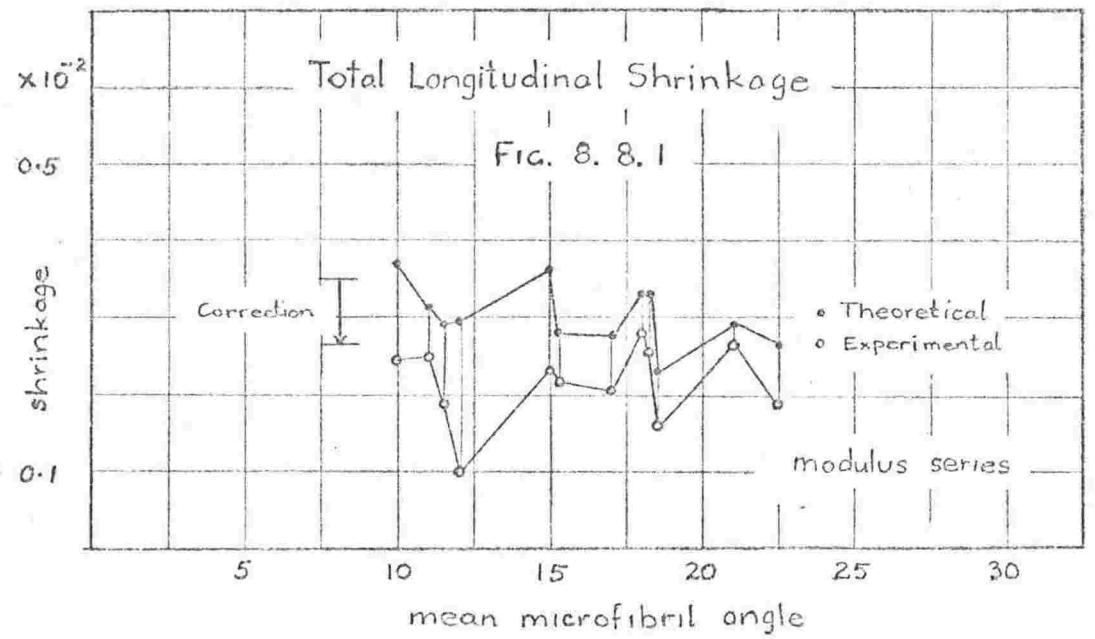
Total Longitudinal Shrinkage
FIG. 8. 8. 1
x10⁻²
0·5
0·1
shrinkage
Correction
• Theoretical
o Experimental
modulus series
5
10
15
20
25
30
mean microfibril angle

swelling stress, and if, as was suggested in Section 8.2.5, the matrix modulus tails off less sharply than indicated in the initial model, then the values at 15% moisture content and higher will be smaller. Thus, the new term does not significantly change the total shrinkage picture from that painted first by Barber and Meylan in 1964. It can, however have a significant effect on some differential shrinkages.

8.8 Model Shrinkage for "Modulus series"

Thus far in this chapter, the "Average tree" model has been used against the extensive block of shrinkage data because the data lacks details on which individual models of cell-wall structure could be built. From this data the initial model of the matrix has been improved. The new matrix model when applied to the individual models of the "Modulus series" Fig. 7.2.1 through the procedures of Section 8.2.1 gives the results for total longitudinal shrinkage shown in Fig. 8.8.1. There is a consistent discrepancy between the theoretical and experimental values that is of no account as it merely represents the mismatch introduced by adopting the full line rather than the dotted matrix water curve (Fig. 8.2.6) which is the one that was fitted to the magnitudes of the 15^{o} experimental adsorption differential shrinkages. All strains should be reduced by about .00085 to compensate for this. The good relative correspondence between pairs of theoretical and experimental points indicates that the basis adopted for modelling the structure of the individual "Modulus series" specimens is generally valid.

8.9 Transverse Shrinkage

It has been pointed out earlier that prediction of transverse shrinkage in whole wood is dependent in large degree upon the geometry and structure of the wood tissue, a matter which has not been considered here. Tangential and radial changes in the dimensions of the cell-wall are the basic cause of transverse shrinkage in wood of course, but the detailed role that each plays in this is not known. The predicted values of total tangential cell-wall shrinkages for the various models in the "Modulus series" range from 0.017 to 0.022 whereas actual values could be expected to be widely scattered in the range 0.04 to 0.08. Thus the predicted changes in cell-wall perimeter fall far short of explaining observed transverse shrinkages; significant contributions must come from other sources. This thesis will not attempt to locate these other sources of transverse shrinkage.

8.10 Miscellaneous Effects

8.10.1 Two outstanding problems

This section briefly draws attention to two other phenomena that lack theoretical interpretation. These are hysteresis in shrinkage and the so-called "moisture induced deformation".

8.10.2 Shrinkage hysteresis

It will have been noted from the comparison of the adsorption and desorption curves in Fig. 8.2.6 that there may be a pronounced hysteresis

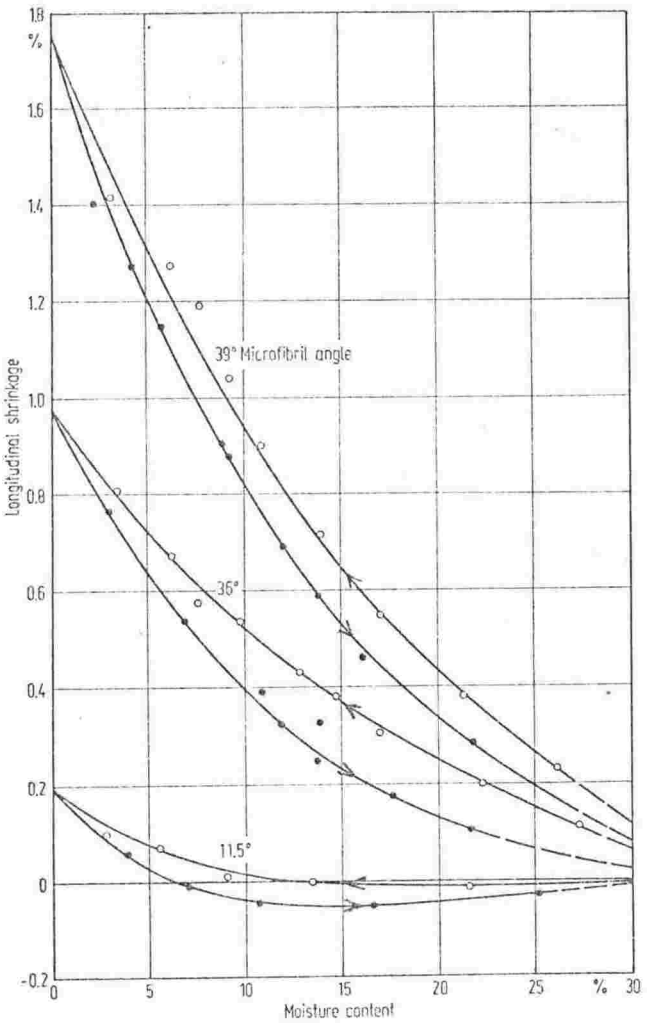

Longitudinal shrinkage as a function of moisture content for one complete moisture content cycle, for samples of different microfibril angles (θ)

FIG. 8.10.1

[After Meylan (1972)]

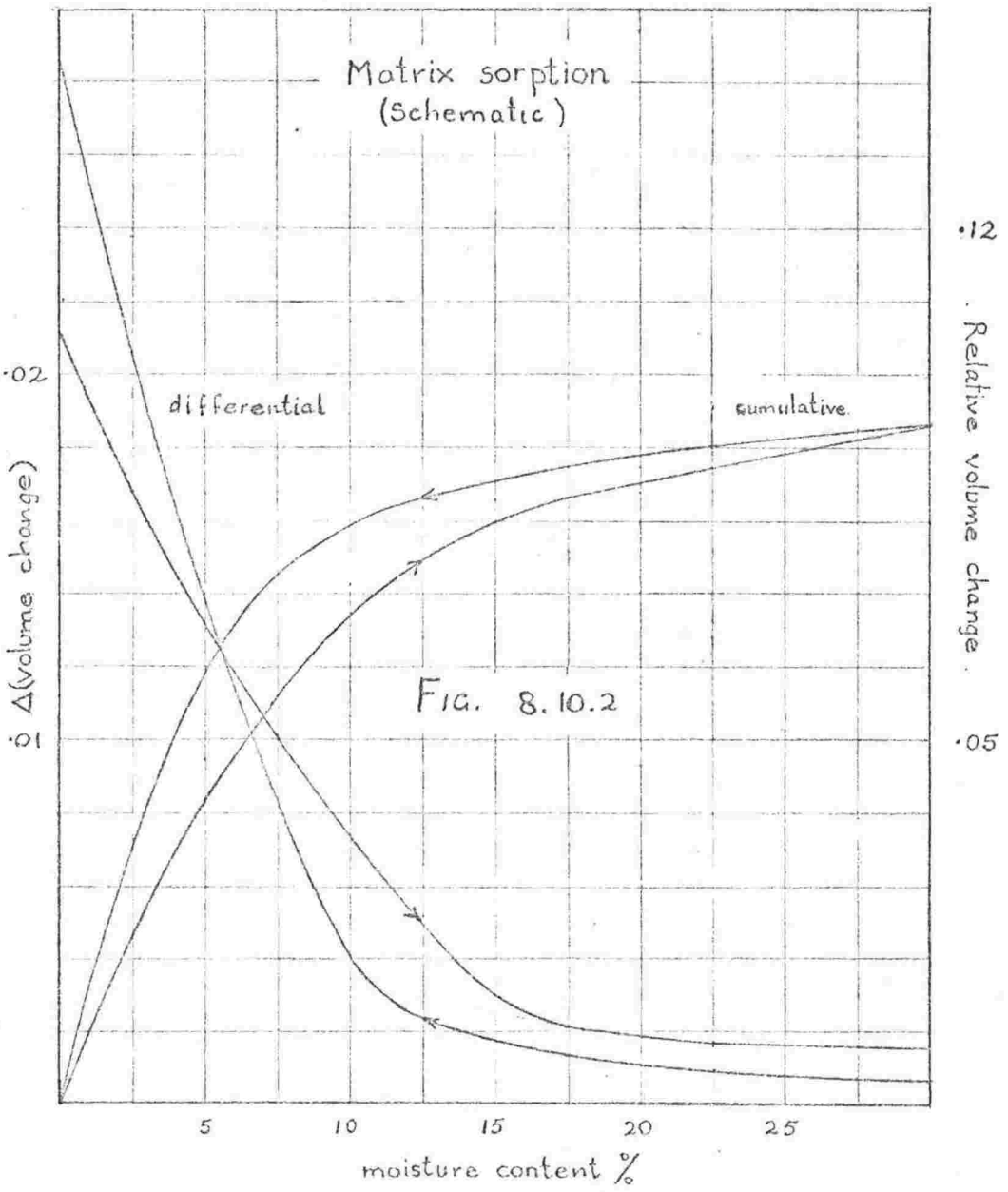
Matrix sorption
(Schematic)
differential
cumulative
·02
·01
Δ(volume change)
·12
·05
Relative volume change
5
10
15
20
25
moisture content %

FIG. 8.10.2

effect in longitudinal shrinkage during moisture cycling. The effect is shown clearly when cumulative shrinkage is plotted against moisture content (Fig. 8.10.1).

It has been reported by Smith (1947) that the amount of "bound" water in wood is greater in desorption than in adsorption at any overall moisture content. The "bound" water has been identified with the matrix water introduced here (Fig. 8.2.7) and means that the fraction of water in the matrix is greater during desorption than during adsorption. This argument would lead to the conclusion that the shrinkage increment at zero moisture content should be greater in the desorption case because the desorption increment is greater than the adsorption increment (see Fig. 8.10.2). The argument, however, ignores the effect that at any given moisture content the stiffness of wood in desorption is lower than that in adsorption (Goulet, 1968), presumably due to variation in the stiffness of the matrix and this would tend to reverse the first effect. There may also be a tendency for the position of the stress free state to migrate in such a way as to minimise internal stress and cause hysteresis in shrinkage.

8.10.3 Moisture induced deformation

When a beam is subject to moisture content cycling, while under continuous loading it exhibits a consequent cyclic pattern of deformation. Contrary to expectation perhaps, the beam deflects when moisture content is decreased and recovers when the moisture content is increased. Recovery is less than deflection and strains up to 8-9 times greater than the

initial elastic deflection can ultimately be achieved. Armstrong and Kingston (1962) found that the extent of deformation was dependent on the size of the moisture content change, while the rate of moisture content change affected only the rate of deformation. Later, Armstrong (1972) disposed of several attempts to explain this behaviour solely in terms of the making and breaking of bonds between water and wood substance while under stress bias occasioned by external load. He demonstrated that volume change and not merely water movement is essential to the process of enhancing deformation by moisture change. He did not, however, attempt any further explanation of the phenomenon.

It appears that volume change can in large degree account qualitatively for moisture-induced deformation. However, the present theory being elastic is reversible and cannot explain the much greater deformation observed in compression. It might be expected that the theory would be better able to account for the observations in tension as the compression observations could be subject to buckling modes of deformation in both the cellulose and the tracheids.

It has been shown that the compliance change component of internal stress is likely to be small and so the behaviour of a specimen in either longitudinal tension or compression could be expected to be approximately given by the expression,

$$C\Delta\bar{\varepsilon} = c^m C^m \Delta\bar{\varepsilon}^\circ \qquad (1)$$

where $\Delta\bar{\varepsilon}^\circ$ is the independent variable indicating moisture change and is now strongly dependent on external stress. Longitudinal tensile breaking stresses of wood substance are typically of the order 15 - 45

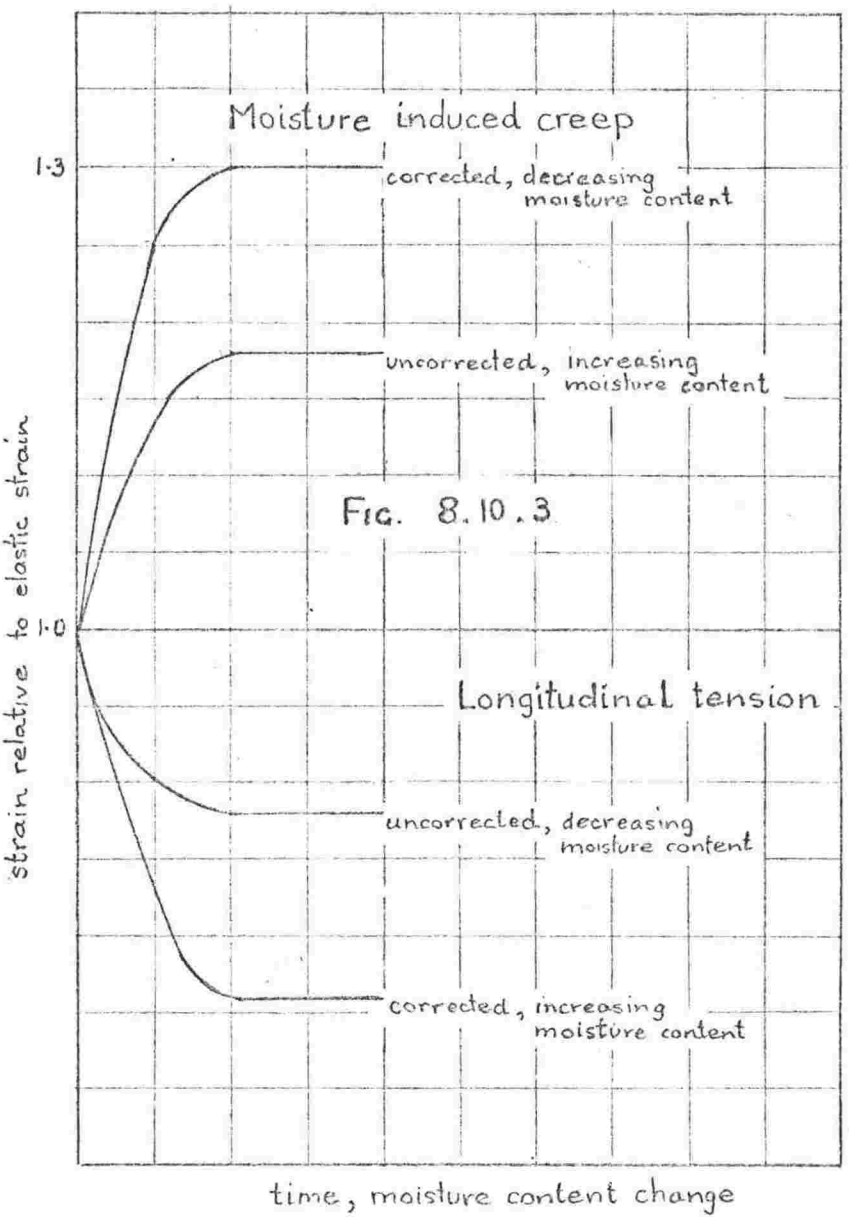
Moisture induced creep
1·3
corrected, decreasing moisture content
uncorrected, increasing moisture content
1·0
Longitudinal tension
uncorrected, decreasing moisture content
corrected, increasing moisture content
strain relative to elastic strain
time, moisture content change

FIG. 8.10.3

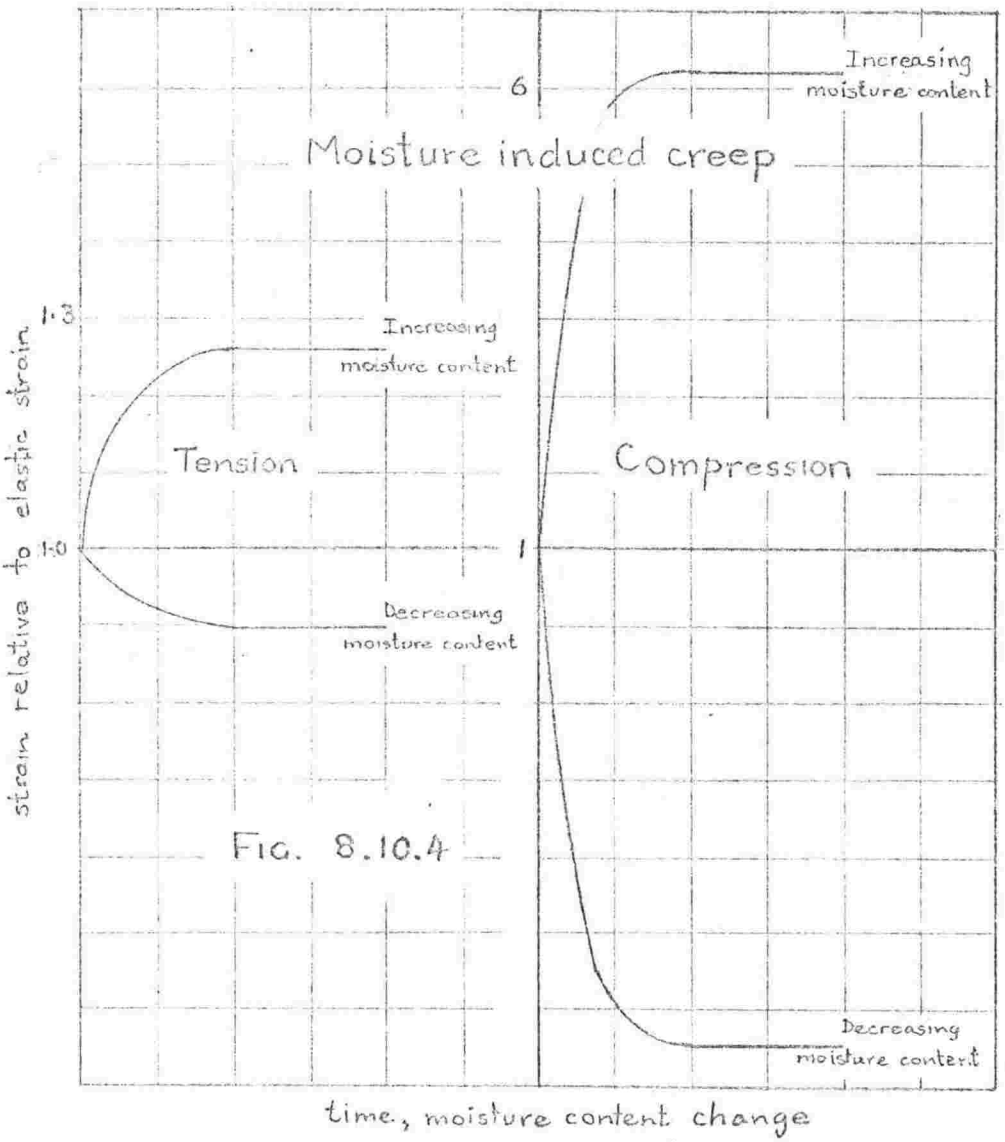
Moisture induced creep
6
Increasing moisture content
1·3
Increasing moisture content
Tension
Compression
1·0
1
Decreasing moisture content
Decreasing moisture content
strain relative to elastic strain
time, moisture content change

FIG. 8.10.4

kp/mm^2, (Pinus radiata earlywood, Cave (1968)) and so on the basis of Table 8.5.1, deflections equivalent to elastic deformation may be expected for reasonably large moisture changes.

The deformations for longitudinal tension and compression as observed by Armstrong and Kingston (1962) and Armstrong (1972) are illustrated in Fig. 8.10.3. These involve large changes in moisture content and it is readily seen that they are compatible, as far as sign is concerned with, Eq. 8.10.1.

The theory fails to account for the observations reported by Armstrong and Kingston (1962) that unloaded deflections exceed loaded deflections for the same relative humidity change. An example, for longitudinal tension, is shown in Fig. 8.10.4. Corrected values refer to the observed deflection under tensile load less the deflection for a specimen under no load. It is apparent from the figure that deflection under no load (i.e. shrinkage or swelling in the usual sense) exceeds that with load. This is a surprising result since it is expected that the moisture content in the loaded specimen will be greater.

According to theory, deformation under tensile load is given approximately by,

$$C_T \Delta\bar{\varepsilon} = c^m C_T^m \left(\frac{\partial\bar{\varepsilon}}{\partial h}\right)_T \Delta h , \qquad (2)$$

and deformation under no load by,

$$C_o \Delta\bar{\varepsilon} = c^m C_o^m \left(\frac{\partial\bar{\varepsilon}}{\partial h}\right)_o \Delta h , \qquad (3)$$

C_o and C_T are composite stiffnesses, and will, therefore, be nearly

identical while C_o^m and C_τ^m will differ mainly because of the difference in moisture content between the loaded and unloaded states. As noted earlier $\left(\frac{\partial \bar{\varepsilon}}{\partial h}\right)_\sigma$ is highly stress dependent, and according to calculations based on Barkas' (1949) p, V, m,h, curves, there could be 2-3 times as much water in the loaded specimen as in the unloaded.

As a first approximation, if we consider the matrix to have both isotropic elastic and swelling behaviour then the products $C_\tau^m\left(\frac{\partial \bar{\varepsilon}}{\partial h}\right)_\tau \Delta h$, $C_o^m\left(\frac{\partial \bar{\varepsilon}}{\partial h}\right)_o \Delta h$ differ only by the amount of water adsorbed in each case and thus,

$$C_m^\tau\left(\frac{\partial \bar{\varepsilon}}{\partial h}\right)_\tau > C_o^m\left(\frac{\partial \bar{\varepsilon}}{\partial h}\right)_o \quad . \tag{4}$$

References

Armstrong, L.D., Kingston, R.S.T. 1962. The effect of Moisture Content Changes on the Deformation of Wood under Stress. Aust. J. App; Sci. 13 : 257-276.

Armstrong, L.D. 1972. Deformation of Wood in Compression during Moisture Movement. Wood Sci. 5 : 81-86.

Barkas, W.W. 1949. The Swelling of Wood under Stress. London. His Majesty's Stationery Office.

Cave, I.D. 1972. A Theory of the Shrinkage of Wood. Wood Sci. & Technol. 6 : 284-292.

Fengel, D., Stoll, M. 1973. Uber die Veranderungen des Zellquerschnitts, der Dicke der Zellwand, und der Wandschichten von Fichtenholz - Tracheiden innerhalls eines Jarringes. Holzforschung. 27 : 1-7.

Goulet, M. 1968. Second order phenomena of Water Sorption in Wood. Note de Recherches No. 3. Département d'Exploitation et Utilization des Bois. Faculté de Foresterie et Géodésie. Université Laval, Québec.

Hailwood, A.J., Horobin, S. 1946. Absorption of Water by Polymers : analysis in terms of a simple model. Trans. Faraday Soc. 42B : 84-92.

Meylan, B.A. 1972. The Influence of Microfibril Angle on the Longitudinal Shrinkage - Moisture Content Relationship. Wood Sci. & Technol. 6 : 293-201.

Skaar, C. 1972. Water in Wood. Syracuse University Press. Syracuse. New York.

Smith, S.E. 1947. The Sorption of Water Vapur by High Polymers. J. Am. Chem. Soc. 69 : 646-651.

Stamm, A.J. 1964. Wood and Cellulose Science. The Ronald Press Company. New York.

Weichert, L. 1963. Investigations on Sorption and Swelling of spruce, beech and compressed beech wood between 20°c and 100°c. Holz als Roh and Werkstoff 21 : 290-300.

Chapter 9

SUMMARY AND CONCLUSIONS

The aim of the present study has been to find a representation of the mechanical properties of wood with respect to moisture content. Previous theories relating mechanical properties to the microstructure of wood have regarded moisture content as constant.

The theory consists of three parts, a constitutive relation which makes provision for variation in moisture content, a model of the properties of the water-reactive matrix, and a model of the structure of the cell-wall. To keep attention directed at the properties of the cell-wall and to avoid complications arising from the structure of the wood tissue as a whole, attention has been confined to the longitudinal properties of wood which are more directly determined by the cell-wall than are the transverse properties.

Two stress situations have been used in determining wood properties. In the first, longitudinal stress has been applied to find longitudinal Young's modulus, and the results have been compared with a set of experimental values in order to infer the properties of the matrix. In the second, stress has been generated by the adsorption of water. Experimental data for longitudinal shrinkage have been used to test the constitutive relation and the model of wood structure and the matrix sorption.

To take account of a varying moisture-content, the constitutive relation includes a new term involving compliance change and the concept of a "stress free state", which is the state of strain at which the forces of reaction of the reinforcing cellulose microfibrils against the water swollen matrix are zero. The likely magnitude of the term has been determined and it seems that as far as total shrinkage (i.e. shrinkage from the saturated to the dry state) is concerned it is not of great significance. However, it could have significance for mid-range moisture content differential shrinkages. The stress free state has been assigned to the zero moisture content condition on the basis of its contribution to shrinkage magnitudes. Barber (1969), using curve shape criteria thought it more likely that the stress free state appeared at the wet end of the moisture content scale. However, it appears that his estimations assigned too great a value to this term and it has been shown here that the appropriate curve shapes can be obtained with the stress free state at zero moisture content. A stress free state at the saturated condition is not intuitively satisfying from the point of view of a fibre composite material as it implies that in dry wood the cellulose is in compression, a rather unlikely role for the reinforcing elements to have to play. It is possible that the stress free state is in the region of virtual negative moisture content where the microfibrils are always in a state of tensional stress.

In a living tree, of course, the situation is different and it may well be that in green wood the stress free state is near the saturated moisture condition. The well known non-repeatable shrinkage patterns exhibited by wood in drying from the green state and then being rewetted

could be due to the stress free state shifting its position from the green condition to the dry by a process of yield in the matrix.

A two-layer model has been used to represent cell-wall structure. One layer represents the predominant S_2 cell-wall and it was supposed that while its chemical constitution was fixed, its thickness varied according to the basic density of the whole wood. Mean microfibril angle could also vary. The rest of the cell-wall was lumped together into a single layer, and was designated the "binding" layer because its microfibrils in general are transverse to the cell axis. An invariant binding layer was tried at first, but it appears that a binding layer that varies in proportion to cell-wall thickness as suggested in the most recent literature on the subject gives predictions that suit the experimental facts better.

The very good correspondence obtained between individual experimental and predicted values for total longitudinal shrinkage indicated the general validity of the procedure used to model individual specimens. This correspondence was obtained by making measurements of basic density, mean microfibril angle and chemical composition, on each specimen individually.

There was little information available prior to this study on the mechanical properties of the matrix and so once the models of structure of the cell-wall had been set up the first task was to derive a shear modulus versus moisture-content function using the experimental Young's modulus data. While there was a disappointingly wide scatter in the results for the matrix shear modulus, three out of twelve specimens gave almost identical

results and the mean of these gave entirely satisfactory values when compared with the relevant information in the literature. The wide scatter obtained was explicable in terms of the method used and the uncertainties in the input data.

At first, the matrix was assumed to be isotropic, but this idea proved untenable and needed substantial modification in light of the fit obtained with the shrinkage data. It was concluded that most of the water taken up into the cell-wall must be mechanically inert, only part entering the matrix and causing changes in length. On deducing from the model, how great this part was, the estimates were found to correspond with the "bound water" or "Langmuir adsorption isotherm" in the literature.

The various theories of sorption of water in wood are agreed that "Langmuir adsorption" (Langmuir, 1918) is a component of the sorption process in wood, even if the detailed interpretation of the remaining sorbed water is open to some doubt, (Skaar, 1972). "Langmuir adsorption" takes place when water interacts with dry wood and forms monomolecular layers on the internal surfaces. The energy of interaction is generally higher than the interaction energy of the secondary water molecules taken up by more moist material. It is generally agreed that secondary low energy adsorption may take place on completed monolayers and some authors (e.g. Smith, 1947) suggest that there may also be low energy sites in the wood substance where secondary water may be directly attached.

From the present considerations it is suggested that -

(i) monomolecular sorption only takes place in the matrix - since the matrix sorption pattern needed to explain longitudinal shrinkage corresponds so closely with the Langmuir adsorption isotherm for wood, and

(ii) as a consequence of (i) all low energy sorption takes place between the lamellae of the cell-wall.

With the introduction of these ideas it will now be necessary to back-track through the procedures used to derive the matrix shear modulus function in order to make compensation for the inert water (see the feed-back loop of Fig. 5.1.1). The effect will be to make the shear modulus function fall with a steadily decreasing rate instead of being virtually linear with moisture content, and this is consistent with the requirements of the differential shrinkage data.

In conclusion, it is apparent that the parameters representing matrix sorption, matrix shear modulus, mean microfibril angle, and the relative size of the S_2 and binding layers are all important to predictions of shrinkage behaviour. It has been possible to obtain very good agreement between the models and the experimental data using justifiable values of these quantities.

At this point the most likely values of the model parameters, not determined directly by measurement would be as listed below (Tables 9.1 - 9.4). Some, such as the matrix sorption property can be accepted with a good deal of confidence, while others such as the matrix shear modulus-moisture

content function should be regarded as informed guesses until such time as they are confirmed by recomputing with updated data.

Table 9.1

Final model values for matrix sorption and matrix shear modulus

Moisture content %	0	5	10	15	20	25	30
Matrix sorption (1)	0.000	0.095	0.143	0.166	0.175	0.182	0.187
Matrix shear modulus, kp/mm^2	620	505	410	335	290	275	275

(1) Volume of sorbed moisture per unit volume of dry matrix.

Table 9.2

Chemical composition of the cell-wall layers

	Lignin Concentration	Cellulose/hemicellulose ratio
M + P	a	0.355(2)
$S_1 + S_3$	0.22(1)	0.615(2)
S_2	0.22(1)	b

a, b values to be fitted from overall chemical data for lignin, cellulose and hemicellulose.

(1) from Fergus, Proctor, Scott & Goring (1969)

(2) from Meier (1961)

Table 9.3

Relative layer thicknesses

Binding layer thickness a constant proportion of total cell-wall thickness. (Value for "Average tree" data - 30%)

Table 9.4

Elastic constants of cellulose

As for Table 5.2.2 but see also Mark 1972

References

Barber, N.F. 1969. The Shrinkage of Wood, Theoretical Models. Institute of Physics and the Physical Society. Conference on the Science of Materials. Univ. of Auckland. N.Z.

Fergus, B.J., Proctor, A.R., Scott, J.A.N., Goring, D.A.I. 1969. The Distribution of Lignin in Spruce Wood as determined by Ultraviolet Microscopy. Wood Sci. Technol. 3 : 117-138.

Langmuir, I. 1918. J. Amer. Chem. Soc. 40 : 1361. (Original not seen.)

Mark, R.E. 1972. Mechanical Behaviour of the Mechanical Components of Fibres. In : Jayne, B.A. (Ed) : Theory and Design of Wood and Fibre Composite Materials. Syracuse, New York. Syracuse Univ. Press. 49-82.

Meier, H. 1961. The Distribution of Polysaccharides in Wood Fibres. J. Polymer Sci. 51 : 11-18.

Skaar, C. 1972. Water in Wood. Syracuse Univ. Press. Syracuse, New York.

Smith, S.E. 1947. The Sorption of Water Vapour by High Polymers. J. Amer. Chem. Soc. 69 : 646-651.

Appendix I

TENSORS AND THEIR REPRESENTATION BY MATRICES

A.I.1 Introduction

Tensors or tensors in their reduced matrix form have been used throughout this work to represent physical quantities. A brief self-contained discussion of tensors and their application to the elasticity of plant cell-walls is given here. However, a full and admirable account of the representation of physical quantities in general by tensors is given by Nye (1967).

Tensors may be defined by their transformation property and this provides an elegant approach to the cell-wall problem.

A.I.2 Definition of a Tensor

The transformation property of a second rank tensor, described in terms of rectangular cartesian co-ordinates is,

$$T'_{ij} = a_{ik}\, a_{jl}\, T_{kl}, \quad i,j,k,l = 1,2,3. \qquad (1)$$

where summation over repeated suffixes is understood.

$\left[T_{ij}\right]$ is an array of 9 coefficients representing the tensor and the coefficients a_{ij} are the direction cosines between the i axis of the new (primed) axes and the j axis of the old (unprimed) system.

Any array of 9 coefficients such as $\left[T_{k\ell}\right]$ that transforms according to Eq. A.I.2.1 is defined by this property as being a tensor (of rank two).

The polar vector transforms according to the law,

$$\rho_i' = a_{ij}\,\rho_j \,, \tag{2}$$

and is therefore said to be a tensor of rank one.

The rank of a tensor is given by the number of subscripts.

A.I.3 Linear Combination of two Tensors is a Tensor

Any array of nine coefficients, A_{ij} $i,j = 1, 2, 3$, that linearly connects the components of two vectors ρ_i, q_j (rank one tensors) in the following manner, is itself a tensor (of rank two),

$$\begin{aligned}
\rho_1 &= A_{11}q_1 + A_{12}q_2 + A_{13}q_3 \\
\rho_2 &= A_{21}q_1 + A_{22}q_2 + A_{23}q_3 \\
\rho_3 &= A_{31}q_1 + A_{32}q_3 + A_{33}q_3
\end{aligned} \tag{1}$$

This statement is proved by noting that,

$$\rho_i' = a_{ik}\,\rho_k \,,$$

with ρ_k related to q_ℓ through,

$$\rho_k = A_{k\ell}\,q_\ell$$

q_ℓ in terms of the new axes is given by,

$$q_\ell = a_{j\ell}\,q_j' \,,$$

so that combining these expressions we have,

$$\rho_i' = a_{ik}\,A_{k\ell}\,a_{j\ell}\,q_j' \,.$$

Thus,

$$A'_{ij} = a_{ik}\, a_{j\ell}\, A_{k\ell},$$

and $\left[A_{ij}\right]$ is by definition a tensor of rank two.

This last theorem is used to show that stress and strain are tensors of rank two and from these results it follows that elasticity which connects stress and strain linearly is a tensor of rank four.

These matters are briefly discussed below. Brief mention of a few relevant properties of stress, strain and elastic tensors is made as each is encountered.

A.I.4 Stress

It can be shown that stress, σ_{ij}, is given by the relation,

$$p_i = \sigma_{ij}\, \ell_j \qquad i,j = 1,2,3, \qquad (1)$$

where p_i is the force and ℓ_j is the outward unit vector normal to a surface element on the body on which the force is acting. p_i and ℓ_j are both vectors and so stress is a second rank tensor.

σ_{11}, σ_{22}, σ_{33} are the normal components of stress and σ_{12}, σ_{21}, σ_{23} etc. are the shear components. Force equilibrium considerations require that stress by a symmetrical tensor, so that,

$$\sigma_{ij} = \sigma_{ji}\,.$$

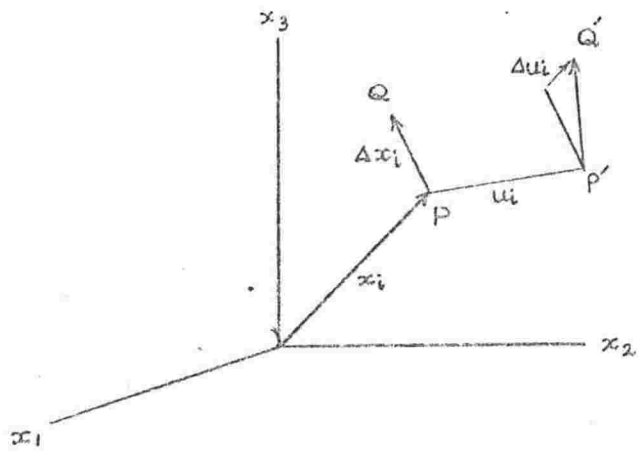

FIG. A. 5. 1

A.I.5 Strain

The deformation, Δu_i, of a general line element, Δx_i, (P Q in figure A.I.5.1) at x_i and displaced by u_i during the deformation process is given by,

$$\Delta u_i = \left(\frac{\partial u_i}{\partial x_j}\right) \Delta x_j ,$$

where $\left(\frac{\partial u_i}{\partial x_j}\right) = e_{ij}$ is the strain.

Because $\left[\Delta u_i\right]$ and $\left[\Delta x_j\right]$ are both vectors it follows that $\left[e_{ij}\right]$ is a tensor of rank two.

$\left[e_{ij}\right]$ is not necessarily symmetric. However, as any tensor may be split into symmetric and anti-symmetric parts strain may be written,

$$\left[e_{ij}\right] = \left[\varepsilon_{ij}\right] + \left[\omega_{ij}\right]$$

where $\varepsilon_{ij} = \tfrac{1}{2}\left(e_{ij} + e_{ji}\right)$ and $\omega_{ij} = \tfrac{1}{2}\left(e_{ij} - e_{ji}\right)$.

It can be demonstrated that the anti-symmetric part, ω_{ij}, represents a rigid body rotation, and that the symmetric part, ε_{ij}, termed the strain tensor, represents deformation. The diagonal components $\left[\varepsilon_{ii}\right]$ are the extensions per unit length parallel to the reference axes, and the off-diagonal components such as ε_{12} measure tensor shear strain.

Any symmetric tensor can be transformed so that its off-diagonal elements are zero.

$$\begin{bmatrix} \varepsilon_{11} & \varepsilon_{12} & \varepsilon_{13} \\ \varepsilon_{12} & \varepsilon_{22} & \varepsilon_{23} \\ \varepsilon_{13} & \varepsilon_{23} & \varepsilon_{33} \end{bmatrix} \longrightarrow \begin{bmatrix} \varepsilon_1 & 0 & 0 \\ 0 & \varepsilon_2 & 0 \\ 0 & 0 & \varepsilon_3 \end{bmatrix}$$

The physical meaning of the principal strains $\varepsilon_1, \varepsilon_2, \varepsilon_3$. is seen by considering a unit cube constructed with its edges parallel to the principal axes. Under deformation it retains its rectangular geometry with its edge lengths extended to $1+\varepsilon_1$, $1+\varepsilon_2$, $1+\varepsilon_3$. The dilation of the cube is then,

$$\Delta = (1+\varepsilon_1)(1+\varepsilon_2)(1+\varepsilon_3) - 1$$

and since the ε_i are small,

$$\Delta = \varepsilon_1 + \varepsilon_2 + \varepsilon_3$$

A.I.6 Elasticity

The generalised Hooke's law takes the form,

$$\varepsilon_{ij} = s_{ijkl}\,\sigma_{kl} ,$$

where the s_{ijkl} are the compliance coefficients. In the inverse form, Hooke's law is written,

$$\sigma_{ij} = s_{ijkl}\,\varepsilon_{kl}$$

where the c_{ijkl} are called stiffness coefficients.

By a similar argument to that used for second rank tensors it can be shown that $[s_{ijkl}]$ and $[c_{ijkl}]$ are fourth rank tensors, since stress and strain are tensors*.

There are 81 stiffness and compliance constants. However, since $[\varepsilon_{ij}]$

*Note : The familiar "technical" elastic constants, Young's modulus, Poisson's ratio and shear modulus do not constitute components of a tensor since they do not relate tensor stress and tensor strain in a linear manner.

and σ_{ij} are symmetric it follows that $c_{ijkl} = c_{jikl}$ etc., so that only 36 of the 81 constants are independent.

A.I.7 Matrix Notation

For computation it is convenient and usual to eliminate the non-independent coefficients by converting from the tensor form to a reduced matrix form. However, it is necessary to remember that it is only in the full tensor form that the physical quantity is completely specified. In particular, when dealing with transformation of axes, one must use the full tensor form. It is quite common, therefore, when dealing with fibre composites with dispersed fibre directions to convert back and forth from the matrix to the tensor forms of compliance and stiffness.

To write the stiffness tensor out in full would require nine, 3 x 3 arrays of the coefficients. If we regard the third and fourth suffixes of as the row and column indices of the two dimensional arrays, the tensor has the form

$$\begin{bmatrix} c_{1111} & c_{1112} & c_{1113} \\ c_{1121} & c_{1122} & c_{1123} \\ c_{1131} & c_{1132} & c_{1133} \end{bmatrix} \quad \begin{bmatrix} c_{1211} & c_{1212} & c_{1213} \\ c_{1221} & c_{1222} & c_{1223} \\ c_{1231} & c_{1232} & c_{1233} \end{bmatrix} \quad \begin{bmatrix} c_{1311} & c_{1312} & c_{1313} \\ c_{1321} & c_{1322} & c_{1323} \\ c_{1331} & c_{1332} & c_{1333} \end{bmatrix}$$

$$\begin{bmatrix} c_{3111} & c_{3112} & c_{3113} \\ c_{3121} & c_{3122} & c_{3123} \\ c_{3131} & c_{3132} & c_{3133} \end{bmatrix} \quad \begin{bmatrix} & & \\ & & \\ & & \end{bmatrix} \quad \begin{bmatrix} c_{3311} & c_{3312} & c_{3313} \\ c_{3321} & c_{3322} & c_{3323} \\ c_{3331} & c_{3332} & c_{3333} \end{bmatrix}$$

Bearing in mind the symmetry property that $c_{ijkl} = c_{ijlk}$ and using the following scheme to condense the tensor suffix notation pair-wise.

tensor notation	11	22	33	23,32	31,13	12,21
matrix notation	1	2	3	4	5	6

the above array may be written,

$$\begin{bmatrix} c_{11} & c_{16} & c_{15} \\ c_{16} & c_{12} & c_{14} \\ c_{15} & c_{14} & c_{13} \end{bmatrix} \quad \begin{bmatrix} c_{61} & c_{66} & c_{65} \\ c_{66} & c_{62} & c_{64} \\ c_{65} & c_{64} & c_{63} \end{bmatrix} \quad \begin{bmatrix} c_{51} & c_{56} & c_{55} \\ c_{56} & c_{52} & c_{54} \\ c_{55} & c_{54} & c_{53} \end{bmatrix} \qquad (2)$$

We may reduce the stress tensor in the same way,

$$\begin{bmatrix} \sigma_{11} & \sigma_{12} & \sigma_{13} \\ \sigma_{21} & \sigma_{22} & \sigma_{23} \\ \sigma_{31} & \sigma_{32} & \sigma_{33} \end{bmatrix} \rightarrow \begin{bmatrix} \sigma_1 & \sigma_6 & \sigma_5 \\ \sigma_6 & \sigma_2 & \sigma_4 \\ \sigma_5 & \sigma_4 & \sigma_3 \end{bmatrix} \qquad (3)$$

so that in the inverse Hooke's law, stress written in the tensor form,

$$\begin{aligned} \sigma_{11} = {} & c_{1111}\varepsilon_{11} + c_{1112}\varepsilon_{12} + c_{1113}\varepsilon_{13} \\ & + c_{1121}\varepsilon_{21} + c_{1122}\varepsilon_{22} + c_{1123}\varepsilon_{23} \\ & + c_{1131}\varepsilon_{31} + c_{1132}\varepsilon_{32} + c_{1133}\varepsilon_{33}\ , \end{aligned} \qquad \begin{aligned} \sigma_{23} = {} & c_{2311}\varepsilon_{11} + c_{2312}\varepsilon_{12} + c_{2313}\varepsilon_{13} \\ & + c_{2321}\varepsilon_{21} + c_{2322}\varepsilon_{22} + c_{2323}\varepsilon_{23} \\ & + c_{2331}\varepsilon_{31} + c_{2332}\varepsilon_{32} + c_{2333}\varepsilon_{33}; \end{aligned} \qquad (4)$$

on reduction becomes,

$$\begin{aligned} \sigma_1 = {} & c_{11}\varepsilon_{11} + c_{16}\varepsilon_{12} + c_{15}\varepsilon_{13} \\ & + c_{16}\varepsilon_{12} + c_{12}\varepsilon_{22} + c_{14}\varepsilon_{23} \\ & + c_{15}\varepsilon_{31} + c_{14}\varepsilon_{32} + c_{13}\varepsilon_{33}\ , \end{aligned} \qquad \begin{aligned} \sigma_4 = {} & c_{41}\varepsilon_{11} + c_{46}\varepsilon_{12} + c_{45}\varepsilon_{13} \\ & + c_{46}\varepsilon_{21} + c_{42}\varepsilon_{22} + c_{44}\varepsilon_{23} \\ & + c_{45}\varepsilon_{31} + c_{44}\varepsilon_{32} + c_{43}\varepsilon_{33}\ , \end{aligned} \qquad (5)$$

Now, if the strain tensor is condensed in the following way,

$$\begin{bmatrix} \varepsilon_{11} & \varepsilon_{12} & \varepsilon_{13} \\ \varepsilon_{21} & \varepsilon_{22} & \varepsilon_{23} \\ \varepsilon_{31} & \varepsilon_{32} & \varepsilon_{33} \end{bmatrix} \rightarrow \begin{bmatrix} \varepsilon_1 & \tfrac{1}{2}\varepsilon_6 & \tfrac{1}{2}\varepsilon_5 \\ \tfrac{1}{2}\varepsilon_6 & \varepsilon_2 & \tfrac{1}{2}\varepsilon_4 \\ \tfrac{1}{2}\varepsilon_5 & \tfrac{1}{2}\varepsilon_4 & \varepsilon_3 \end{bmatrix}, \qquad (6)$$

the inverse Hooke's law may be represented by the two dimensional array,

$$\begin{aligned}\sigma_1 &= c_{11}\varepsilon_1 + c_{12}\varepsilon_2 + c_{13}\varepsilon_3 + c_{14}\varepsilon_4 + c_{15}\varepsilon_5 + c_{16}\varepsilon_6\\ &\vdots\\ \sigma_4 &= c_{41}\varepsilon_1 + c_{42}\varepsilon_2 + c_{43}\varepsilon_3 + c_{44}\varepsilon_4 + c_{45}\varepsilon_5 + c_{46}\varepsilon_6\\ &\vdots\end{aligned} \qquad (7)$$

which in the index notation is,

$$\sigma_i = c_{ij}\,\varepsilon_j \qquad i,j = 1,2,\ldots 6. \qquad (8)$$

This is known as the matrix form as it consists of a single two dimensional 6 x 6 array.

In order that an inverse relation between stress and strain may be written in the same form, with the same definition for the stress and strain matrices it is necessary that the compliance coefficients be reduced by observing the following rules,

s_{ijkl} becomes s_{mn} when m and n are 1, 2, or 3,

$2s_{ijkl}$ becomes s_{mn} when either m or n are 4, 5, or 6,

and $4s_{ijkl}$ becomes s_{mn} when both m and n are 4, 5, or 6.

Thus ε_{11} and ε_{23} become,

$$\begin{aligned}\varepsilon_1 = {} & s_{11}\sigma_1 + \tfrac{1}{2}s_{16}\sigma_6 + \tfrac{1}{2}s_{15}\sigma_5\\ & + \tfrac{1}{2}s_{16}\sigma_6 + s_{12}\sigma_2 + \tfrac{1}{2}s_{14}\sigma_4\\ & + \tfrac{1}{2}s_{15}\sigma_5 + \tfrac{1}{2}s_{14}\sigma_4 + s_{13}\sigma_3\end{aligned} \qquad \begin{aligned}\varepsilon_4 = {} & \tfrac{1}{2}s_{41}\varepsilon_1 + \tfrac{1}{4}s_{46}\sigma_6 + \tfrac{1}{4}s_{45}\sigma_5\\ & + \tfrac{1}{4}s_{46}\sigma_6 + \tfrac{1}{2}s_{42}\sigma_2 + \tfrac{1}{4}s_{44}\sigma_4\\ & + \tfrac{1}{4}s_{45} + \tfrac{1}{4}s_{44}\sigma_4 + \tfrac{1}{2}s_{43}\sigma_3,\end{aligned} \qquad (9)$$

or $\varepsilon_1 = s_{1j}\,\sigma_j$, $\varepsilon_4 = s_{4j}\,\sigma_j$

or $\varepsilon_i = s_{ij}\,\sigma_j \qquad i,j = 1,2,\ldots 6.$ (10)

The definitions of c_{ij} and s_{ij} given above conform with established practice. (Nye (1967)).

An additional symmetry property of elasticity arising from consideration of strain energy results in the equalities,

$$c_{ij} = c_{ji} \quad , \quad s_{ij} = s_{ji} \quad ,$$

and brings about a further reduction of the number of independent elastic constants from 36 to 21.

A.I.8 Transformation of Elastic Tensors

The evaluation of the elastic coefficients of cell-wall material in terms of the cell-wall reference system is basic to cell-wall mechanics. The execution of the transformation required for this is easily accomplished by the use of the transformation law.

The elemental volume of cell-wall material has transverse isotropy (Section 4.2) and so the stiffness matrix is of the form,

$$\begin{matrix} c_{11} & c_{12} & c_{13} & \cdot & \cdot & \cdot \\ & c_{11} & c_{13} & \cdot & \cdot & \cdot \\ & & c_{33} & \cdot & \cdot & \cdot \\ & & & c_{44} & \cdot & \cdot \\ & & & & c_{44} & \cdot \\ & & & & & c_{66}, \; c_{66} \quad \tfrac{1}{2}(c_{11} - c_{12}), \end{matrix} \qquad (1)$$

when the axis of isotropy is parallel to the x_3 axis of a cartesian set (x_1, x_2, x_3).

For a fourth rank tensor the transformation law is,

$$T'_{ijkl} = a_{im}\, a_{jn}\, a_{ko}\, a_{lp}\, T_{mnop} \ ,$$

and it is required that we rotate the tensor about the $1'$ axis by an angle θ equal to the microfibril angle of the cell-wall element.

The construction of an array of direction cosines aids the transformation process, and so we have,

"new" \ "old"	x_1	x_2	x_3
x'_1	1	0	0
x'_2	0	$\cos\theta$	$\sin\theta$
x'_3	0	$-\sin\theta$	$\cos 0$

.

Proceeding with the transformation for c_{22} for example, we have with simultaneous reference to both the full tensor array A.I.7.1 and the matrix array of the stiffness coefficients A.I.8.1 in order to pick out equalities and zeros in the coefficients,

$$c'_{22} \equiv c'_{2222} = 0 \qquad \text{from matrix II of array A.I.7.1}$$

$$+0 \qquad " \quad " \quad 12 \quad " \quad " \quad "$$

$$+0 \qquad " \quad " \quad 13 \quad " \quad " \quad "$$

$$+0 \qquad " \quad " \quad 21 \quad " \quad " \quad "$$

$$+\cos^4\theta\, c_{11}\,(c_{2222}) + \cos^2\theta \sin^2\theta\, c_{13}\,(c_{2233}) \qquad " \quad " \quad 22 \quad " \quad " \quad "$$

$$+2\cos^2\theta \sin^2\theta\, c_{44}\,(c_{2323}),(c_{2332}) \qquad " \quad " \quad 23 \quad " \quad " \quad "$$

$$+0 \qquad " \quad " \quad 31 \quad " \quad " \quad "$$

$$+2\cos^2\theta \sin^2\theta\, c_{44}\,(c_{3223}),(c_{3232}) \qquad " \quad " \quad 32 \quad " \quad " \quad "$$

$$+\cos^2\theta \sin^2\theta\, c_{13}\,(c_{3322}) + \sin^4\theta\, c_{33}\,(c_{3333}) \qquad " \quad " \quad 33 \quad " \quad " \quad "$$

where the contents of the brackets indicates only the tensor coefficients from which the preceding matrix coefficient is derived.

i.e. $c'_{22} = c_{11}\cos^4\theta + c_{33}\sin^4\theta + 2\left(c_{13} + 2c_{44}\right)\cos^2\theta\sin^2\theta$

As a second example consider the transformation of c_{24} . Dropping the explanatory notes, we can write by inspection,

$c'_{24} = c_{2223}$ (for example; other possible terms are $c_{2232}, c_{2322}, c_{3222}$)

$$\begin{aligned} &= -\cos^3\theta\sin\theta c_{11} + \cos^3\theta\sin\theta c_{13} \\ &\quad +\cos^3\theta\sin\theta c_{44} - \cos\theta\sin^3\theta c_{44} \\ &\quad +\cos^3\theta\sin\theta c_{44} - \cos\theta\sin^3\theta c_{44} \\ &\quad -\cos\theta\sin^3\theta c_{13} + \cos\theta\sin^3\theta c_{33} \end{aligned}$$

$$\text{i.e. } c'_{24} = \left(c_{33}\sin^2\theta - c_{11}\cos^2\theta + \left(c_{13} + 2c_{44}\right)\left(\cos^2\theta - \sin^2\theta\right)\right)\cos\theta\sin\theta$$

The full table of coefficients for this transformation is given below.

Table A.I.7.1

Transformation for the matrix coefficients of stiffness when a transversely isotropic body is rotated by an angle, θ, about the '1' axis

$$c'_{11} = c_{11}$$

$$c'_{22} = c_{11}\cos^4\theta + c_{33}\sin^4\theta + 2(c_{13} + 2c_{44})\cos^2\theta\sin^2\theta$$

$$c'_{33} = c_{11}\sin^4\theta + c_{33}\cos^4\theta + 2(c_{13} + 2c_{44})\cos^2\theta\sin^2\theta$$

$$c'_{12} = c_{12}\cos^2\theta + c_{13}\sin^2\theta$$

$$c'_{13} = c_{12}\sin^2\theta + c_{13}\cos^2\theta$$

$$c'_{23} = \left(c_{11} + c_{33} - 2(c_{13} + 2c_{44})\right)\cos^2\theta\sin^2\theta + c_{13}$$

$$c'_{44} = \left(c_{11} + c_{33} - 2(c_{13} + 2c_{44})\right)\cos^2\theta\sin^2\theta + c_{44}$$

$$c'_{55} = c_{44}\cos^2\theta + c_{66}\sin^2\theta$$

$$c'_{66} = c_{44}\sin^2\theta + c_{66}\cos^2\theta$$

$$c'_{14} = (c_{13} - c_{12})\cos\theta\sin\theta$$

$$c'_{24} = \left(c_{33}\sin^2\theta - c_{11}\cos^2\theta + (c_{13} + 2c_{44})(\cos^2\theta - \sin^2\theta)\right)\cos\theta\sin\theta$$

$$c'_{34} = \left(c_{33}\cos^2\theta - c_{11}\sin^2\theta - (c_{13} + 2c_{44})(\cos^2\theta - \sin^2\theta)\right)\cos\theta\sin\theta$$

$$c'_{56} = (c_{44} - c_{66})\cos\theta\sin\theta$$

With all other $c'_{ij} = 0 \quad i,j = 1,2,3,4,5,6.$

A.I.9 Relations between Stiffness and Compliance Coefficients

To conclude, the relationship between compliance and stiffness is briefly considered. The problem is most readily approached through the matrix form of the elastic relations by the process of matrix inversion.

From $\sigma_i = c_{ij}\,\varepsilon_j$ and its inverse $\varepsilon_i = s_{ij}\,\sigma_j$ it is evident that,

$$\left[s_{ij}\right] = \left[c_{ij}\right]^{-1},$$

and so,

$$\left[s_{ij}\right] = \left[\frac{\left[\Gamma_{ji}\right]}{\det\left[c_{ij}\right]}\right]$$

where Γ_{ji} is the cofactor of the element c_{ji} in the determinant $\det\left[c_{ij}\right]$ formed from the array, c_{ij} , $i, j = 1,2,3$.

The process is illustrated by deriving Young's modulus for an isotropic material in terms of the stiffnesses.

Young's modulus $E = \frac{1}{s_{11}}$,

$$= \frac{\det\left[c_{ij}\right]}{\Gamma_{11}},$$

$$= \frac{c_{11}\left(c_{11}^2 - c_{12}^2\right) - 2c_{12}\left(c_{12}c_{11} - c_{12}^2\right)}{c_{11}^2 - c_{12}^2},$$

$$i.e. \quad = \frac{(c_{11} + 2c_{12})(c_{11} - c_{12})}{c_{11} + c_{12}} \quad .$$

It is readily shown that,

$$c_{11} + 2c_{12} = 3k$$

where k is the bulk modulus, and

$$c_{11} - c_{12} = 2\mu$$

where μ is the shear modulus, so that more familarly,

$$E = \frac{9k\mu}{3k+\mu} \quad .$$